ROLE OF EARLY B-CELL FACTORS (EBFs) IN THE DEVELOPMENT OF THE CEREBRAL CORTEX

A thesis submitted to University College London for the Degree of Doctor of Philosophy

By

Francesca Chiara

Department of Cell and Developmental Biology
University College London
London WC1E 6BT
UK

February, 2011

I, Francesca Chiara, confirm that the work presented here in this thesis is my own.

Where information has been derived from other sources, I confirm that it has been indicated clearly in the thesis.

……

ABSTRACT

Early B-cell factor 2 (*Ebf2*) is one of four mammalian members of the helix-loop-helix transcription factor family *Collier/Olf/Ebf* (*COE*). COE proteins EBF1, EBF2 and EBF3 have been implicated in various aspects of neural development including neurogenesis, cell differentiation, neuronal migration and axonal fasciculation. Here, I examined the role of one of these proteins, EBF2, on the development of the cerebral cortex.

Ebf2 mRNA, detected by *in situ* hybridisation, was transiently expressed in the developing mouse cerebral cortex. In particular, it was found in the cortical hem, septum and preplate/marginal zone, which are known sites of origin and migration for Cajal-Retzius cells, respectively. In order to permanently label *Ebf2* positive cells even after the downregulation of the gene expression, the transgenic line $Ebf2^{GFPiCre}$ was crossed with the reporter line $Rosa26R^{YFP}$. It was found that the expression of *Ebf2* matched the expression of markers for Cajal-Retzius cells, subplate cells and a subpopulation of layer V pyramidal neurons. Although $Ebf2^{-/-}$ mice showed a delay in the migration of Cajal-Retzius cells at early stages of development, which was rescued by the end of gestation, they did not present any other gross defect in cortical topography and cellular organisation. *In vivo* and *in vitro* studies have suggested that *Ebf1* and *Ebf3*, also expressed in the cortical hem and septum, may be involved in complementing the lack of *Ebf2* function. These results suggest a role for the EBF family in controlling Cajal-Retzius cell development.

ACKNOWLEDGEMENTS

I am really grateful to my supervisor Professor John Parnavelas for giving me the opportunity to join his lab, but most importantly, for his incredible support during my entire PhD.

My sincere gratitude goes to my "master", Dr Sonja Rakic, for patiently teaching me the developmental neurobiology and helping me to carry out all the experiments I have shown in this thesis. I would like also to thank her for giving me the passion and the strength to reach my goals.

Thanks to Dr Anna Cariboni for the precious help in the Lab but most importantly for the sincere friendship. Thanks to all the other Parnavelas Lab members: Bill, Claire, Tilly, Fani, Arianna, Mary for sharing long working hours and moments of fun, and Mason for the incredible help with EndNote and References of this thesis.

I am thankful to Dr Yoshiuki Yamamoto (YAMA) for allowing me to use his microscope and his friendly support.

I would like also thank Dr Giacomo Consalez and lab members for sharing mouse lines and plasmids; Dr Zoltan Molnar and Prof Tomomi Shimogori for the collaboration in the realisation of some of the experiments presented in this thesis.

I am thankful to BBSRC for funding three years of PhD university fees.

Thanks to Chris, Tim and Daniel at the Confocal Unit; Mary and Pala at the Molecular Biology Lab; Tina at the Animal Facility and Ian at the Anatomy Store for the technical support.

A special thanks to my friend Mandy Tsang for her sincere support throughout these three years.

My deepest gratitude goes to my parents, Osvaldo and Ada; and, my brother and sister, Jacopo and Elena, for their belief in me.

PUBLICATIONS

Chiara, F., A. Cariboni, A. Badaloni, G. G. Consalez, J. G. Parnavelas, S. Rakíc. "*Ebf2* plays a role in Cajal-Retzius cell development." (In preparation)

Qian, H., A. Badaloni, **F. Chiara**, J. Zetterblad, N. Polisetti, K. Nihlberg, G. G. Consalez, M. Sigvardsson. "Prospective isolation and characterization of highly purified mesenchymal stem cells in mouse bone marrow based on expression of Ebf2." **Blood**. (Submitted)

Hernández-Miranda, L. R., J. G. Parnavelas, **F. Chiara** (2010). "Molecules and Mechanisms involved in the generation and migration of cortical interneurons." ASN Neuro 2:e00031. **PMID: 20360946**

TABLE OF CONTENTS

TABLE OF FIGURES

INDEX OF TABLES

ABBREVIATIONS

α-Tub	Alpha-Tubulin
µm	Micrometer
µm	Micromolar
ACSF	Artificial cerebrospinal fluid
AEP	Eteropeduncolar area
Am	Amygdala
ApoE	ApolipoproteinE
BAC	Bacterial artificial chromosome
β-Gal	beta-Galactosidase
BMP	Bone morphogenetic protein
BNST	Bed nucleus stria terminalis
bp	Base pair
Cc	Corpus callosum
Calb	Calbindin
Calr	Calretinin
Cb	Cerebellum
cDNA	Complementary-Deoxyribonucleic acid
CGE	Caudal ganglionic eminence
CH	Cortical hem
CNS	Central nervous system
CO	Cytochrome oxidase
COE	Collier Olf Ebf
CoP	Comminsural plate
COUP-TF	Chicken ovalbumin upstream promoter-transcription factor

CP	Cortical plate
CR	Cajal-Retzius
Ctip	COUP-TF interacting protein
Cux	Cut homeobox gene
d	Dorsal
Dab1	Disabled 1 gene
DAPI	4',6-Diamidino-2-Phenylindole
DBD	DNA binding domain
Dbx1	Developing brain homeobox gene 1
Dlx	Distalless gene
DMEM	Dulbecco modified eagle's medium
DNA	Deoxyribonucleic acid
DTB	Diencephalic-telencephalic boundary
E	Embryonic day
Ebf	Early B-cell factor
EGF	Epidermal growth factor
Emx	Empty spiracles gene
Ep	Electroporated
Er81	Ets domain transcription factor
Et	Epithalamus
F	Forebrain
FBS	Fetal bovine serum
FGF	Fibroblast growth factor
Foxg1	Forkhead box G1
FSH	Follicle stimulating hormone
gm	Grams
GABA	γ-Aminobutyric acid
GE	Ganglionic eminence
GFP	Green fluorescent protein
Gli	Glioma associated gene
GnRH	Gonadotropin-releasing hormone
Gp	Globus pallidus
Gsh	Glutathione sinthetase gene
H	Hippocampus

h	Hour
HB	Hindbrain
HLH	Helix loop helix
HOM	Homology
Hox	Homeobox gene
Hy	Hypothalamus
ICD	Intracellular domain
Ig	Immunoglobulin
IGF	Insulin like growth factor
IPT/TIG	Immunoglobulin-like fold in plexins transcription factor/Transcription factor immunoglobulin
IZ	Intermediate zone
kDa	kilo Dalton
LacZ	Lactose Z
LGE	Lateral ganglionic eminence
LH	Luteinizing hormone
Lhx	LIM-homeobox gene
LV	Lateral ventricle
Mm	Millimetres
Mm	Millimolar
M	Molar
Mash	Mammalian achaete-scute homolog gene
MB	Midbrain
MGE	Medial ganglionic eminence
Min	Minutes
mRNA	messanger Ribonucleic acid
mTOR	Mammalian target of rapamycin
MZ	Marginal zone
NCx	Neocortex
N-Ep	Non-electroporated
NFAT	Mouse fat orthologue
NF-kB	Nucleofactor-kB
Ngn	Neurogenin
Nkx	Homeobox protein

Nurr1	Nuclear receptor related 1 protein
OB	Olfactory bulb
OE	Olfactory epithelium
Opg	Osteoprotegerin
P	Postnatal
P<	Probability
p21	Cyclin-dependant kinase inhibitor 1
p73	Tumor protein 73
PA	Polyadenylation
Pax6	Paired box gene 6
PBS	Phosphate buffered saline
PCR	Polymerase chain reaction
PCx	Pyriform cortex
PFA	Paraformaldehyde
PI3K	Phosphatidylinositol 3-kinases
PNS	Peripheral nervous system
POA	Preoptic area
PPL	Preplate
PSPB	Pallial subpallial boundary
Pv	Paravalbumin
Reln	Reelin gene
RNA	Ribonucleic acid
ROAZ	Rat O/E-1-associated zinc finger protein
RT	Room temperature
SDF	Stromal derived factor
Sec	Seconds
SEM	Standard error of the mean
shEbf	Short hairpin ebf
Shh	Sonic hedgehog
shMock	Short hairpin scrambled Ebf
SP	Subplate
Sp	Septum
Sp8	Zinc finger transcription factor
St	Striatum

SVZ	Subventricular zone
Tbr	T-Box brain gene
TCA	Thalamo-cortical axon
TE	Thalamic eminences
TGF	Transforming growth factor
Th	Thalamus
v	Ventral
Vax	Ventral anterior homeobox containing gene
Vldlr	Very low density lipoprotein receptor
VZ	Ventricular zone
WNT	Wingless gene
wt	Wild type
Zi	Zona incerta
Zic	Zinc finger transcription factor

Above all do not fear difficult moments, the best comes from them.
(Rita Levi Montalcini)

CHAPTER 1

STRUCTURE AND GENETIC REGULATION OF THE DEVELOPMENT OF THE CEREBRAL CORTEX

The nature, structure, and regulation of genes have been a central topic of interest for more than 100 years. However, early theories of heredity, even without any scientific support, can be found as early as in Greek philosophers', such as Hippocrates and Aristotle, doctrines. Aristotle's major biological works formulated in *On the Generation of Animals* raises the fundamental questions about reproduction, development, and heredity. In attempting to explain how animals produce offspring like themselves, Aristotle examined two major models of development known as preformation and epigenesis. Preformationist theories hold that a miniature individual pre-exists in either the egg or the semen and begins to grow into its adult form when properly stimulated. The theory of epigenesis, which Aristotle favoured, asserts that the new organism is gradually produced from an undifferentiated mass by the addition of parts. Artistotle's theories formed the core of biological thought for hundreds of years.

The history of modern genetics is generally thought to have started with the work of the Augustinian friar, Gregor Mendel. It was his work on pea plants, published in 1866, that described for the first time what is now widely known as the Mendelian inheritance theory. Wilhelm Johannsen, however, only coined the name "gene" in 1909. Later, the work on *Drosophila* of Thomas Hunt Morgan and his colleagues established that genes were located on chromosomes and, in 1940; Oswald Avery demonstrated that genes were composed of deoxyribonucleic acid (DNA). It was only the discovery of the structure of DNA in 1953 by James Watson and Francis

Crick that set the beginning for years of research into gene function. Moreover, the generation of the first knockout mouse by Mario Capecchi, Martin Evans and Oliver Smithies, awarded the Nobel Prize in Medicine in 1989, and the various genome sequencing projects, made possible to study the effects of loss of genes and gain of function. This allowed medical and biological research to understand how genes influence the development and functions of different organs in model animals as well as in humans. Moreover, mutations of different genes have been now linked with different diseases.

So far, many genes have been identified and studied for their roles in brain development, which is one of the most complex and finely regulated organs in the human body. However, the nature of thousands of genes expressed in the nervous system is still poorly understood prompting the efforts of many scientists to keep researching for new discoveries (Mayr, 1984).

1.1. ADULT CEREBRAL CORTEX STRUCTURE

The cerebral cortex is the most elaborate structure of the mammalian brain, and is related to the achievement of complex brain functions such as motor and sensory processing, and cognitive capabilities. Proper assembly of the cortex requires precise gene expression patterns and regulation of neuronal migration during its development. Disruptions of these processes lead to abnormalities that can result in severe neurological diseases.

1.1.1 Organization of the adult cortex

Phylogenetically, the cerebral cortex is subdivided in allocortex (evolutionary older region) and neocortex (or isocortex, evolutionary younger region). The allocortex is further subdivided in paleocortex and archicortex. The paleocortex gives rise to olfactory regions whereas the archicortex contains the hippocampus (Gotz, 2001).

Mainly two types of neurons populate the adult cerebral neocortex: projection neurons, also called pyramidal cells, and interneurons. These cells are organised into six different layers consecutively arranged from the pial surface to the subcortical white matter (Kandel, 2000): I - molecular layer; II - external granular layer; III – external pyramidal layer; IV - internal granular layer; V - internal pyramidal layer; VI - multiform or fusiform layer (Figure 1.1).

Figure 1.1 Layer organisation in the adult cerebral cortex

Roman numbers from I to VI indicate the different cortical layers.

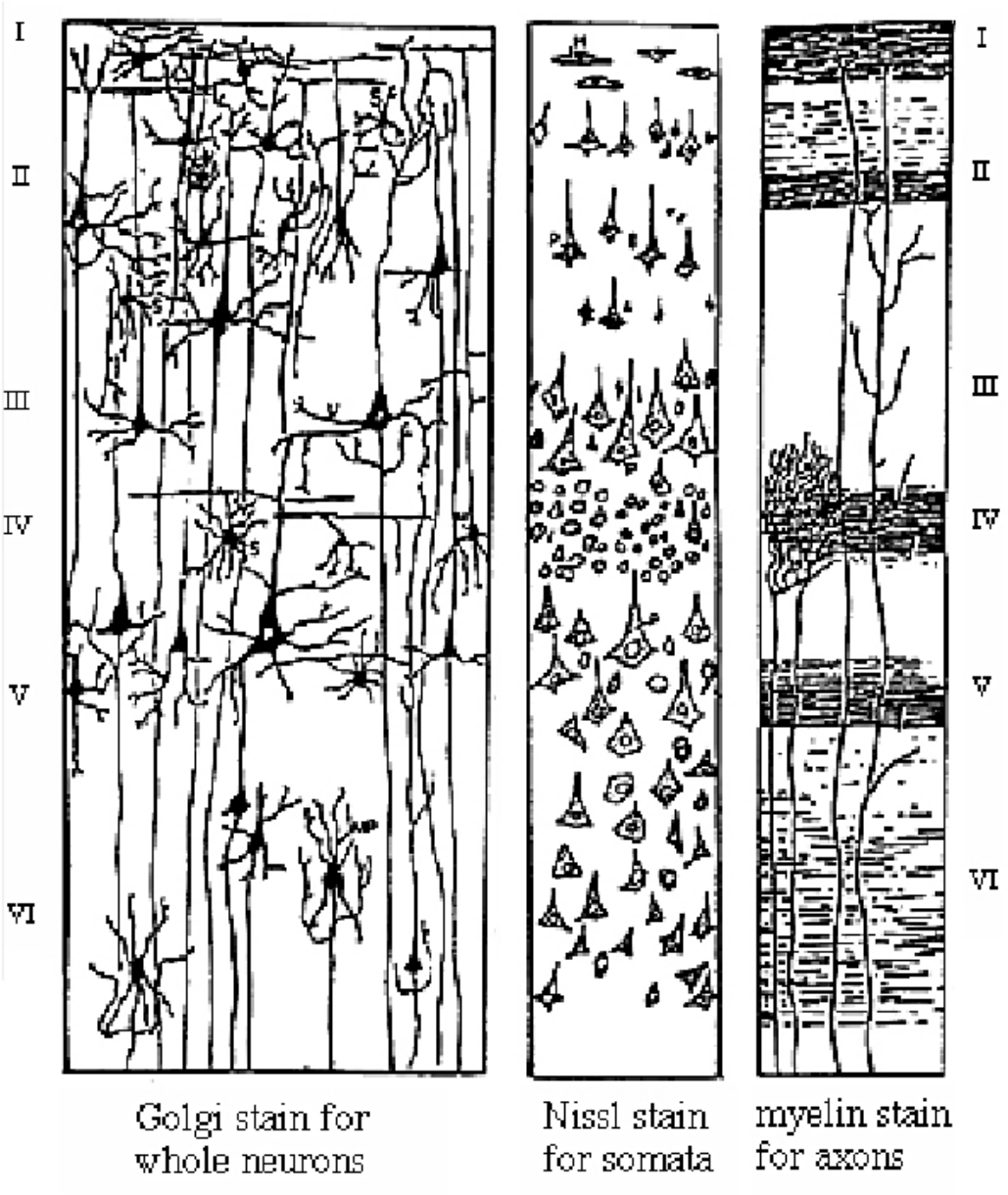

(Modified from 'The human body', 2nd Ed Mosby, 1988)

1.1.2 Neuron populations

Projection cells, called pyramidal neurons after their soma shape, are the most abundant population in the neocortex. Morphologically, they have a long apical dendrite that ascends vertically to reach the cortical surface and basal dendrites that are directed horizontally. Dendrites bear spines that are the sites of synaptic contacts. Pyramidal cells project a long axon towards different territories and, as such, they are the main output neurons of the cortex. They use the excitatory amino acid glutamate as neurotransmitter (Kandel, 2000).

Interneurons or local circuit neurons are inhibitory in function; they use the neurotransmitter γ-amino-butyric acid (GABA). Interneurons represent approximately the 25% of the cortical neuronal population, and they are distributed in all six layers. Several types of interneurons have been described based on their pattern of connections and morphological appearance. It is possible to distinguish basket cells, chandelier cells, bipolar cells and stellate cells. Moreover, interneurons express different calcium binding proteins such as Calbindin (Calb), Calretinin (Calr) and Paravalbumin (Pv), as well as neuropeptides and enzymes. Interneurons make synapses with other interneurons and pyramidal cells, but their axons are distributed entirely within the cortex (Kandel, 2000).

1.1.3 Connections

Cortical afferents that arise from the thalamus, called thalamocortical axons, reach mainly layer IV as well as layers I, III and VI. Afferents from cortical neurons of the same or opposite hemisphere contact, instead, layers II and III. There are three different types of cortical efferents or corticofugal projections: corticothalamic fibers that reach the thalamus from layer VI, corticocortical from layers II and III and corticosubcortical from layer V. Corticocortical efferents are subdivided into controlateral fibers, which connect neurons in the two hemispheres (also called commissural fibers), and ipsilateral fibers, which connect areas in the same hemisphere. Corticosubcortical efferents connect the neocortex with the striatum,

superior collicus, pons and spinal cord (later known as corticospinal or pyramidal tract (Kandel, 2000).

1.2 DEVELOPMENT OF THE EMBRYONIC CEREBRAL CORTEX

The cerebral cortex is a very complex structure, composed by different areas, which have specialised functions such as sensory processing and motor control. The areal identity seems to be determined by mechanisms suggested by two hypotheses. On one hand, the protomap hypothesis (Rakic, 1988) is in favour of a genetic specification of cortical neurons in the proliferative zone at the time of birth. According to this model, the early neuroepithelium is programmed to generate specific cohorts of neurons in different cortical regions, and the relative positions and sizes of cortical areas are so pre-specified. In contrast, the protocortex model (O'Leary, 1989) supports the role of thalamo-cortical connections in specifying functional areas of the cortex (O'Leary *et al.* 1994).

1.2.1 Regional organization

In mammals, the central nervous system (CNS) arises from the neural plate. During neurulation, the neural plate folds to form the neural tube, which will differentiate into brain and spinal cord. At embryonic day 9.5 (E9.5) in the mouse, the anterior end of the neural tube expands unequally producing a series of swellings that will form the forebrain (prosencephalon), the midbrain (mesencephalon) and the hindbrain (rhombencephalon) regions. The forebrain contains the telencephalon and the diencephalon. The telencephalon is subdivided into a dorsal domain called the pallium and a ventral domain called the subpallium. The two primary structures of the pallium are the cerebral cortex and the hippocampus. The main subpallial structures are the basal ganglia and the entopeduncular/preoptic area (AEP/POA). The basal ganglia arise from two bulges surrounding the later ventricles, the medial ganglionic eminence (MGE or globus pallidus primordium) and the lateral ganglionic eminence (LGE or striatum primordium). A third eminence, called the

caudal ganglionic eminence (CGE), is thought to give rise to the amygdala (Gotz, 2001) (Figure 1.2).

Figure 1.2 Anatomical organization of the developing forebrain.

***A*:** Schema of a sagittal section through the brain of an E12.5 mouse showing forebrain, diencephalon and telencephalon. The pallium is in light grey colour.
B: Schema of a transverse section through the telencephalon of an E12.5 mouse indicating its main subdivisions.

MGE: medial ganglionic eminence, LGE: lateral ganglionic eminence, POA: anterior preoptic area.

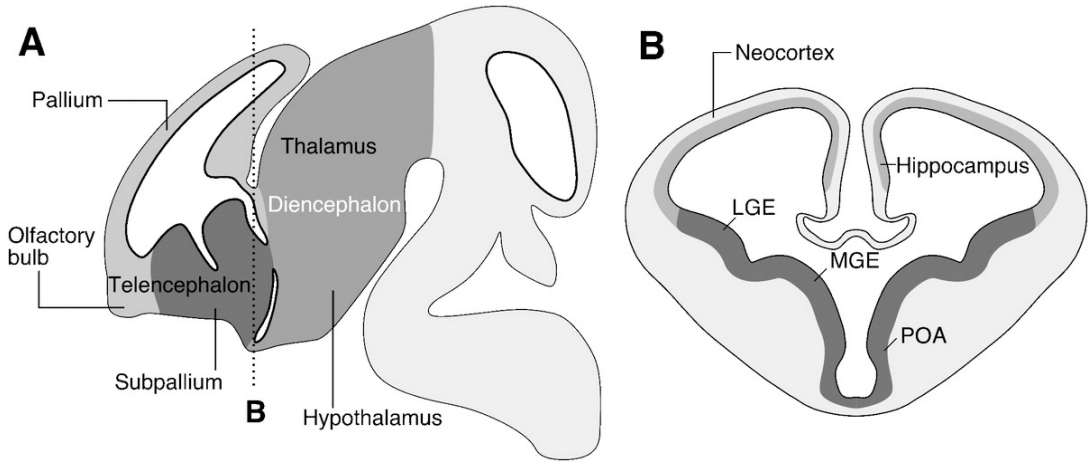

(Modified from Marin *et al.* 2003)

1.2.2 Laminar organization

Cortical neurogenesis is characterised by generation of post-mitotic neurons that arise from the ventricular surface and settle beneath the pial surface. This event transforms the neuroepithelium in a layered structure composed at the beginning by the ventricular zone (VZ) and the preplate (PPL), which contains the first generated neurons. At E13.5, the PPL splits in two parts due to the arrival of the cortical plate (CP), the marginal zone (MZ) and the subplate (SP) (Marin-Padilla, 1978; 1988). The MZ, which will became layer I, is populated by Cajal Retzius (CR) cells and interneurons. The CP is populated by pyramidal cells, whereas the SP by subplate cells and interneurons. Birth-dating experiments have demonstrated that layers in the CP are formed in an "inside-out" manner. This means that layer VI neurons are born before those in layer V, and the last neurons to be generated are in layers II and III. Thus, later generated neurons migrate through the entire CP to reach and to settle at its surface (Gotz, 2001). A secondary germinal zone, called subventricular zone (SVZ), forms superficial to the VZ around E15.5. The intermediate zone (IZ), prospective white matter, appears early (E13.5), and contains fibers and migrating neurons. Neurogenesis of the neocortex is completed before birth in rodents. However, in the dentate gyrus (part of the hippocampus) and in the anterior SVZ, neurogenesis continues throughout life (Rakic, 1988; Gotz, 2001) (Figure 1.3).

Figure 1.3 Cortical layer development

The development of the cerebral cortex is shown at different embryonic stages.

CP: cortical plate, IZ: intermediate zone, MZ: marginal zone, PPL: preplate, SP: subplate, SVZ: subventricular zone, VZ: ventricular zone.

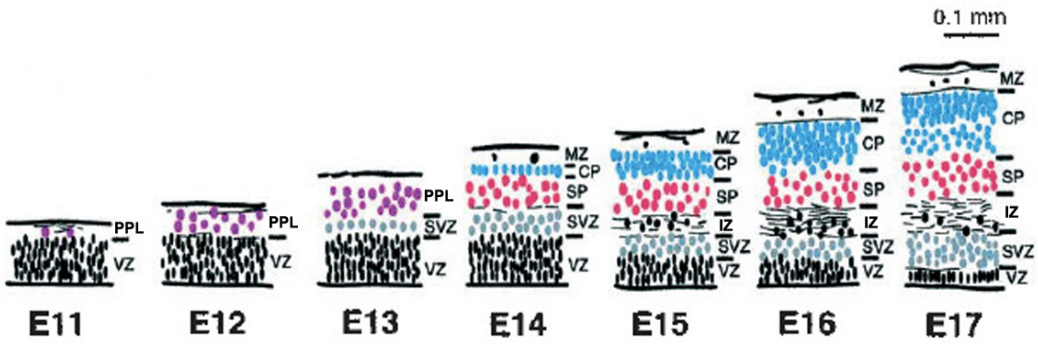

(Modified from Molnar *et al.* 2006)

1.2.3 Formation of cortico-thalamic connections and the function of subplate cells

The pathfinding of thalamic axons towards the isocortex involves several phases. Thalamic axons first grow towards the cortex through the internal capsule, part of basal ganglia, and after their arrival in the cortex they extend tangentially along the IZ without entering the CP. This mechanism is regulated by the presence of growth promoting molecules, such as fibronectin, tenascin and proteoglycans, in the IZ and in the SP layer and of repulsive cues in the CP. This is necessary to avoid the arrival of thalamic axons in the cortex when the generation of their target cells in layer IV is not yet complete. In fact, prior to the establishment of neurons in layer IV, the thalamic fibers reside in the SP layer (Kanold *et al.* 2010; Wang *et al.* 2010).

Subplate neurons play a key role in early cortical development in coordinating reciprocal thalamocortical innervation. Subplate cells at early developmental stages are found in the PPL. Following the splitting of this layer, these cells are localised in the SP layer (Konig *et al.* 1981). Subplate cells acquire a neuronal phenotype early during embryonic development, even before CP neurons (Clancy *et al.* 2001; Arias *et al.* 2002), including the formation of synaptic inputs and the generation of action potentials. These cells project axons into the internal capsule where they serve an important role in innervating the thalamus and providing a scaffold for the innervation of the cortex by the thalamocortical axons (Kanold *et al.* 2003). It has been shown that if the SP cells are lesioned during development, thalamic axons fail to reach their correct cortical targets (McConnell *et al.* 1994), and cortical columnar organisation does not develop normally (Kanold *et al.* 2003).

After serving as transient innervation targets for thalamocortical axons, most of SP cells die, and layer IV neurons become innervated by thalamic axons. However, 10-20% of these cells survive, remaining at the bottom of layer VI and in the white matter in adult life.

1.3 GENE EXPRESSION SPECIFIES TELENCEPHALIC DEVELOPMENT

1.3.1 Patterning of the cerebral cortex at early developmental stages

The onset of neurogenesis coincides with the appearance of patterning centers positioned at the perimeters of the telencephalon that generate across the developing cortex the graded expression of various transcription factors (TF) (for example COUP-TFI, EMX2, PAX6 and *Sp8*) that promote area specification. The two major dorsal telencephalic patterning centers are: the commissural plate (CoP) at the anterior margin of the forebrain, which expresses several members of the fibroblast growth factor family (FGFs, in particular *Fgf8* and *Fgf17*), and the cortical hem (CH) at the posteromedial border, which expresses bone morphogenetic proteins (BMPs) and vertebrate orthologs of *Drosophila Wingless* (*Wnts*) genes (O'Leary *et al.* 2007). Moreover, two other additional patterning centers have been identified: the first, located in the ventral telencephalon, expresses *Sonic hedgehog (Shh*) and is implicated in the regional patterning of the diencephalon and, indirectly, in cortical arealisation (Grove *et al.* 1999). The second, the antihem, located in the lateral area of the GE, secretes the Wnt antagonist Secreted Frizzled Related Protein-2 (SFRP-2), FGF7, Epidermal Growth Factors (EGF) family members (such as *Neuregulins 1,2, 3*) and Transforming Growth Factor-α (TGF-α) (Assimacopoulos *et al.* 2003). The CH and antihem have been suggested to cooperate with the CoP to establish the anterior-posterior and medial-lateral axes of the developing cortex. For example, ectopic expression of FGFs and SHH inhibit the expression of BMPs and WNTs (Shimogori *et al.* 2004).

It has been shown that *Fgf8*, secreted by the CoP, promotes also the graded expression of *Chick Ovalbumin Upstream Transcription Factor I* (*COUP-TFI)* and *Empty Spiracles homeobox 2* gene (*Emx2)*. These factors are characterised by a low anterior and high posterior expression gradient. *In utero* electroporation experiments have shown that *Fgf8*, whose expression is initiated by *Hox* genes and maintained by *Shh* and zinc finger TF *Sp8* (related to *Buttonhead* gene in *Drosophila*), controls the formation of motor areas in the anterior part of the telencephalon (Fukuchi-Shimogori *et al.* 2001). It seems that *Emx2* is able to repress *Fgf8* by suppressing the

function of *Sp8* (Sahara *et al.* 2007). In fact, in the absence of *Emx2*, *Fgf8* shows extended expression to posterior domains (Rakic *et al.* 2009). Moreover, pallial neuroblasts in *Emx2* mutants are converted into subpallial neuroblasts, which accumulate in an aberrant structure resembling the basal ganglia (Muzio *et al.* 2002). Analysis of the cerebral cortex has detected the expression of EMX2 not only in the VZ but, interestingly, also in CR cells (Mallamaci *et al.* 1998). *Emx2* expression in the proliferative layer of the developing cerebral cortex and in the CR cells suggests a potential role for the gene in the control of neuronal proliferation, migration and differentiation processes.

Furthermore, *COUP-TFI* is also involved in the specification of posterior telencephalic area together with *Emx2*. In fact, *COUP-TFI* null mice show lack of somatosensory areas and posterior expansion of anterior frontal and motor domains (Zhou *et al.* 2001). On the other hand, the CH (called roof plate together with the choroid plexus) is specified by *LIM-homeodomain 5* gene (*Lhx5*). Loss of *Lhx5* expression leads to loss of choroid plexus, CH and a defective hippocampal formation (Sheng *et al.* 1997; Zhao *et al.* 1999). In contrast, the lack of *Lhx2*, which is expressed in the cortical VZ, allows the choroid plexus and CH to dramatically expand, whereas the neocortex is reduced in size (Bulchand *et al.* 2001). Moreover, in the absence of *Forkhead box G1 (Foxg1),* neocortical progenitors are not specified and progenitors of the hippocampus and CH, in particular the CR cell population, are expanded (Monuki *et al.* 2001).

Other regulatory genes are also involved in the specification of the cortical areas; among these *Paired box gene 6* (*Pax6)* plays multiple roles in the development of the cerebral cortex (Scardigli *et al.* 2003; Guillemot *et al.* 2006). Firstly, *Pax6* is involved in the dorso-ventral specification of telencephalic progenitors and its expression is opposite to *Emx2*. In the cortical primordium, the early expression of *Pax6* and the homeobox gene *Gsh2* outline the anlage of the pallium and subpallium, respectively, and cross-repressive interactions between these two genes establish the pallial–subpallial border (PSPB) (Toresson *et al.* 2000; Yun *et al.* 2001). Disruption of the PSPB in the *Pax6–Small eye* mutant, where *Pax6* is not expressed, leads to an expansion of subpallial markers such as *Dlx1*, *Dlx2*, *Gsh2*, *Mash1*, *Vax1* into the pallium (Corbin *et al.* 2000; Stoykova *et al.* 2000; Toresson *et al.* 2000; Kroll *et al.* 2005). In addition, to these intrinsic mechanisms involving gene regulation, extrinsic mechanisms have also been considered especially at later stages of telencephalic

development. In fact, it has been shown that thalamo-cortical axons (TCAs) may influence the specification of its different areas. However, further studies are required to clarify these mechanisms (O'Leary *et al.* 2007)(Figure 1.4).

Figure 1.4 Patterning centers and genes expressed in the developing forebrain.

A: Positions of the different patterning centers in the developing embryos. The table lists key molecules and their corresponding expression patterns.

B: Graded expression of *Emx2*, *Pax6*, *Coup-TFI*, and *Sp8* along the anterior-posterior and lateral-medial axes. *Emx2* is expressed in a high P-M to low A-L gradient. *Pax6* expression pattern is opposite to that of *Emx2*, with a high A-L to low P-M gradient. *Coup-TFI* has a high P-L to low A-M gradient. *Sp8* is expressed in a high A-M to low P-L gradient. While the expression of *Emx2*, *Pax6*, and *Coup-TFI* is sustained in the VZ, *Sp8* expression is quickly downregulated around the onset of cortical neurogenesis.

C: In the anterior signaling center, *Fgf8* establishes the low anterior-graded expression of the TFs *Emx2* and *COUP-TFI* by repression, and promotes the high anterior gradient of *Sp8* expression. *Fgf8* expression is also regulated positively by direct transcriptional activation by Sp8 and indirectly by *Emx2*, which represses the ability of Sp8 to directly induce Fgf8. Putative posterior signaling molecules *Bmps* and *Wnts*, expressed in the CH, positively regulates the high caudal gradient of *Emx2* expression.

D: Summary of all reports of loss-of-function or gain-of-function mouse mutant for TFs that regulate area patterning. Reducing *Emx2* levels in the cortex of the heterozygote mutant mice results in posterior shifts of areas, while overexpression of *Emx2* under the control of the *Nestin* promoter shifts areas anteriorly. The *small eye* mutant shows anterior area shifts and YAC transgenic mice of *Pax6* do not show area changes other than a slight, but significant, reduction in the size of S1 (asterisk). Loss of *COUP-TFI* in cortical progenitors transforms the fate of primary sensory areas into frontal/motor areas. The analysis of *Sp8* conditional knockout mice shows anterior shifts of gene markers.

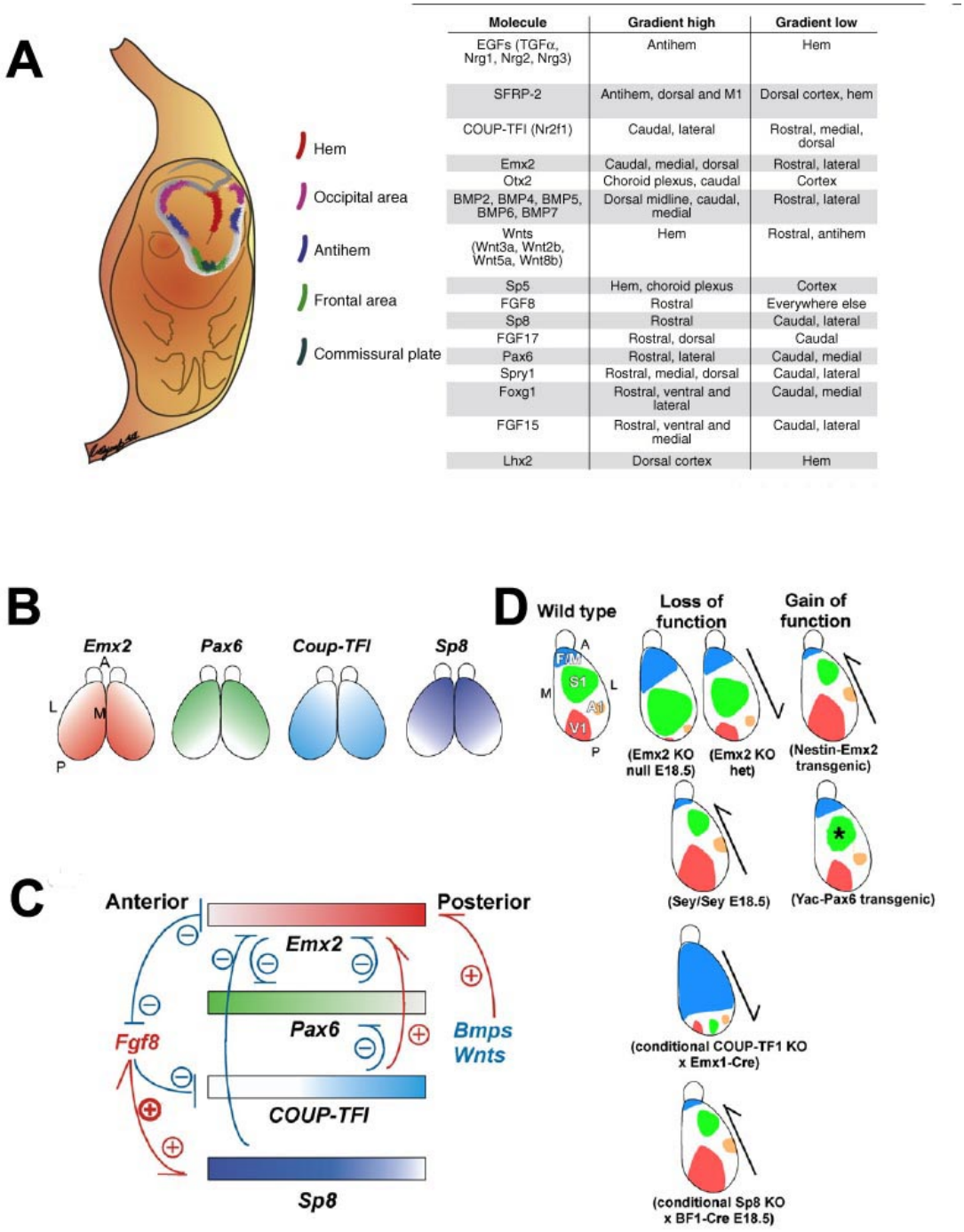

Molecule	Gradient high	Gradient low
EGFs (TGFα, Nrg1, Nrg2, Nrg3)	Antihem	Hem
SFRP-2	Antihem, dorsal and M1	Dorsal cortex, hem
COUP-TFI (Nr2f1)	Caudal, lateral	Rostral, medial, dorsal
Emx2	Caudal, medial, dorsal	Rostral, lateral
Otx2	Choroid plexus, caudal	Cortex
BMP2, BMP4, BMP5, BMP6, BMP7	Dorsal midline, caudal, medial	Rostral, lateral
Wnts (Wnt3a, Wnt2b, Wnt5a, Wnt8b)	Hem	Rostral, antihem
Sp5	Hem, choroid plexus	Cortex
FGF8	Rostral	Everywhere else
Sp8	Rostral	Caudal, lateral
FGF17	Rostral, dorsal	Caudal
Pax6	Rostral, lateral	Caudal, medial
Spry1	Rostral, medial, dorsal	Caudal, lateral
Foxg1	Rostral, ventral and lateral	Caudal, medial
FGF15	Rostral, ventral and medial	Caudal, lateral
Lhx2	Dorsal cortex	Hem

(A is modified from Rakic *et al.* 2009; B-D are modified from O'Leary *et al.* 2007)

1.3.2 Specification of pyramidal neurons

As neurogenesis begins, cortical neuroepithelial cells start to differentiate. Specific TFs are involved in maintaining the right equilibrium between proliferation and differentiation. The basic Helix-Loop-Helix (bHLH) molecules are among the TFs tightly involved in these processes. For example, the telencephalic proneural genes *Neurogenin1 (Ngn1)* and *Neurogenin2 (Ngn2)* (Fode *et al.* 2000; Nieto *et al.* 2001) regulate the key steps of commitment of stem cells to the neuronal fate, cell cycle exit and initiation of a neuronal differentiation program. Double mutants for *Ngn2* and *Mash1* show reduced cortical neurogenesis (Fode *et al.* 2000; Nieto *et al.* 2001). In wild-type mice, expression of *Ngn1* and *-2* in dorsal telencephalic progenitors, direct the differentiation of neurons towards a glutamatergic phenotype (Schuurmans *et al.* 2004). *Ngn1* and *2* mutant animals present defects in expression of laminar-specific markers in early-born neurons in layers VI and V, while late-born neurons in layers IV and II/III appear to be normal (Schuurmans *et al.* 2004).

Once cells are committed, additional TFs, such as *Tbr1, Ctip2* and *Cux1/2,* consolidate differentiation of the projection neuron phenotype and begin to specify projection neuron subtypes related to their laminar fate. In the developing cortex, *Cux1* and *Cux2*, two homologues of *Drosophila Cut* gene, are specifically expressed in the VZ and in mitotically active cells of the SVZ, respectively, whereas later on their expression is confined to distinct subpopulations of the upper cortical layers (Schuurmans *et al.* 2004; Zimmer *et al.* 2004). Interestingly, the expression of *Cux2* and *Cux1* in the upper cortical layers is severely diminished in the *Pax6*-mutant cortex, suggesting that these two genes might also act in the specification of the upper cortical layer neurons in a *Pax6*-dependent pathway (Schuurmans *et al.* 2004; Zimmer *et al.* 2004). *Tbr1* and *Ctip2* have been involved, instead, in the specification of neurons in lower layers (Molyneaux *et al.* 2007; Guillemot *et al.* 2006).

1.3.3 Specification of interneuron progenitors

The embryonic subpallium or ventral telencephalon contains amongst other structures the MGE, LGE, CGE and AEP/POA domains. These subpallial domains express specific genes, such as *Dlx1*, *Dlx2*, *Gsh1*, *Mash1*, *Gsh2*, *Nkx2.1*, *Nkx5.1*, *Isl1*, *Six3* and *Vax1* that define their identities and are involved in the specification of interneurons and oligodendrocytes (Marin *et al.* 2003). *Dlx* homeobox genes are transcription factors that act as critical molecular determinants in forebrain development (Panganiban *et al.* 2002). They are specifically required to co-ordinate the timing of GABAergic interneuron migration and neuronal process formation (Anderson *et al.* 1997; Yun *et al.* 2002). In double *Dlx1* and *Dlx2* null mutants, migration is almost abolished and cells accumulate in the GEs (Cobos *et al.* 2005; 2006; 2007). Ectopic expression of *Dlx* has been shown to induce GAD65/67 expression in neuronal progenitors of the cerebral cortex normally committed to a glutamatergic phenotype (Stuhmer *et al.* 2002). Interestingly, *Dlx1* single null mutants show no migrational defects. Recent studies suggest that DLX factors do not only have a role in migration, but also in morphogenesis of interneuron subtypes. Thus, abnormal dendritic morphology has been reported in subsets of somatostatin (SST) and Calr interneurons in *Dlx1* and *Dlx2* double-null mutants (Cobos *et al.* 2005). Another homeobox transcription factor, *Nkx2.1*, appears to play a pivotal role during the commitment of interneuron progenitors. In fact, *Nkx2.1* is fundamental for the correct MGE specification (Sussel *et al.* 1999), whereas LGE development is affected by the expression of *Gsh2* (Hsieh-Li *et al.* 1995). Expression of *Pax6* also distinguishes the LGE from the MGE and may contribute to the specification of the former. The AEP/POA territory, adjacent to the MGE, is also specified by *Nkx2.1* expression but, although the expression of common transcription factors indicates that MGE and AEP/POA may share some properties, progenitors arising from these structures appear molecularly distinct (Flames *et al.* 2007). These results suggest that the MGE and AEP/POA are anatomically defined sites characterised by distinct gene expression domains, *Gsh2* and *Lhx7* for the former and *Nkx5.1* for the latter. As such, they give rise to distinct populations of cortical interneurons (Xu *et al.* 2004; Butt *et al.* 2005).

Earlier *in vitro* and *in vivo* experiments on the origins of interneuron subtypes suggested that they arise from different subpallial progenitor pools (Fishell, 2007). More recent *in vitro* experiments have shown that expression of *Nkx2.1* in the MGE is required for the specification of MGE-derived interneurons. Upstream of *Nkx2.1*, the morphogen *Shh* appears to play a critical role in the establishment of *Nkx2.1* expression in the MGE (Sussel *et al.* 1999; Fuccillo *et al.* 2004) and in the maintenance of its expression during neurogenesis (Xu *et al.* 2005). Thus, mice carrying mutations in *Shh* expression within the neural tube fail to express the interneuron fate-determining gene *Nkx2.1* in the MGE. This effect was also reproduced by inhibiting SHH signalling in slice cultures (Gulacsi *et al.* 2006). Recent lineage experiments using the *Cre/loxP* system have shown that another member of the *Nkx* gene family, *Nkx5-1,* appears to specify a population of early post-mitotic AEP/POA cells towards interneuron fate (Gelman *et al.* 2009) (Figure 1.5).

Figure 1.5 Drawings of medial (A), caudal-intermediate (B) and caudal (C) coronal sections of E13.5 mouse brain showing the expression of different genes in the subpallial domain

Broken lines delineate the VZ. Sub-domains that express two or more genes are marked with stripes.

D: A summary of the expression of different genes in the LGE, MGE, CGE and POA.

++: High level of expression, +: lower level of expression, -: lack of expression.

CGE: caudal ganglionic eminence, Gp: globus pallidus, H: hippocampus, MGE: medial ganglionic eminence, NCx: neocortex, LGE: lateral ganglionic eminence, POA: preoptic area, St: striatum, Th: thalamus.

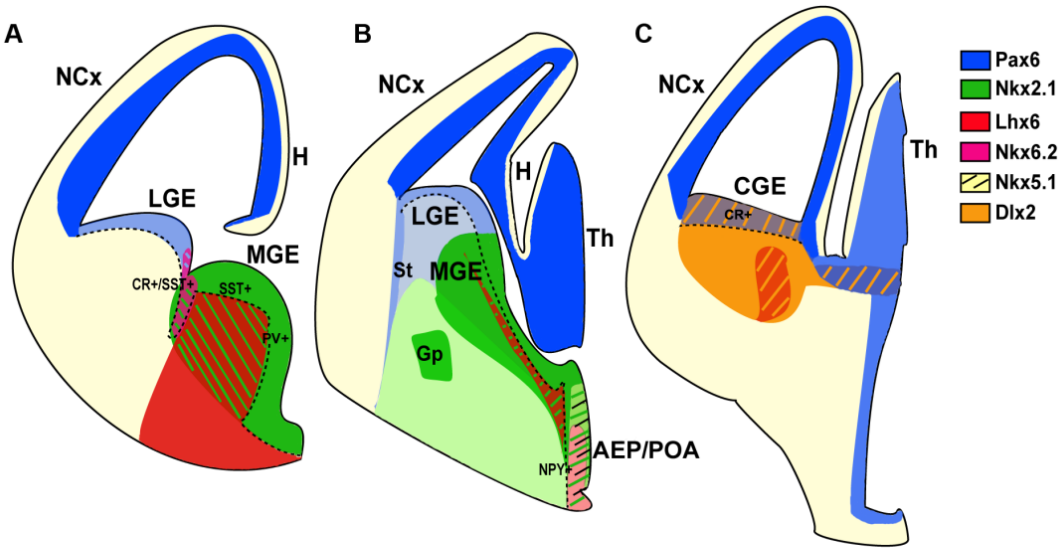

D

	LGE	MGE	CGE	POA
Dlx2	++	++	++	++
Gsh2	++	++	++	-
Couptf1	++	++	++	++
Lhx6	-	++	+	-
Lhx7	-	++	-	-
Nkx2.1	-	++	-	++
Nkx5.1	-	-	-	+
Nkx6.2	-	+	-	+
Olig2	+	++	+	+
Pax6	+	-	+	-

(F. Chiara from review Hernandez-Miranda *et al.* 2010)

1.4 MODES OF CELL MIGRATION IN THE EMBRYONIC CORTEX

Cell migration is a crucial process involved in the proper assembly of the cerebral cortex. Two major types of neuronal migration have been implicated in corticogenesis: radial migration of pyramidal neuron precursors and tangential migration of interneurons as well as of CR cells.

1.4.1 Radial migration of pyramidal cell precursors

Pyramidal cell progenitors, born in the pallial VZ/SVZ, migrate radially towards the CP and eventually form the cortical layers. The formation of the cortical lamination in an "inside–out" manner requires precise guidance of these neurons from the VZ to CP (Ayala *et al.* 2007). Generation of these cells occurs through a combination of three different modes of cell division: symmetrical division that expands the pool of neuronal progenitors, asymmetrical division that gives rise to a self-renewed progenitor and a neuron, and symmetrical terminal division that produces two neurons, thus depleting the pool of proliferating cells (Mione *et al.* 1997). Retroviral labeling techniques and time-lapse experiments have shown that radial glia cells mainly populate the VZ. These cells predominantly undergo asymmetrical division giving rise to a self-renewed radial glia cell and a daughter cell, which migrates away from the ventricle. A small percentage of asymmetric divisions produce a self-renewed radial glia cell and an intermediate progenitor cell that undergoes symmetrical division in the SVZ to produce upper cortical layer neurons (Noctor *et al.* 2004). The process of migration progresses through different phases. Firstly, the newborn neuron assumes a bipolar shape and migrates in the SVZ where it acquires a multipolar shape. Subsequently, the neuron contacts the ventricle through a leading process and migrates retrogradely. Finally, after contacting the ventricle, it acquires a bipolar morphology and migrates towards the CP (Noctor *et al.* 2004). Radial glia cells born in the VZ at early stages during development mostly guide radial migration of pyramidal cells. Structurally, each cell has its body in the VZ and a long process that reach the pial surface. Radial glia cells have two main

functions during embryonic development: they are a source of neuronal precursors and also provide a scaffold for their radial migration (Parnavelas *et al.* 2001). After birth, radial glia cells differentiate into astrocytes. Molecular abnormalities that affect radial glia development can also cause defects in neuronal progenitor migration (Hatten 1999; Marin *et al.* 2003). Two major modes of radial neuronal migration have been identified in the cortex: somal translocation and glia-guided locomotion (Nadarajah *et al.* 2001; Borrell *et al.* 2006; Rakic *et al.* 2007). During early corticogenesis, somal translocation is the predominant mode and some neurons appear to migrate solely by this mode. At later stages, locomotion becomes more common, but these neurons switch to somal translocation when their leading processes reach the pial surface. The cells that undergo somal translocation typically have a long, radially oriented basal process that terminates at the pial surface, and a short, transient trailing process. By contrast, cells that adopt glia-guided locomotion have a shorter radial process that is not attached to the pial surface and require a continuous formation and breakage of adhesive interactions with the radial glia. Integrins, a family of cell adhesion receptors mediating cell–extracellular matrix and cell–cell interactions, were long speculated to play a role in this process (Anton *et al.* 1999; Schmid *et al.* 2004). Two main cellular events take place during neuronal locomotion: growth of the leading process and movement of the cell body and nucleus (nucleokinesis) (Tsai, *et al.* 2005).

1.4.2 Tangential migration of interneurons

Unlike projection neurons, the vast majority of GABA-ergic interneurons are first born in the subpallial VZ and migrate tangentially towards the cortex. This migration pattern by interneurons was originally established based on dye labelling of migrating cells as well as analysis of *Dlx1/2* double mutant mice (De Carlos *et al.* 1996; Anderson *et al.* 1997). The main source of cortical interneurons is the MGE. The LGE and the CGE also contribute in a small part (Marin *et al.* 2003; Metin *et al.* 2006). Interneurons are guided from the ventral to the dorsal telencephalon by a combination of chemorepulsive (SLIT1 and semaphorins) and chemoattractive (neuregulin, SDF-1) factors. Tangential migration is independent of interactions with radial glia. Initially, interneurons enter in the developing cortex in defined streams at

the level of the PPL and IZ and, after the splitting of the PPL, through the MZ, SP and SVZ. It seems that, once interneurons reach areas where they will reside, they start to migrate radially, inward and outward, in the direction of the CP. Recent studies using time-lapse imaging and tracer-labelling techniques have also shown that interneurons, after reaching the developing cortex, migrate in the direction of the cortical VZ. This ventricle-directed morphological feature suggests the hypothesis that interneurons actively seek the cortical VZ to receive layer information that is essential for their correct positioning into the developing cortex (Nadarajah *et al.* 2002). Finally, cortical interneurons position themselves in layers in an "inside-out" manner, together with pyramidal cells born at the same time. This suggests that projection neuron lamination and interneuron positioning are tightly coordinated. Indeed, in *reeler* cortex, interneurons have been found to adopt a similar inverted pattern of laminar positioning as projection neurons despite their independence of Reelin signalling (Pla *et al.* 2006). Recent studies found that the chemokine Cxcl12, also known as Stromal Cell Derived Factor-1 (SDF-1), plays a key role in this process (Lopez-Bendito *et al.* 2008). Cxcl12 is highly expressed along the streams of migrating interneurons in the MZ and SVZ, whereas its receptor Cxcr4 is expressed in interneurons. The specific migration patterns shown by different neuronal types in the developing cortex suggest that the genetic program regulating cell migration is part of neuronal cell fate specification.

1.5 CAJAL-RETZIUS CELLS

Cajal–Retzius cells are a transient population that cover, like a sheet, the entire cortex early during development (Ramón y Cajal, 1911; Retzius, 1894; Soriano *et al.* 2005). Cajal–Retzius cells, which are found in the PPL and subsequently in the MZ, display characteristic radial ascending processes that contact the pial surface, and a horizontal axon located in the deep MZ. These cells secrete Reelin, a molecule important for the correct formation of the cortical lamination (Soriano *et al.* 2005). In the dentate gyrus, Reelin expression by CR cells provides positional cues for organising granule cell lamination (Zhao *et al.* 2004). Transplantation of embryonic CR cells into the adult cerebellum also induces a transient rejuvenation of host Bergmann glia (Soriano *et al.* 1997). Moreover, ectopically positioned CR cells can reverse the direction of granule cell migration in cerebellar slices (Soriano *et al.* 1997). Lastly, loss of function studies suggest that lack of the transcription factor *Foxg1*, which acts as a positive regulator of neuron proliferation and repressor of cell cycle exit in the pallial VZ, leads to abnormal differentiation of early-born cortical progenitors that adopt CR cell fate (Hanashima *et al.* 2004). This consequently causes an increased production of Reelin that alters the expression of a HLH transcription factor called *Early B-cell factor 2* (*Ebf2)*. The same effect (hyperproduction of CR cells and Reelin) has been observed in *Glioma-associated gene 3* (*Gli3)* mutants (Hanashima *et al.* 2007).

1.5.1 Origin, migration, functions and postnatal fate of CR cells

More than a century after their discovery, CR neurons are still surrounded by controversy. Firstly, the origin of these cells has been elusive for a long time, but recent lineage tracing experiments have finally begun to clarify it. Cajal-Retzius neurons are amongst the earliest born cells in the neocortex, starting around E10–12 in the mouse (Hevner *et al.* 2003). Electroporation experiments suggest that the vast majority of CR neurons are most likely generated in three locations: the CH (Takiguchi-Hayashi *et al.* 2004; Garcia-Moreno *et al.* 2007), the septum and the

ventral pallium (Bielle *et al.* 2005). In fact, fate mapping experiments using a *Wnt3a-Cre* line to trace cells derived from the CH, confirmed that this structure gives rise to the vast majority of CR cells (Yoshida *et al.* 2006). Interestingly, ablation of the CH did not result in major perturbation of cortical layer formation (Yoshida *et al.* 2006). Further experiments, using a *Dbx1-Cre* line, have identified two additional sources for CR cells outside the cortex, including the ventral pallium and septum (caudally identified as AEP/POA) (Bielle *et al.* 2005). Recently, thalamic eminence has also been proposed as a possible source of CR cells (Tissir *et al.* 2009; Abellan *et al.* 2010). After their birth, CR cells migrate tangentially to cover the entire cortical MZ. Cortical meninges have been found to act as substrate for CR cells as well as chemoattractant system during their migration. In fact, the chemokine Cxcl12 (or SDF-1) is expressed by the meninges and plays a role in attraction and dispersion of CR cells (Borrell *et al.* 2006). In addition, loss of Cxcr4, which is the receptor for Cxcl12, expressed by CR cells, results in failure of their migration. In fact, Paredes *et al.* (2006) found that, a disrupted meningeal basement membrane with loss of Cxcl12 expression, results in CR cell displacement.

A number of different TFs and nuclear proteins have been implicated in the control of CR cell differentiation, migration and survival. These TFs have also been used as markers of different CR cell populations: *Tbr1, Pax6, Emx1 and Emx2* (Mallamaci *et al.* 1998; Hevner *et al.* 2001; Muzio *et al.* 2003; Stoykova *et al.* 2003), *p73* (Meyer *et al.* 2002), *p21* (Siegenthaler *et al.* 2008), *Zic 1-3* (Inoue *et al.* 2008) specify septal and hem derived cells, *Er81* septal cells (Zimmer *et al.* 2010) and *Ebf2* the ventral pallium (Hanashima *et al.* 2007) (Figure 1.6 and Table 1.1).

The postnatal fate of CR neurons is another subject of debate. Cells with the typical CR morphology are difficult to find in the adult cortex. One theory is that they undergo a morphological changes in order to become resident interneurons in adult neocortex (Parnavelas *et al.* 1983; Sarnat *et al.* 2002). Others have proposed that the decrease in CR neuron density is caused by dilution following the expansion of the cortex during development, without any morphological transformation (Marin-Padilla, 1990). Recent experiments, using a *Ebf2-GFP* mice for *in vivo* two-photon imaging, have shown that the majority of CR neurons die by apoptosis during the second postnatal week and less than 3% of the population survive into adulthood (Chowdhury *et al.* 2010). So far, the best understood function of CR neurons is in cortical lamination. In fact, these cells secrete Reelin (Ogawa *et al.* 1995; Rice *et al.*

2001) to orchestrate neuronal migration in the typical "inside-out" pattern (Caviness, 1982). However, in the last decade, studies showing phenotypic variability (Radnikow *et al.* 2002; Soda *et al.* 2003) and multiple origins of CR neurons (Bielle *et al.* 2005; Garcia-Moreno *et al.* 2007) support the hypothesis that these cells could evolve to carry out different functions throughout cortical development. It is known that CR neurons are capable of firing action potentials (Radnikow *et al.* 2002; Soda *et al.* 2003) and are spontaneously active (Schwartz *et al.* 1998; Aguilo *et al.* 1999; Soda *et al.* 2003). Moreover, gap junctions exist between CR cells and pyramidal neurons (Radnikow *et al.* 2002) and these cells can fire synchronously (Soda *et al.* 2003). Lastly, Portera-Cailliau and colleagues have previously demonstrated that the axon tips of CR neurons have large growth cones that continue to grow during postnatal development (Portera-Cailliau *et al.* 2005). Together, these data suggest that CR neurons could influence network activity of pyramidal neurons.

Figure 1.6 Origins and migration of CR cells

A-C: Schematic figures showing rostral and medial coronal sections of E11.5 and E13.5 mouse brain. PSPB, Sp, AEP/POA and CH between E10-E11.5 give rise to different subpopulation of CR cells that eventually will cover the surface of the entire pallium. Recently, TE has also been proposed as possible source of CR cells. These cells migrate tangentially into the pallium and their process of migration is completed by E13.5/E14.5. Different sites of origin for CR cell populations are characterised by the expression of different genes (See Table 1.1).

AEP/POA: entopeduncolar area/preoptic area, CH: cortical hem, NCx: neocortex, PSPB: pallial subpallial boundary, PCx: pyriform cortex, Sp: septum, TE: thalamic eminences.

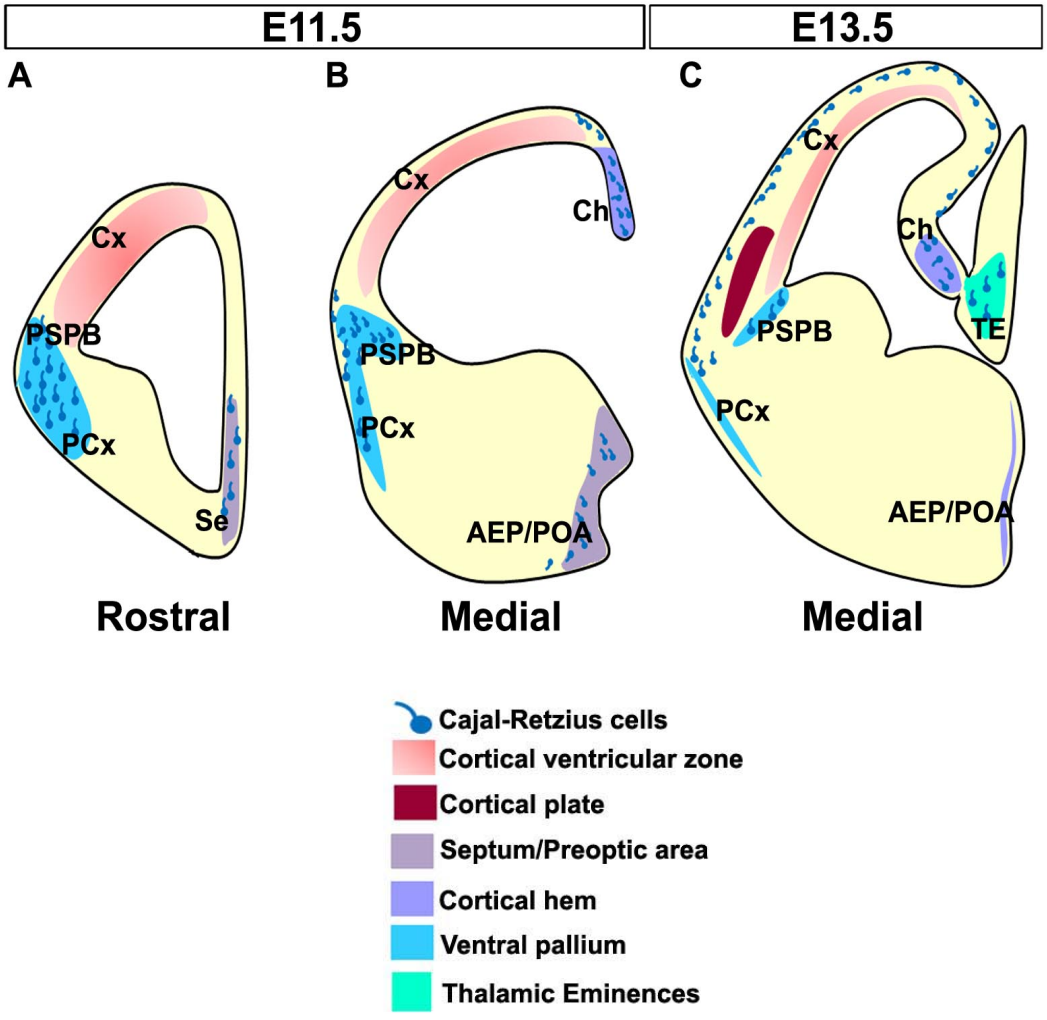
E11.5
E13.5
A
B
C
Cx
PSPB
PCx
Se
Ch
AEP/POA
TE
Rostral
Medial
Medial
Cajal-Retzius cells
Cortical ventricular zone
Cortical plate
Septum/Preoptic area
Cortical hem
Ventral pallium
Thalamic Eminences

Table 1.1 Gene expressions in the different site of origins of CR cells

Area	Gene expression
Cortical hem	*Tbr1, Pax6, Emx1, Emx2, p73, p21, Zic 1-3, Ebf2-3, Calretinin, Reelin, Lhx6, Wnt-3a*
PSPB (Ventral Pallium)	*Dbx1, Reelin, Calretinin*
AEP/POA	*Tbr1, Pax6, Emx1, Emx2, p73, p21, Zic 1-3, Ebf2-3, Reelin, Er81*
Septum	*Dbx1, p73, Ebf2, Ebf3, Reelin,*
TE	*Δnp73, Reelin, Ebf3*

1.5.2 Reelin

Reelin is a secreted extracellular matrix protein containing 3461 amino acids, encoded by the *Reln* gene (D'Arcangelo *et al.* 1995; Ogawa *et al.* 1995; Tissir *et al.* 2003). In *Reeler* mutants, a spontaneous mouse line carrying *Reln* mutation, the normal inside-out pattern of cortical formation is replaced by an inverted cortical lamination, where the PPL fails to split and neurons incorrectly position in the lower layers of the cortex (Caviness *et al.* 1973). Defects observed in mutant mice are more severe in the cerebral cortex, hippocampus and cerebellar cortex, but anomalies have also been found in other structures, such as the olfactory bulb and inferior olive. However, it is still poorly understood how *Reln* influences neuronal migration and proper lamination of the cortex. Reelin signal is received by migrating neurons by two redundant cell surface receptors, Very Low Density Lipoprotein Receptor (Vldlr) and Apolipoprotein E Receptor 2 (ApoER2), and double mutation of Vldlr and ApoER2 results in cortical lamination defects similar to *Reeler* mutants (D'Arcangelo *et al.* 1999; Hiesberger *et al.* 1999). Downstream of Vldlr and ApoER2, the adaptor protein Disabled-1 (Dab-1) is required for mediating Reelin signalling and *Dab-1* mutant mice also display *Reeler*-like cortical lamination phenotypes (Howell *et al.* 1997). Thus, Reelin signalling is essential for cortical neurons for proper radial neuron migration and cortical layer formation.

Recent analysis have shown that Vldlr and ApoER2 may play distinct roles in regulating cortical neuron migration: Vldlr may mediate a stop signal for migrating neurons, whereas ApoER2 may promote the migration of late born cortical neurons (Hack *et al.* 2007). Moreover, *Reln* has also been implicated in regulating neuronal dendrite and spine development (Niu *et al.* 2004; 2008). Interestingly, phosphatidylinositol 3-kinase (PI3K) signalling is required to mediate Reelin signaling downstream of Dab-1 in both neuronal migration and dendrite development, but neuronal migration is independent of mTOR (mammalian target of rapamycin) signalling which, in contrast, is required for *Reln* regulation of dendrite growth (Jossin *et al.* 2007).

An alternative mechanism of Reelin signaling has been recently shown by Rakic and colleagues who implicated Notch signaling in Reelin regulation of radial neuron migration (Hashimoto-Torii *et al.* 2008). These authors found that Notch

Intracellular Domain (ICD), the proteolytic fragment of Notch that translocates to the nucleus when Notch receptor is activated, is significantly reduced in the *Reeler* cortex. Indeed, simultaneous deletion of Notch 1 and 2 from migrating neurons results in a phenotype similar to that in *Reeler* cortex. Most importantly, overexpression of Notch ICD in cortical neurons of *Reeler* mouse mitigates their migration defects.

1.6 THE TRANSCRIPTION FACTOR FAMILY Collier/Olf/Ebf

One of the most important mechanisms to regulate cell-type function in somatic cells is the differential activation of tissue-specific genes. This is controlled by TF proteins that promote gene transcription by directly interacting with DNA. So far, many TF families have been characterized during cellular differentiation; one of these is the group of HLH proteins. The *Collier/Olfactory/Early-Bcell (COE)* TFs are a conserved family of HLH proteins present in vertebrate and invertebrate species. The first member of the COE family, *Ebf1/OE-1* (or the rat orthologue *Olf-1*), was isolated as a TF that specifically binds promoters of various olfactory genes and the *Mb-1* gene in developing B-lymphocytes (Hagman *et al.* 1995; Wang *et al.* 1997). Subsequently, additional members of the same family were isolated in mouse: *Ebf2/OE-3*, *Ebf3/OE-2* and *0/E*-4 (Garel *et al.* 1997; Malgaretti *et al.* 1997; Wang *et al.* 1997). Furthermore, EBF orthologues have been found in other organisms. In *C. elegans*, *Unc-3* determines the ventral nerves fasciculation (Prasad *et al.* 1998; Liberg *et al.* 2002). In *Drosophila*, mutations in the *Collier* gene, a member of the COE family, lead to wing, head and muscle defects (Crozatier *et al.* 1996). Finally, in *Xenopus Xebf2* and *Xebf3* are involved in neuronal cell differentiation (Pozzoli *et al.* 2001). The mouse EBF proteins show 75% identity. EBF1 and EBF3 are the most similar, whereas EBF2 differs at the carboxy-terminal domain used to interact with other proteins. In humans, four *Ebf* orthologous genes were discovered: *Ebf1-related* (chromosome 5), *Ebf2-related* (chromosome 8), *Ebf3-related* (chromosome 10) and *OE-4- related* (chromosome 20). Phylogenetic analysis has revealed that the exons-introns structure of *Ebfs* is conserved in different species (Crozatier *et al.* 1999; Dubois *et al.* 2001).

1.6.1 The structure of EBF proteins

The *COE* family contains several conserved regions. This indicates that the specific structure is of crucial importance for the correct function of EBF proteins. Firstly, these factors, through a histidine and cysteine-rich domain of 250 amino acids located in the amino-terminal region of the protein, bind the specific DNA sequence. The DNA binding occurs in the presence of Zn^{2+} ions that binds a zinc finger-like motif made up by three cysteines and one histidine. Moreover, this structure, which is required for the DNA binding process, is highly conserved in all the COE proteins (Crozatier *et al.* 1999).

Downstream of the DNA binding domain (DBD), there is a second conserved region with apparent similarity to an IPT/TIG (immunoglobulin-like, plexins, transcription factors/transcription factor immunoglobulin) domain also present in the DNA binding region of transcription factors such as *NFAT* and *NF-kB* (Aravind *et al.* 1999). The role of this region is unclear although it has been suggested to be involved in the interaction with the *Rat O/E-1 associated zinc finger* (*ROAZ*) (Tsai *et al.* 1997). Another possibility comes from the findings that IPT plexin-rich domains are involved in axonal guidance and semaphorin signaling, suggesting a role of the COE proteins in neuronal migration (Prasad *et al.* 1998; Yu *et al.* 1999; Tamagnone *et al.* 2004).

EBF1, EBF2, EBF3 and OE-4 bind DNA as homo- or heterodimers, and dimerisation is dependent on a region downstream of the DBD containing a HLH domain. The typical HLH contains two dissimilar amphipathic helices, helix 1 and helix 2, connected by a loop. EBFs do not contain any sequence corresponding to helix 1 but rather a duplication of helix 2 resulting in a domain that mediates dimerisation. The helix 2 duplication is only present in vertebrate EBFs and it can be deleted without affecting the capacity of the proteins to bind DNA (Wang *et al.* 2002).

EBF factors contain two transactivation domains, TSI located within the DBD and TSII in the C-terminal part of the protein with the ability to interact with other proteins. This region is poorly conserved amongst all the family members,

suggesting the potential of EBF proteins to interact with different factors and, as a result, play different roles during development (Hagman *et al.* 1995) (Figure 1.7).

Figure 1.7 COE proteins structure

A: Structure of mammalian EBFs.

Green- Transactivation domain I. This includes the DNA binding domain and the zinc finger domain. Orange- IPT/TIG domain. Red- Helix1. Blue- dupliacated Helix2.Yellow- Transactivation domain II.

B: Comparison between EBFs from different species. Mouse (mCOE), human (hCOE) and *Xenopus* EBF (*x*COE) show high sequence similarity. Members of other species, such as *Drosophila* (dCOE), Zebrafish (zCOE) and *C.elegans* (cCOE) present variation at the transactivation domain II.

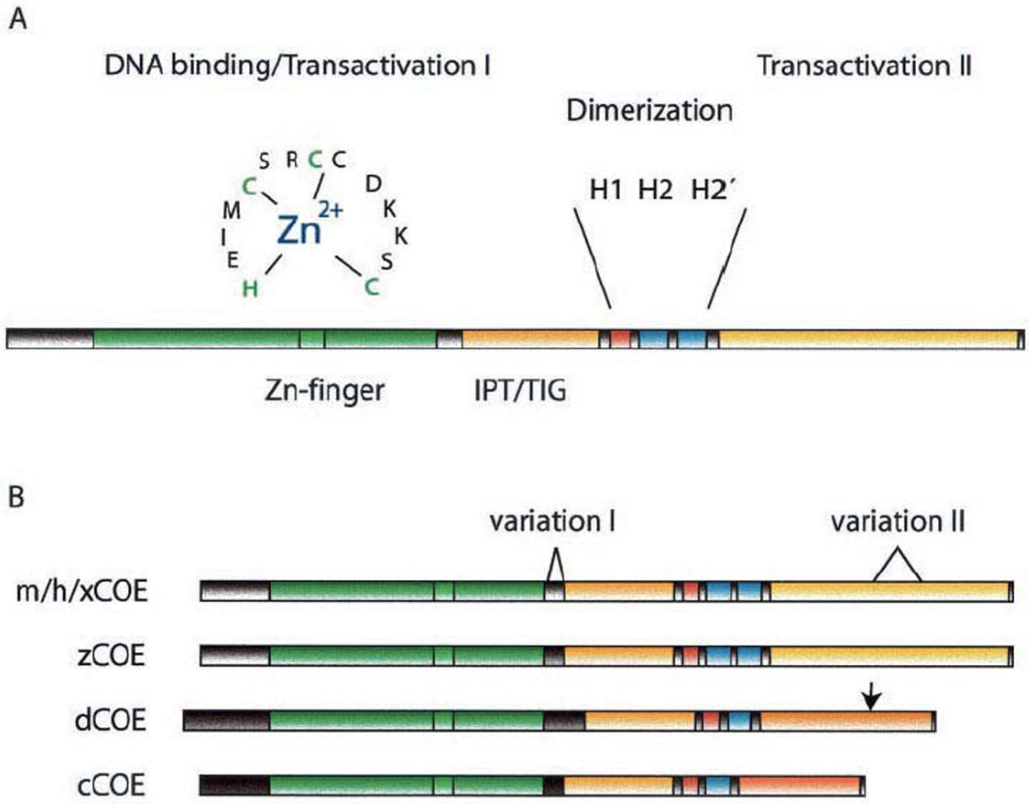

(Modified from Liberg *et al.* 2002)

1.6.2 The function of EBF proteins

COE proteins play important roles during embryonic development, in particular during neurogenesis in different model systems. The *Collier* gene in *Drosophila* is fundamental for head and trunk segmentation and in the formation of a specific embryonic somatic muscle (Crozatier *et al.* 1996; 1999).

COE proteins are also closely linked to *Notch* signalling during later inhibition events, which occurs during neuronal development. In *Xenopus*, *Notch* signalling suppresses neuronal differention downregulating the proneural gene bHLH *X-neurogenin-1*. *Xebf2* appears to act downstream of this protein, but upstream of the neurogenic *xNeuroD*, which seems to be activated by *Xebf2*. *Xebf2* is, therefore, involved in maintaining high neural potential of precursor cells, but at the same time in promoting the commitment into neuronal fate by the activation of *XneuroD*. Instead, *Xebf3* acts downstream of *XneuroD* stimulating the development of specific cell subtypes such as cranial sensory ganglia cells (Pozzoli *et al.* 2001). Furthermore, in *C. elegans,* the loss of expression of *Unc-3*, which is a member of the *COE* family, causes defects in specific motor neurons of the ventral nerve cord and in nerve fasciculation (Liberg *et al.* 2002).

In chick embryos, *Ebf* gene function is necessary to initiate neuronal differentiation and migration towards the mantle layer in neuroepithelial progenitors, but is not required for cell cycle exit (Garcia-Dominguez *et al.* 2003). *Ebf* genes, therefore, appear to control neuronal differentiation and migration, and may also play a role in cell commitment and specification. In mouse, *Ebf1*, *Ebf2* and *Ebf3* were originally studied for their expression in the olfactory epithelium, but they are also transiently expressed in postmitotic neurons during embryonic development in overlapping as well as in different territories (Garel *et al.* 1997; Malgaretti *et al.* 1997; Wang *et al.* 1997). *Ebf1* and *Ebf3*, which map on mouse chromosomes 11 and 7, respectively (Garel *et al.* 1997), are co-expressed at most sites in the mantle layer of the developing neural tube, whereas *Ebf2*, which maps on mouse chromosome 14, is expressed by postmitotic neural cells located in the subventricular layer of the spinal cord primordium (Garel *et al.* 1997; Malgaretti *et al.* 1997). In the developing nervous system, the functions of *Ebf1* and *Ebf3* appear to be redundant. The *Ebf1* null mouse was originally reported to develop normally due to the redundant function of

Ebf3. However, there are defects in the striatum and in the facial motor nucleus, where *Ebf1* is the only gene of the COE family to be expressed (Garel *et al.* 1997; 1999). Moreover, in *Ebf1* null animals a subset of thalamic axons does not reach the neocortex, and the projections that do form between thalamic nuclei and cortical domains have a shifted topography in the absence of regionalisation defects in thalamus or cortex (Garel *et al.* 1999; 2000).

There is evidence to suggest that COE proteins interact with *ROAZ* that is involved in bone morphogenetic signalling (BMP). *ROAZ*, acting together with *Smad*, activates *Xvent-2*. The impaired ability of *ROAZ* to stimulate *Xvent -2* in response to *BMP-2*, due to ectopic expression of COE, suggests that COE might be involved in modulation of BMP signaling during development (Hata *et al.* 2000). So far, target genes of EBFs have not yet been identified, but it has shown recently that IGF-1 (Insuline growth factor-1) may be a target candidate gene of *Ebf2* involved in Purkinje cell survival (Croci *et al.* 2011).

COE proteins are also expressed in the developing cerebellum. *Ebf1* and *Ebf3* are broadly expressed during embryonic development and postnatally in the Purkinje cells, whereas *Ebf2* is expressed in a specific subpopulation of postmitotic Purkinje cells (Corradi *et al.* 2003; Croci *et al.* 2006). Furthermore, studies have shown that *Ebfs* are transiently expressed in the cerebral cortex; specifically *Ebf2* and *Ebf3* have been found to be expressed in CR cells during corticogenesis (Yamazaki *et al.* 2004; Hanashima *et al.* 2007; Chowdhury *et al.* 2010). Outside the nervous system, EBFs are involved in the development of B-lymphocytes and in the genetic control of the adipogenic cascade (Sigvardsson *et al.* 2002; Jimenez *et al.* 2007) (Table 1.2).

Table 1.2 Expression roles and putative targets of the *COE* factors

(Dubois *et al.* 2001)

Species/gene name		Expression	Role
Rodent	***Ebf1/ Olf-1***	CNS and PNS: differentiating post-mitotic neurons	Differentiation of striatal neurons
			Control of fbm migration
		Olfactory neuron precursors and mature neurons	Cerebellum development
			Specification of B-cells
		Subventricular zone of laterl ganglionic eminence	(*Ebf1*$^{-/-}$ mouse available)
	Ebf2	Differentiating facial brachiomotor (fbm) neurons	Purkinje cells development in the cerebellum. Expressed in Cajal-Retzius cells in the cerebral cortex.
		Pro-B and pre-B lymphocytes	(*Ebf2*$^{-/-}$ mouse available)
		PNS, CNS subventricular zone of neural tube	
	Ebf3	Progenitors of fbm neurons	Expressed in Cajal-Retzius cells and Purkinje cells. (*Ebf3*$^{-/-}$ mouse is not available)
		Bones development and adipogenic cascade	
		CNS and PNS: differentiating post-mitotic neurons	
		Progenitors of fbm neurons	
Xenopus	***xEbf2***	Precursors of primary neurons	Commitment of primary neurons. (Notch signaling)
	xEbf3	Differentiating primary neurons	Differentiation of primary neurons (Notch signaling)
Drosophila	***Collier***	Embryonic head	Formation of head
		Progenitor and precursor cells of somatic muscle DA3	Muscle specification
		Central region of the wing disk	Patterning of the wing
C.elegans	***Unc-3***	Ventral motor neurons	Axonal pathfinding

1.6.3 *Ebf2*$^{-/-}$ mice

Ebf2 $^{-/-}$ mice were generated by target mutation within the insertion of a promoterless LacZ cDNA that replaced the translation initiation site and the first five exons of the gene. Although *Ebf2*$^{-/-}$ mice complete the embryonic development successfully, mutants show defects in different territories (Corradi *et al.* 2003). Firstly, in the CNS, the migration of gonadotropin-releasing hormone (GnRH) neurons from the vomeronasal organ to the hypothalamus is defective, although *Ebf1* is co-expressed with *Ebf2*. However, *Ebf2* is not required for the birth of these neurons. As a result, the formation of the neuroendocrine axis is impaired and homozygotes adult mice show hypogonadotropic hypogonadism characterised by testis hypoplasia in the absence of Leydig cell hyperplasia and sterility (Corradi *et al.* 2003). Moreover, *Ebf2*$^{-/-}$ mice are characterised by disruption of the cerebellar corticogenesis. In fact, the cerebellum is dramatically reduced in size with foliation defects, especially in the anterior vermis. *Ebf2*$^{-/-}$ mice show a typical ataxic gait closely associated with the abnormalities of the cerebellar development. During embryogenesis, *Ebf2* is strongly expressed in a postmitotic subpopulation of Purkinje cells, in domains that are also positive for *Ebf1* and *Ebf3*. The fact that the cerebellar cortex is malformed in the *Ebf2*$^{-/-}$ suggests that EBF2, despite the tight structural similarity to EBF1 and EBF3, may actually exert distinct functions in Purkinje cell development. The *Ebf2*$^{-/-}$ mutation does not affect cell proliferation or cell cycle exit, and the development of Bergmann glia cells appears normal. Conversely, the mutant cerebellum displays a clear defect in the migration of a subset of Purkinje cells. At birth, numerous delayed-migrating Purkinje cells accumulate in the proximity of the ventricular zone and subsequently die by apoptosis. Furthermore, *Ebf2* expression in the wild-type cerebellum is restricted to ZebrinII (ZII)-negative Purkinje cells, and in the *Ebf2*$^{-/-}$ cerebellum ZII-negative Purkinje cell stripes are selectively disrupted leading to strong changes in the cerebellar topography (Croci *et al.* 2006). In addition to defects in the CNS, *Ebf2*$^{-/-}$ mice feature glial and axonal defects in the sciatic nerve. These include incomplete axon sorting, which results in defective axonal fasciculation. In parallel, mutant nerves feature signs of segmental dysmyelination and hypomyelination (Corradi *et al.* 2003). *Ebf2*$^{+/-}$ animals are reported to develop

normally, suggesting that *Ebf2* function could be gene dosage dependent (Croci *et al.* 2006).

Finally, outside the nervous system, EBF2 is expressed in osteoblast progenitors as a regulator of osteoclastogenesis and bone homeostasis through the activation of *osteoprotegerin* (*OPG*). *Ebf2*$^{-/-}$ mice show reduced bone mass and an increase in the number of osteoclasts due to a downregulation of the expression of *OPG* (Kieslinger *et al.* 2005) (Figure 1.8).

Figure 1.8 β-Gal expression in *Ebf2*$^{-/-}$ mice

A- C: *Ebf2* expression in three mouse embryos at different developmental stages. *Ebf2* is strongly expressed in the telencephalon at E11.5, but its expression is subsequently downregulated in this region at E13.5 (black arrows) (Croci L., G. G. Consalez, unpublished).

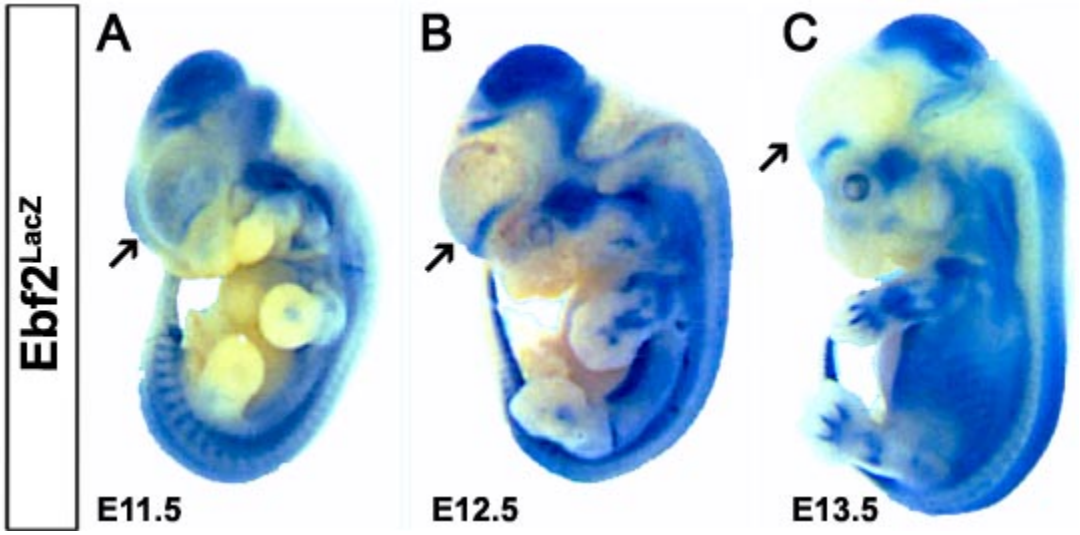
Ebf2LacZ
A
E11.5
B
E12.5
C
E13.5

1.7 AIMS

The regulated expression of specific genes is tightly associated with the correct development of different organs (e.g. brain) into the complex structure that characterise adult animals. Mutations that disrupt these mechanisms may lead to dramatic defects. In this work, I will analyse the role of a novel group of genes, called *Ebf*s, in telencephalic specification. So far, it is known that EBF factors play a pivotal role in various aspects of neuronal development. In particular, it has been found that *Ebf2* is involved in neuronal fate determination and migration. Absence of this factor leads to striking defects in mice, especially in the correct development of the cerebellar cortex. Studies on *Ebf2* have been focused on its characterisation in the midbrain and hindbrain, but the role *Ebf2* expression during forebrain development still needs to be clarified. In particular, recent studies have suggested a correlation between CR cells and *Ebf2* expression, but it is still unkown whether lack of expression of this gene could lead to severe defects in this specific cell population. Moreover, due to the high sequence similarity between the COE members, I will assess whether EBF2 function in the cerebral cortex could be influenced by other EBF proteins.

CHAPTER 2

MATERIALS AND METHODS

2.1 MATERIALS

2.1.1 Buffers

All solutions were prepared with reagents from Sigma-Aldrich Company Ltd (Dorset, England) unless otherwise stated.

Artificial Cerebrospinal Fluid (ACSF)

25 mM KCl, 2 mM KH_2PO_4 25 mM HEPES, 37 mM D-Glucose, 10 mM $MgSO_4$, 175 mM Sucrose, 0.5 mM $CaCl_2$ in double-distilled (dd)H_2O. Adjust pH to 7.4 with NaOH. Add penicillin/streptomycin (5000 units of Penicillin/5000 µg Streptomycin, Gibco-Invitrogen Ltd, Paisley, UK) and filter with 0.2 µm membrane (Millipore, Watford, UK)

In Situ Hybridisation Buffer

50% Formamide (Roche), 5X SSC, 1% SDS, 500 µg/ml tRNA (Roche-Applied Science, Newhaven, UK), 200 µg acetylatedBSA, 50 µg/ml Heparin

NTMT

100 mM NaCl, 100 mM Tris-HCl pH 9.5, 50 mM $MgCl_2$, 1% Tween20, 2 mM Levamisole in ddH_2O

1X Phosphate Buffered Saline (PBS)

2 mM KH_2PO_4, 8 mM Na_2HPO_4, 2.5 mM KCl, 140 mM NaCl, add ddH_2O and adjust
pH to 7.2-7.3. For PBST 0.2% of TritonX-100 was added

4% Paraformaldehyde (PFA)

4 % PFA, 1X PBS to volume, adjust to pH 7.4 by adding 10 M NaOH

Proteinase K (PK) Buffer for genotyping

50 mM Tris-HCl pH8, 100 mM EDTA pH8, 100 mM NaCl, 0.5% SDS(20%) in ddH_2O

Permeabilisation (P) Solution

10 g Sucrose, 1 ml 5 M NaCl, 300 µl 1 M $MgCl_2$, 2 ml 1 M Hepes pH 7.4, 2.5 ml 20% TritonX100

10X Running Buffer

250 mM Tris Base, 1.9 M Glycine, 10% Methanol, 1% SDS

Ripa Buffer

150 mM NaCl, 1% NP-40, 0.5% DOC (deoxycholic acid), 0.1% SDS, 50 mM Tris pH 8.0, ddH_2O to volume

20X Saline Sodium Citrate Buffer (SSC)

175.3 g di NaCl and 88.2 g di NaCitrate add ddH_2O to volume of 1 L

TE STOP Buffer

10 mM Tris-HCl pH7.5, 10 mM EDTA pH 8.0 and ddH_2O to volume

10X Transfer Buffer

250 mM Tris Base, 1.9 M Glycine, 10% Methanol

1X Tris Acetate Buffer (TAE)

0.4 M Tris pH8, 0.2 M Sodium Acetate, 20 mM EDTA pH8 in ddH_2O

10X Tris Buffered Saline (TBST)

100 mM Tris-HCl pH 7.5, 150 mM NaCl, 1% Tween-20 in ddH_2O. Working solution was diluted to 1X in ddH_2O

2.1.2 Cell Culture Buffers

Cell Line Culture (CLC) Medium

Dulbecco's Modified Eagle Medium (DMEM), 10% Fetal Bovine Serum (FBS, Gibco), 2 mM L-Glutammine (Gibco), 2500 units Penicillin/2500 μg Streptomycin (Gibco)

Slice Medium

DMEM-F12, 5% FBS (Gibco), 1X N2 Supplement (Gibco), 100 μM L-Glutammine (Gibco), 2.4 g/L D-Glucose, 2500 units Penicillin/2500 μg Streptomycin (Gibco)

2.1.3 Animals

Animals were maintained by UCL Biological Services. Experiments were performed in accordance to the personal licence and to Animal Act 1986 (UK).

Mice

The mouse lines *Ebf2* $^{+/-}$, *Gt(ROSA)26Sor*$^{tm1(EYFP)Cos}$ (*R26R*^{YFP}; Jackson Laboratories, first described in Srinivas et al., 2001) and *Ebf2*^{GFPiCre} were kindly provided by Dr. G. G. Consalez (San Raffaele Scientific Institute, Milan, Italy). Experiments on *Ebf2*$^{-/-}$ mice were carried out on F1 hybrids obtained by crossing *Ebf2*$^{+/-}$ pure-bred FVB/N (N9) females with *Ebf2*$^{+/-}$ pure-bred C57BL/6J males. This hybrid strain was chosen to obviate the low fertility and poor maternal behavior of C57BL/6J heterozygous mothers, as described before (Croci *et al.* 2006). All studies were conducted using wild-type control littermates. CD1 pure-bred mice were used for *in utero* electroporation experiments.

2.2 TABLES OF MATERIALS

Table 2.1 Primers for genotyping

MOUSE LINE	FORWARD (5'→3')	REVERSE (5'→3')	FRAGMENT SIZE (bp)
Ebf2 $^{-/-}$	GAGGCGGCAGATCTGAAG	Wt-CCAATGCTGCCAGCAAATG Mutant- CATTCAGGCTGCGCAACTGTT	Wt-250 Mutant-600
Ebf2 ^{GFPiCre}	ATGGTGCCAAGGATGACTCT	CCTCGAGCAGCCTCACCA	250
R26R ^{YFP}	Wt- GCGAAGAGTTTGTCCTCAACC Mutant- AAAGTCGCTCTGAGTTGTTAT	GGAGCGGGAGAAATGGATATG	Wt-600 Mutant-250

Table 2.2 Primers for RT-PCR

GENE	PRIMER SEQUENCE (5'→3')	FRAGMENT SIZE (bp)	SPECIES
m*Ebf1*-F	AGGTTGGATTCTGCTACGAAAGTT		mouse
m*Ebf1*-R	TCAGGCCTTTTTAAGAGGAATCA	80	
m*Ebf2*-F	TGGAGAATGACAAAGAGCAAG		mouse
m*Ebf2*-R	TTTGAAAACAGCGGGAAACCC	330	
m*Ebf3*-F	TCGTGAATATGCACCGTTTTG		
m*Ebf3*-R	CCTCGAGACATTTTTTCTGTACTCAT	76	mouse

Table 2.3 Plasmids for cell transfection

NAME	5' TAG	PLASMID	SUPPLIER
Ebf1-flag	FLAG	pcDNA 3.1	G. G. Consalez
Ebf2-flag	FLAG	pcDNA 3.1	G. G. Consalez
Ebf3-flag	FLAG	pcDNA 3.1	G. G. Consalez
shEbf1	GFP	pcDNA 6.2	G. G. Consalez
shEbf2	GFP	pcDNA 6.2	G. G. Consalez
shEbf3	GFP	pcDNA 6.2	G. G. Consalez
shEbf1-2-3	GFP	pcDNA 6.2	G. G. Consalez
shMock	GFP	pcDNA 6.2	G. G. Consalez

Table 2.4 *In situ* probes

NAME	ENZYME for linearization	POLYMERASE	SPECIES	SUPPLIER
Dbx1	EcoRI	T7	mouse	T. Shimogori
Ebf1	XhoI	T3	mouse	G.G. Consalez
Ebf2	XhoI	T3	mouse	G.G. Consalez
Ebf3	SalI	T3	mouse	G.G. Consalez
FoxG1	BamHI	T7	mouse	A. Mallamaci
GFP	BamHI	T3	mouse	T. Shimogori
Reelin	HindIII	T3	mouse	T. Shimogori
Wnt3a	EcoRI	T7	mouse	T. Shimogori

Table 2.5 Primary antibodies

ANTIGEN	HOST	CLONE	DILUTION	SUPPLIER
Ctip2	rat	Polyclonal	1/1000^{H}	Abcam
GFP	rabbit	Polyclonal	1/3000^{H}	Abcam
GFP	chicken	Polyclonal	1/500^{H}	Aves
pan-Ebf	rabbit	polyclonal	1/2000^{WB}	Gift from G. G. Consalez
Reelin	mouse	Monoclonal	1/3000^{H}	Gift from F. Goffinet
Nurr1	rat	Polyclonal	1/100^{H}	Gift from Z. Molnar
p73	goat	Polyclonal	1/100^{H}	Santa Cruz
Cux1	rabbit	Polyclonal	1/100^{H}	Santa Cruz
α-tubulin	mouse	Monoclonal	1/5000^{WB}	Sigma
Paravalbumin	mouse	Monoclonal	1/500^{H}	Sigma
α-FLAG	mouse	Monoclonal	1/100^{H}	Sigma
Calbindin	Rabbit	Polyclonal	1/5000^{H}	Swant
Calretinin	Rabbit	Polyclonal	1/2000^{H}	Swant

H: Immunohistochemistry, WB: western blot.

Abcam, Cambridge, UK; Aves Labs, Oregon, USA; RnD Systems, Abingdon, UK; Santa Cruz, Heidelberg, Germany; Swant, Bellinzona, Switzerland

Table 2.6 Secondary antibodies

ANTIBODY	HOST	CONJUGATED WITH	DILUTION	SUPPLIER
Anti-mouse IgG	goat	Biotin	1/200	Vector
Anti-rabbit IgG	goat	Biotin	1/200	Vector
Anti-rat IgG	goat	Biotin	1/200	Vector
Anti-goat IgG	donkey	Biotin	1/200	Vector
Anti-chicken IgG	goat	FITC	1/1000	Invitrogen
Anti-mouse IgG	goat	FITC	1/1000	Invitrogen
Anti-rabbit IgG	goat	FITC	1/1000	Invitrogen
Anti-rat IgG	goat	FITC	1/1000	Invitrogen
Anti-rat IgG	donkey	TRITC	1/1000	Invitrogen
Anti-mouse IgG	goat	TRITC	1/1000	Invitrogen
Anti-rabbit IgG	goat	TRITC	1/1000	Invitrogen
Anti-mouse IgG	goat	HRP	1/5000	Amersham
Anti-rabbit IgG	goat	HRP	1/5000	Amersham

FITC: fluorescin-5-isothiocyanate (Alexa Fluor 488), TRITC: tetramethilrhodamine-5-(and 6)- isothiocyanate (Alexa Fluor 568), HRP: horse radish peroxidase.

Vector, Peterborough, UK; Amersham, GE Healthcare, Netherlands

2.3 METHODS

2.3.1 Extraction of nucleic acids from tissues/cells

DNA extraction from tissues

DNA was extracted from mouse tissues (ear notches for adults and yolk sacs for embryos) and analyzed by PCR reaction.

Tissues were incubated overnight (ON) in PK Buffer plus Proteinase K (1mg/ml, Sigma) at 55°C. Genomic DNA was extracted with phenol-chloroform, precipitated with 100% iso-propanol and eluted in ddH_2O.

DNA was analyzed by Polymerase chain reaction (PCR) using different primers to discriminate wild-type, heterozygous and knock-out/transgenic animals (See Table 2.2.1).

RNA extraction from cells

RNA was extracted from cells using a commercially available kit from Qiagen (West Sussex, UK). RNA was eluted in ddH_2O. Genomic DNA contamination was eliminated by treating with DNAaseI (Invitrogen) according to manufacter's instructions. RNA was retro-transcribed into DNA prior to analysis according to the protocol shown below. Specific primers were used for the analysis of extracted RNA (See Table 2.2.2).

2.3.2 Analysis of DNA/RNA samples

Reverse Transcription Polymerase Chain Reaction (RT-PCR)

First strand DNA was synthetised from RNA using the kit SuperscriptII RT (Invitrogen). Briefly, 500 ng of RNA were mixed with Oligo dT, dNTPs and ddH_2O up to 12 µl following the manufacturer's instructions. The mix was incubated at 65°C for 5 minutes (min) and chilled on ice. First Strand Buffer, DTT and RNAasin were added to the mix and incubated at 42°C for 2 min. Subsequently, 200 units of

Superscript II Polymerase were added and the samples incubated at 42°C for 1 hour (h). The reaction was stopped by heating the sample at 75°C for 15 min.

Each reaction was performed in a total volume of 20 µl. Products were amplified by using a non-proof reading Taq Polymerase (Promega, Dublin, IR). The mixture was composed of 50 ng of DNA, 1X Taq Buffer, 1.5 mM MgCl2, 0.2 mM dNTPs, 0.5 µM Forward and Reverse primers, 1.25 units of Taq and ddH_2O to final volume.
The general PCR conditions used were the following:
INITIAL DENATURATION: 95°C, 2 min;
DENATURATION: 95°C, 30 secends (sec);
ANNEALING: temperature was set according to the composition of the primers (Tm=2x (nA+nT) +4x (nG+nC)) and duration was usually between 30 sec and 1 min.
EXTENSION: temperature was set at 72°C and duration was set according to the size of the fragment to be amplified and the processing capacity of Taq (1 kb for 1 min).
FINAL EXTENSION: 72°C, 5 min.
PCR products were analyzed on 1 or 2% agarose gel electrophoresis as described below.

Agarose gel electrophoresis

1%-2% agarose gel was used to resolve DNA samples according to the size of amplified product. Agarose powder was melted in 1X TAE by heating the mix with a microwave and 0.2 µg/ml Ethidium Bromide was added. The solution was poured in a gel tray with a comb and left to set at RT for 30 min. Samples were mixed with Loading Buffer (Promega) and the gel was run in the appropriate apparatus (Bio-Rad, Hertfordshire, UK). For fragment size identification a ladder (Promega) was run together with the PCR samples.

2.3.3 Cell cultures

COS7 cells

COS7 cells were obtained from African green monkey kidney and transformed with SV40. These cells were cultured in CLC medium at 37°C in 5% CO_2 in a humified incubator. They were passaged by trypsinasation in 0.25% trypsin/1 mM

EDTA (Gibco) until cells were detached from the plate. Activity of trypsin was stopped by adding NCC medium. COS7 cells were transfected with *Ebfs-flag* plasmids and/or *shEbfs* (see Table 2.2.3) with Lipofectamine2000 according the manufacturer's instructions (Invitrogen). Three days after transfection, cells were either fixed with 4% PFA for immunohistochemistry or collected for RNA and/or proteins extraction. The transfection efficiency was calculated 48 h post-transfection by counting the number of flag/GFP-positive cells in 10 random fields imaged with a 20 X objective.

GN11 cells

The GN11 cell line was obtained by genetically targeted tumorigenesis of gonadotropin-releasing hormone (GnRH) neurons in mice (Radovick *et al.*, 1991). This cell line was a kind gift of A. Cariboni and R. Maggi (University of Milan, Italy). GN11 cells show high migratory behavior *in vitro* and are, therefore, a good model for studying molecular mechanisms of neuronal migration (Maggi *et al.* 2000). Cells were cultured, propagated and treated as described for COS7 cells. GN11 cells were transfected with *Ebfs-flag* and *shEbfs* (Table 2.2.3) using Lipofectamine2000 (Invitrogen) and used to perform *in vitro* migratory assays, RNA/proteins extraction or fixed with 4% PFA for immunohistochemistry. The transfection efficiency was calculated 48 h post-transfection by counting the number of flag/GFP-positive cells in 10 random fields imaged with a 20 X objective.

2.3.4 *In vitro* migration assays

Chemomigration assay of GN11 neurons (Boyden chamber)

Chemotaxis is a migratory response of cells to chemotropic gradients that can be studied with Boyden's chamber (Boyden, 1962; Neuroprobe). The Boyden chamber contains two compartments, the upper cell chamber and the lower chemotropic chamber separated by PVP-free polycarbonate filter through which cells migrate. Filters have different pore sizes depending on cell type. For GN11 cells, pourous filter are treated with 0.5 M acetic acid, rinsed in 1X PBS and coated with gelatin.

Transfected GN11 were trypsinised and resuspended in normal medium without FBS, as this was used as chemoattractant at a concentration of 1%. The same number

of cells was loaded in each well, and different conditions were tested (GN11 towards DMEM or towards DMEM+FBS). A gelatine coated membrane of pore size 8 μm was placed between the two compartments. GN11 cells were incubated for 3 h at 37°C in a 5% CO_2 humified incubator to allow migration. Subsequently, the migrated cells were fixed in methanol for 2 min, whereas the non migrated cells that had not migrated were attached to the upper surface of the membrane, and were scraped. Migrated cells were then stained with Tiazin and Eosin for 2 min each, rinsed in ddH_2O and mounted onto a glass slide. The total cell number in 1 mm^2 of three different fields for each well was counted. Results were expressed as a mean number of migrated cells per well+/- the standard error of the mean (SEM) and significance was calculated by the Student's t-test (Microsoft Excell 2007).

2.3.5 Extraction and analysis of proteins from cells or tissues

Protein isolation from cells

Cells were lysed in RIPA BUFFER containing protease (PMSF 1 mM, aprotinin 2 μg/ml, leupeptin 5-10 μg/ml, pepstatin 1 μg/ml) and phosphatase inhibitors, and left on ice for 20 min. Adherent cells were scraped off the dish using a cold plastic cell scraper and then gently transferred into a pre-cooled tube.

Cell suspension was centrifuge microcentrifuged using a at 4°C at 12,000 rpm for 20 min and the supernatant collected. Protein concentration was determined using Bio-Rad Protein assay based on the method of Bradford. It utilizes the dye comassie blue g-250 wich is red of a pH below 1, but turns blue when binding to a protein causing a shift in the pKa of the bound dye. 1 μl of protein lysate was added to 800 μl of ddH_20 and 200 μl of Bio-Rad reagent. The absorbance (OD) reading of these samples was recorded at the wavelength of 595 nm. These values were then compared to a curve drawn from a standard curve (BSA curve), and 30 μg of protein was usually used for Western blot analysis.

Protein sample preparation

Laemmli sample (Bio-Rad) buffer added to β-mercaptoethanol is especially formulated for protein sample preparation. 2X Laemmli buffer was added to each protein sample at a ratio of 1:1 and heated on a heating block for 1-5 min.

Sodium dodecyl sulphate polyacrylamide gel electrophoresis (SDS-PAGE)

Gels were prepared in a vertical gel electrophoresis separation system (Bio-Rad). Resolving gel was prepared according to protein size (EBFs proteins are about 65 kDa) containing 10% Bis/Acrylamide, 1.5 M Tris-HCl pH8.8, SDS (pH 7.2), ddH_2O, ammonium persolfate (APS) and TEMED. The stacking gel contained 5% acrylamide in Tris pH6.8, SDS, APS and TEMED. Proteins were loaded into the gel and resolved at a constant voltage (100 V) in 1X Running Buffer. Rainbow marker (Amersham) was run together with proteins samples (Sambrook, Fristsch and Maniatis, 1989).

Transfer of proteins onto a nitrocellulose membrane

Transfer was done on nitrocellulose membrane (Amersham) which was placed next to the gel. The two are sandwiched between absorbent 3 MM paper and sponges (sponge/paper/gel/membrane/paper/sponge), and the sandwich is clamped between solid supports to maintain tight contact between the gel and membrane after ensuring no air bubbles have formed between the gel and membrane. The sandwich was then submerged in transfer buffer to which an electrical field was applied. The negatively-charged proteins travel towards the positively-charged electrode, but the membrane stops them, binds them, and prevents them from continuing on. The transfer was made ON at 30 V at 4ºC.

Visualization of proteins on membranes

The morning after the membrane was washed in 1X PBST and then placed in blocking solution containing 5% non-fat milk (Marvel) in PBST at RT for 1 h. The membrane was then transferred into the blocking solution to which the primary antibody was added and left ON at 4°C in agitation. The morning after, the membrane was washed several times in PBST while agitating, 5 min or more per wash, to remove residual primary antibody and then placed in blocking solution to which the secondary antibody was added at the suggested dilution for 1-2 h at RT with agitation. Enhanced Chemiluminiscence reagent (ECL, Amersham) was used, according to manufacturer's instructions, to detected bound antibodies. The reaction was detected using GEL-DOC detection machine (Bio-Rad). The camera inside the machine detects the chemiluminescence emanating from the membrane, transforming

the signal into a digital image for rapid analysis with software provided with the detection machine.

2.3.6 Immunohistochemistry

Specimens' collection and preparation

While collecting brains of different embryonic stages, the day of the plug formation was considered as E0.5. The day of birth was considered as P0. Pregnant animals were culled by cervical dislocation. Embryos and P0 animals were anesthetized by hypothermia prior decapitation. Adult animals were anaesthetized with isoflurane and subsequently perfused through the heart with PFA. Embryos and adult brains were dissected in cold 1X PBS and placed in PFA for 30 min up to 4 h at 4°C depending on age.

Coronal sections were obtained by cutting either with cryostatat (20 µm, embryonic tissues) or freezing microtome (40 µm, embryonic tissue for *in situ* hybridization or adult tissues). For cryostat sections, brains werecryoprotected in 30% sucrose in 1X PBS and frozen in OCT with isopenthane prior to cutting. For freezing microtome sections, adult brains were cryoprotected in 30% sucrose and frozen directly on dry ice dust. Cryo-sections were collected onto superfrost plus glass slide (VWR, Leicestershire, UK), whereas freezing microtome sections were left free-floating and mounted at later stage.

Immunoperoxidase

Firstly, sections were treated with 0.3% H_2O_2 in 1X PBST for 20 min at RT followed by 3 washes in 1X PBST. They were subsequently, incubated in P-solution for 10 min at RT and in Retrival solution (BD Pharmagen, Erembodegem, Belgium) at 70°C for 15 min and left to cool down at RT for 10 min. Sections were then rinsed in 1X PBST and incubated in DAKO blocking solution for 1 h (DAKO, Cambridgeshire, UK), and then ON at 4°C with the primary antibody (See Table 2.2.5) diluted in DAKO solution. The following day, sections were washed in 1X PBST and incubated with secondary antibodies (See Table 2.2.6) at RT for 1h. They were then treated with the avidin-biotin-peroxidase complex (ABC-HRP kit, dilution 1/100, Vector) at RT for 2 h. The activity of the peroxidase was revealed using DAB (0.005% 3,3'diaminobenzidinetetrachloride in H_2O, Sigma) as chromogen and

0.005% H_2O_2 as substrate. The reaction was stopped with 1X PBS, and sections dehydrated through ascending ethanol concentrations (70, 80, 95, and 100% for 1 min each) and mounted in DPX (VWR).

Immunofluorescence

Sections were incubated in P-solution at RT for 10 min and in Retrival solution (BD Pharmagen) at 70°C for 15 min and then, left to cool down at RT for 10 min. They were subsequently rinsed in 1X PBST and incubated in DAKO blocking solution for 1 h (DAKO). Sections were incubated ON at 4°C with the primary antibody (See table 2.2.5) diluted in DAKO solution. Different primary antibodies raised in different hosts were used for double labeling. The following day, sections were washed in 1X PBST and incubated with fluorescent conjugated secondary antibodies at RT for 1 h (See Table 2.2.6). The secondary antibody was washed out with several washes with 1X PBS and tissues were treated with DAPI (4', 6-diamidino-2-phenylindole**,** 2.5 µg/ml, Sigma) for 5 min. Sections were mounted in Mowiol (Sigma).

Immunohistochemistry

Cells were fixed in 4% PFA for 10 min and rinsed in 1X PBST. Immunoreaction was performed as described for tissue sections, except that coverslips were placed culture side up on strips of parafilm mounted on glass slides.

2.3.7 Nissl Staining

In order to visualize cortical layers, sections were stained with 0.025% thionin solution, dehydrated through ascending ethanol concentrations (70, 80, 95, and 100% for 1 min each) and mounted in DPX (VWR).

2.3.8 RNA expression analysis in organic specimens

Non-radioactive *in situ* hybridization with labelled probes

Brains were placed in 4% PFA/30% Sucrose for up to one week, and cut with a freezing microtome at 40 µm. Embryonic brains were embedded in gelatin solution prior freezing (20% Sucrose, 10% Porcine Gelatine in 1X PBS).

Preparation of digoxygenin/fluorescin-labelled probes

20 µg of plasmid DNA was linearised with the correct restriction enzyme, extracted twice with equal volumes of phenol-chloroform, precipitated with 2.5 volumes of ethanol and 1/25 of 2 M NaCl, washed with 70% ethanol, resuspended in 20 µl DEPC-ddH_2O.

In vitro transcription reactions were composed by: 1 µg linear template DNA, 1X transcription buffer (Promega), 100 µM DTT; 1X digoxigenin (DIG) or Fluorescin (F) RNA labelling mix (10 mM each of ATP,CTP,GTP, UTP, DIG-UTP) (Roche), 20 units RNasin (Promega), 20 units of the appropriate RNA polymerase in 20 µl of DEPC-ddH_2O. The mixture was incubated at 37˚C for 2 h. The RNA was precipitated with 2.5 volumes of ethanol and 1/25 of 2 M NaCl, washed with 70% ethanol, resuspended in 100 µl of DEPC-ddH_2O and stored at -80˚C.

Different probes were tested (See Table 2.2.4)

First day: Hybridization

Sections were placed in plastic slide mailers (Sigma) and fixed for 20 min in 4%PFA, washed in 1X PBS 3 times, and placed in buffer containing 100 mM Tris-HCl pH 8 and 50 mM EDTA pH8 added with proteinase K (PK, Roche) at 0.5 µg/ml for 20 min. The reaction was stopped by fixing the sections in 4% PFA for 15 min. In the meantime, 70 µl of probe was added in 15 ml of Hybridization solution. For two-colours *in situ*, a DIG-labelled probe and F-labelled probes were added. The slides were either placed in hybridization solution without probes and frozen for up to six months at -20°C or added in the mailer with the probes and incubated at 70°C ON in a water bath.

Second day: post-hybridization washes and antibody staining

After overnight hybridization, slides were washed in a solution containing 50% formamide, 2X SSC and 1% SDS at 70˚C for 45 min, 3 times.

The slides were incubated in 1X TBST blocking solution containing 2% blocking reagent (Boehringer) and 10% heat-inactivated sheep serum at RT for 1 h. The blocking solution was then replaced with anti-digoxygenin AP-conjugated antibody (Fab fragments; Roche) diluted 1:5000 in blocking solution, and the incubation continued overnight at 4˚C (or 2 h at RT).

Third day: Post-antibody washes and colour reaction

The slides were washed 3 x 5 min in 1X TBST; then 2 x 10 min in NTMT buffer. Subsequently, 0.2 mM 5-bromo-4-chloro-3-indolyl-phosphate (BCIP, Roche), 0.2 mM nitroblue tetrazolium salt (NBT, Roche) were added in NTMT buffer in order to stain the sections. Sections were incubated in the dark at 37˚C until the signal reached a satisfactory intensity (usually a few hours to overnight). The slides were then washed in 1X TBST to clear the background and the reaction stopped in TE STOP buffer and mounted with Glicergel Cytomatic (DAKO).

Second colour reaction

For the second colour reaction with fluorescein, slides were incubated in solution containing 50% Formamide, 2X SSC and 1% SDS at 70ºC for 15 min in order to remove the first antibody for 2 times. The slides were incubated in 1X TBST blocking solution containing 2% blocking reagent (Roche) and 10% heat-inactivated sheep serum for 1 h at RT. The blocking solution was then replaced with anti-fluorescein AP-conjugated antibody (Fab fragments; Roche) diluted 1:5000 in blocking solution, and the incubation continued overnight at 4˚C (or 2 h at RT). The slides were washed 3 x 5 min in 1X TBST; then 2 x 10 min in NTMT buffer. Subsequently, 0.2 mM 5-bromo-4-chloro-3-indolyl-phosphate (BCIP, Roche), 0.2 mM trinitroblue tetrazolium salt (TNT, 50 mg/ml in 85% Dimethylformamide, Sigma) were added in NTMT buffer in order to stain the sections. Sections were incubated in the dark at 37˚C until the signal reached a satisfactory intensity (usually a few hours to overnight). The reaction was stopped in TE STOP buffer and slides mounted with Glicergel Cytomatic (DAKO).

2.3.9 Electroporation experiments

In vivo in utero electroporation in mouse embryonic brain

The *in utero* electroporation is a technique that allows a quick and direct approach to studying the function of genes, rather than a generation of a transgenic or knock-out line. This technique involves an electrical mediated transfer of DNA into a specific tissue. The electricity causes the formation of pores in cell membranes allowing the uptake of large molecules such as DNA (Fukuchi-Shimogori *et al.* 2001; Shimogori *et al.* 2008).

Time-pregnant mice (CD1 background) were anesthetized with sodium pentobarbital (50 µg per gram bodyweight; intraperitoneally; Sigma) and the abdomen was shaved. After an abdominal incision, the uterine horns were exposed on PBS-moistened cotton gauze. The embryos were visualized placing a flexible fibre cable (Leica, Japan) under the uterus, without the use of a microscope. The uterus was positioned between the light source and the thumb and squeezed gently in order to push up the embryos close to the uterine wall. DNA (1 µg) (See Table 2.2.3 for list of plasmids used) mixed with fast green (Sigma) was then injected in one of the two telencephalic ventricles via a glass capillary with the use of a micromanipulator (KD Scientific, Japan). The target region was placed in between of two electrodes made of tungsten, negatively charged, and platinum, positively charged. A three square wave current pulse (7-10 V, 100 ms) using a pulse generator (A-M Systems 2100, Japan) was then passed three times at interval of 1sec. When all the embryos were electroporated, the uterine horns were placed back into the abdomen and the surgical incision was sutured. Mice were kept in a warm place until they were fully recovered.

2.4 DATA ANALYSIS

2.4.1 Image analysis

Bright field pictures of specimens were taken using a LEICA DM500 microscope. Fluorescence pictures were taken using either the same microscope or confocal microscope LEICA SPE-I. Different magnifications were used. Scale bars were adjusted every time according to magnification.

Pictures were processed using Adobe Photoshop CS3 program.

2.4.2 Data Collection and Statistical analysis

Cortical thickness, white matter thickness and thalamic area were measured using ImageJ software. The same scale bar was set up prior to every measurement.

Cell counts were performed using the Methamorph software. Only cells showing visible neurites or nuclei were considered for cytoplasmic staining and nuclear staining, respectively. Quantification of cell numbers was carried out at medio-caudal levels. In embryonic stages, at E13.5, all the cells in the pallial area present in the section were counted, or as otherwise stated, and; at E16.5, the number of cells was counted in boxes that were placed over pallial regions matching control and mutant sections. All measurements realised in these boxes were normalised in number of cells per 250 μm (measured at the pial surface). In postnatal tissue, the number of cells was counted in boxes in regions matching control and mutant sections. All measurements realised in these boxes were normalised in number of cells per 500 μm (measured at the pial surface) and radial column.

For all experiments, we calculated the mean of at least three independent samples. Data are expressed as mean ± standard error of the mean (SEM); error bars represent the standard error of the mean. To determine the statistical significance, we used a paired t test; p-value of < 0.05 was considered significant and indicated with an

asterisk; a p-value of < 0.01 was indicated with two asterisks and a p-value of <0.001 with three asterisks. Statistical analysis was performed using Excel 2008 (Microsoft).

CHAPTER 3

EBF2 IS EXPRESSED IN THE DEVELOPING CEREBRAL CORTEX, BUT LOSS OF FUNCTION DOES NOT LEAD TO MAJOR CORTICAL DEFECTS

3.1 INTRODUCTION

As discussed in Chapter 1, *Ebf2*$^{-/-}$ mice show multiple defects, especially in the cerebellum, suggesting that this gene may play important roles in brain development (Corradi *et al*. 2003; Croci *et al.* 2006). So far, *Ebf2* expression and the effects of its loss of function on the development of the cerebral cortex have not been extensively studied. Garel and colleagues (1997) reported that *Ebf2* is transiently expressed in post-mitotic neurons of the developing mouse forebrain, although it has always been difficult to establish the neuronal cell types that depend on its expression for their development. In this chapter, I have analysed in detail the expression of *Ebf2* with two different approaches. Firstly, by *in situ* hybridisation at different developmental stages in wild type (wt) mice of different developmental ages; secondly, to overcome the early downregulation of the gene expression, *Ebf2*$^{+}$ cell fate was followed using a genetic approach. Specifically, *Ebf2*$^{+}$ cells were permanently labelled using a transgenic mouse line, which expressed the improved *Cre* recombinase gene (*iCre*; Shimshek *et al.* 2002) under the control of the *Ebf2* promoter (Gong *et al.* 2003; Heintz, 2004). Finally, *Ebf2* loss of function defects were analysed using an *Ebf2*$^{-/-}$ mouse line kindly provided by Dr. Giacomo G. Consalez (San Raffaele Scientific Institute, Milan). These studies were focused on the analysis of the anatomical and cellular integrity of the embryonic and adult forebrain in *Ebf2*$^{-/-}$ mice.

3.2 CHARACTERISATION OF *Ebf2*-EXPRESSING CELLS IN THE DEVELOPING FOREBRAIN

3.2.1 *Ebf2* mRNA expression in the developing mouse forebrain

To identify the pattern of expression of *Ebf2* during forebrain development, brains of mice of different embryonic stages, ranging from E10.5 to adult, were analysed using *in situ* hybridization. *Ebf2* was expressed in different areas of the developing forebrain. In the telencephalon, it was expressed in post-mitotic regions of the pallium, namely septum, CH, hippocampus, neocortex (PPL/MZ) and piriform cortex (PCx). Expression was not detected in the pallial proliferative zone or in any of the subpallial domains. In the diencephalon, it was expressed in the VZ of the epithalamus, hypothalamus, thalamic eminences (TE) and diencephalic-telencephalic boundary (DTB). Expression was first detected around E10.5 in the CH, hippocampus and neocortical PPL (Figure 3.1, A). At E11.5 (Figure 3.1, B) and E12.5 (Figure 3.1, C), its expression was extended to PCx. At E13.5, *Ebf2* showed maximum expression and it was found rostrally, in the cortical PPL and septum (Figure 3.2, A), while medially and caudally, it was detected in the dorsal PPL, in the lateral MZ and SP (as PPL splits due to the arrival of CP; Figure 3.2, B and C; Figure 3.3, B), hippocampus, CH, PCx, epithalamus, DTB and TE (Figure 3.1, D; Figure 3.2, B and C). The expression in the telencephalon did not show a rostro-caudal gradient (Figure 3.2, A-C).

Cajal-Retzius cells, located in the cortical PPL/MZ, are believed to originate in the CH, septum and pallial-subpallial boundary (PSPB) (Bielle et al., 2005). The expression of *Reelin mRNA*, which is a specific marker for this cell population, matched the expression of *Ebf2* in the cortical PPL, the CH and the septum (Figure 3.4, A-E). Interestingly, *Ebf2* expression did not coincide with *Reelin mRNA* expression in the PCx (Figure 3.4, F). The hypothesis that the *Ebf2* transcription factor plays a role in the development of CR cells and, possibly, in the regulation of the Reelin pathway was extensively analysed in the *Ebf2*$^{-/-}$ mouse (see Chapter 3.3). Between E14.5 and E15.5, a general downregulation of the *Ebf2* gene occurred in the PPL/MZ, hippocampus and CH (Garel et al., 1996) (Figure 3.3, C), whereas the

expression in the PCx, TE and DTB persisted (Figure 3.1, E and F). At P0, *Ebf2* expression was detected only in subcortical nuclei identified as *zona incerta* and bed nucleus of *stria terminalis*, probably derivates of DTB and TE (Figure 3.1, G).

3.2.2 *Ebf2*^{GFPiCre} line: a genetic approach to map *Ebf2*-derived cells

In order to overcome the difficulty of tracking the lineage of *Ebf2*$^{+}$ cells due to early downregulation of the gene in the telencephalon, *Ebf2*^{GFPiCre} transgenic females were crossed with reporter animals expressing the yellow fluorescent protein under the control of the ubiquitous promoter *Rosa 26* (*R26R*^{YFP}) to permanently label *Ebf2*$^{+}$ cells (Figure 3.6). The *Ebf2*^{GFPiCre} transgenic line was generated in the laboratory of Dr. Giacomo G. Consalez by using the Bacterial Artificial Chromosome Recombinogenic Engineering (BAC Recombineering; Copeland *et al.* 2001; Lee *et al.* 2001; Testa *et al.* 2003), based on the homologous recombination in specific *E. coli* strains (Figure 3.5, A). In order to produce a classic transgenic mouse by this approach, the integration of a green fluorescent protein fused with an improved Cre recombinase protein (*GFPiCre)* construct (Badaloni A, unpublished) was targeted into the first coding exon of the *Ebf2* locus in the BAC RP24-283N8 (Figure 3.5, A) (Gong *et al.* 2003; Heintz 2004; Chiara F. and A. Badaloni, unpublished). This BAC contains the *Ebf2* promoter, the beginning of the *Ebf2* coding sequence located in exon 2 and the first seven exons of the gene (for BAC specifications: Gene Expression Nervous System Atlas, GENSAT, www.gensat.org). The transgenic line obtained, coupled with a *Cre*-inducible reporter transgene, permits the execution of fate mapping experiments, allowing *GFPiCre*-expressing cells and their progeny to be indelibly labelled *in vivo*, even long after the *Ebf2* gene is developmentally downregulated (Figure 3.6, A-C). Preliminary characterisation of the transgene expression, particularly focused on the cerebellum, compared to the endogenous gene expression, has demonstrated that BAC RP24-283N8 contains most of the regulatory sequences necessary for correct transgene expression in the brain (Chiara F., A. Badaloni and G. G. Consalez, unpublished).

The expression of the *GFPiCre* transgene was also analysed by *in situ* hybridisation in the telencephalon and compared with the expression of the endogenous *Ebf2* (Figure 3.5 B-E). At E13.5, *GFPiCre* expression matched the expression of *Ebf2* in the CH, septum, hippocampus, cortical PPL/MZ, SP and PCx

(Figure 3.5, B compared to C). At E15.5, dowregulation of transgene signal occurred in the expected territories such as CH, septum, hippocampus and MZ, but persisted in the PCx (Figure 3.5, D compared to E). The expression of *GFPiCre* gene in the MZ and PCx was less intense compared to that of the endogenous gene in the same areas. This difference is explained by the use of *in situ* probes of different length as well as a different *mRNA* stability of the transgene compared to the *mRNA* of the endogenous gene (Figure 3.5, B-E). Subsequently, $Ebf2^{GFPiCre/R26RYFP}$ mice were collected at different developmental stages and the expression of YFP was followed from E11.5 to postnatal life. YFP immunohistochemistry at E13.5 and E16.5 revealed that *Ebf2* was expressed in pallial structures, such as neocortex, CH, septum, hippocampus and PCx (Figure 3.7, A and B). Moreover, YFP-expressing cells in the neocortex were detected in the PPL/MZ, the CP and in the SP (Figure 3.7, A-E). In the diencephalon, the transgene was expressed in the epithalamus, hypothalamus and DTB (Figure 3.7, B). No expression was detected in the thalamic nuclei or axons arising from this area (Figure 3.7, B). At P7, $Ebf2^{+}$ cells in the cerebral cortex were positioned in layer I (former PPL/MZ), layer V and in the SP at the bottom of layer VI (Figure 3.7, E).

Next, YFP signal was compared with the expression of different markers for known cortical cell populations. Only medial sections of coronally cut forebrains were considered. At E11.5, YFP was expressed in the PPL and its expression coincided with that of p73 (Figure 3.8, A-D'). As previously described, p73 protein is an early specific marker for CR cells originating from the septum and CH (Meyer *et al.* 2002). *Ebf2,* as previously shown by *in situ* hibrydisation, was specifically expressed in CH and septum, thus explain the correlation between p73 and YFP signals (Figure 3.8, D'). Moreover, the expression of YFP matched the expression of Reelin in the PPL (Figure 3.8, E-H; H' shows double positive cells in the circle). However, not all YFP^{+} cells did express Reelin (Figure 3.8, H'; arrowhead points to YFP^{+} cells only). Reelin is a marker of all CR cells, however it has been shown that its expression in the CH appears later compared to p73 protein (Meyer *et al.* 2002; Hanashima *et al.* 2007). Thus, YFP^{+}/$Reelin^{-}$ cells were most likely derived from the CH, whereas YFP^{-}/$Reelin^{+}$ cells (Figure 3.8, H'; arrow points to $Reelin^{+}$ cells only) possibly came from the PSPB, where *Ebf2* was not expressed. A third marker, Calr, was also used to label specifically CR cells, although it has been shown that the polyclonal anti-Calr antibody produced by Swant and used in these experiments does

not recognise a subpopulation of $Calr^+$ CR cells deriving from the septum (Bielle *et al.* 2005). At E11.5 the majority of cells were $Calr^+/YFP^+$ indicating that *Ebf2* was expressed in CR cells as confirmed previously with other CR-specific markers (Figure 3.8, I-L; L' shows double positive cells in the circle). Thus, $YFP^+/Calr^-$ cells were derived from the septum (Figure 3.8, L'; arrowhead points to green cells only) and $YFP^-/Calr^+$ cells from the PSPB (Figure 3.8, L'; arrow points to red cells only). At E13.5, Calr labelled CR cells in the MZ (PPL is split in MZ and SP), but also SP cells (Figure 3.9, A-D) positioned underneath the CP at this stage (Figure 3.9, C; circle shows SP cells). In the MZ, $YFP^+/Calr^+$ were CR cells derived from CH (Figure 3.9, D; square), and in the SP layer $YFP^+/Calr^+$ represented *Ebf2* expression in SP cells (Figure 3.9, D; circle). YFP^+ cells localised in the CP and not expressing Calr (Figure 3.9, D), were most likely early-born pyramidal cell precursors that will later occupy layer IV and V in the developed neocortex (see below). Moreover, at E13.5 cortical migrating interneurons were also positioned in the MZ (Figure 3.9, G; arrow) and specifically labelled by Calb antibody. Calbindin immunoreactivity was not detected in YFP^+ cells, suggesting that *Ebf2* was not expressed in migrating interneurons (Figure 3.9, H; rectangle). These results were confirmed also postnatally (Figure 3.10). At P7, caudal sections of the cerebral cortex showed that YFP was expressed in CR cells, labelled with Calr antibody in layer I (Figure 3.10, C and C'). However, postnatally Calr was also expressed in a subpopulation of interneurons, which did not co-express YFP/*Ebf2* (Figure 3.10, C and C''; layer IV). Moreover, a small percentage of layer IV cells were also found to be YFP^+, but not $Calr^+$, suggesting that at caudal level *Ebf2* was also expressed in pyramidal cells (Figure 3.10, A and C). Nuclear receptor related 1 (Nurr1) (Figure 3.10, D-F'), a postnatal marker for SP cells, was also found to be expressed in YFP^+ cells at the bottom of layer VI (Figure 3.10, F and F'). Moreover, YFP-expressing cells seen in the lower parts of developing CP at E13.5 and E16.5 (Figure 3.7, A-D; Figure 3.9, D) were positioned in layer V postnatally, representing a small percentage of COUP-TF interacting protein 2 $(Ctip2)^+$ cells (Figure 3.10, G-I'), which is a marker of pyramidal cells in lower cortical layers (V-VI). Thus, *Ebf2* is expressed in a subpopulation of layer V neurons (Figure 3.10, I and I').

In conclusion, during the *Ebf2*-expressing phase, YFP is found in the septal and hem-derived CR cell subpopulations and SP cells. Moreover, long after the disappearance of *Ebf2* expression from the cortex, YFP could still be detected in

these cells postnatally, making the *Ebf2*^{GFPiCre} mouse line an excellent tool to follow the fate of these two transient, but very important cortical cell populations.

Figure 3.1 *Ebf2* expression during cortical development

In situ hybridisation; coronal sections, 40 µm.

A-C: At E10.5, E11.5 and E12.5, *Ebf2* is detected in the PPL, CH and hippocampus of the telencephalon. At E11.5 and E12.5, the gene is found expressed in the PCx.
D: At E13.5 *Ebf2* is expressed in the PPL, CH, hippocampus and PCx of the pallium. Moreover, the gene is expressed in diencephalic regions such as the TE and Et.
E, F: *Ebf2* is dowregulated in pallial regions from E15.5. However, expression persists in the PCx and TE.
G: Postnatal expression of *Ebf2* is localised in Zi and BNST.

BNST: bed nucleus of stria terminalis, CH: cortical hem, Et: epithalamus, MZ: marginal zone, H: hippocampus, PCx: pyriform cortex, PPL: preplate, TE: thalamic eminences, Zi: zona incerta.

Scale bars: (A-D) 100 µm, (E-G) 200 µm

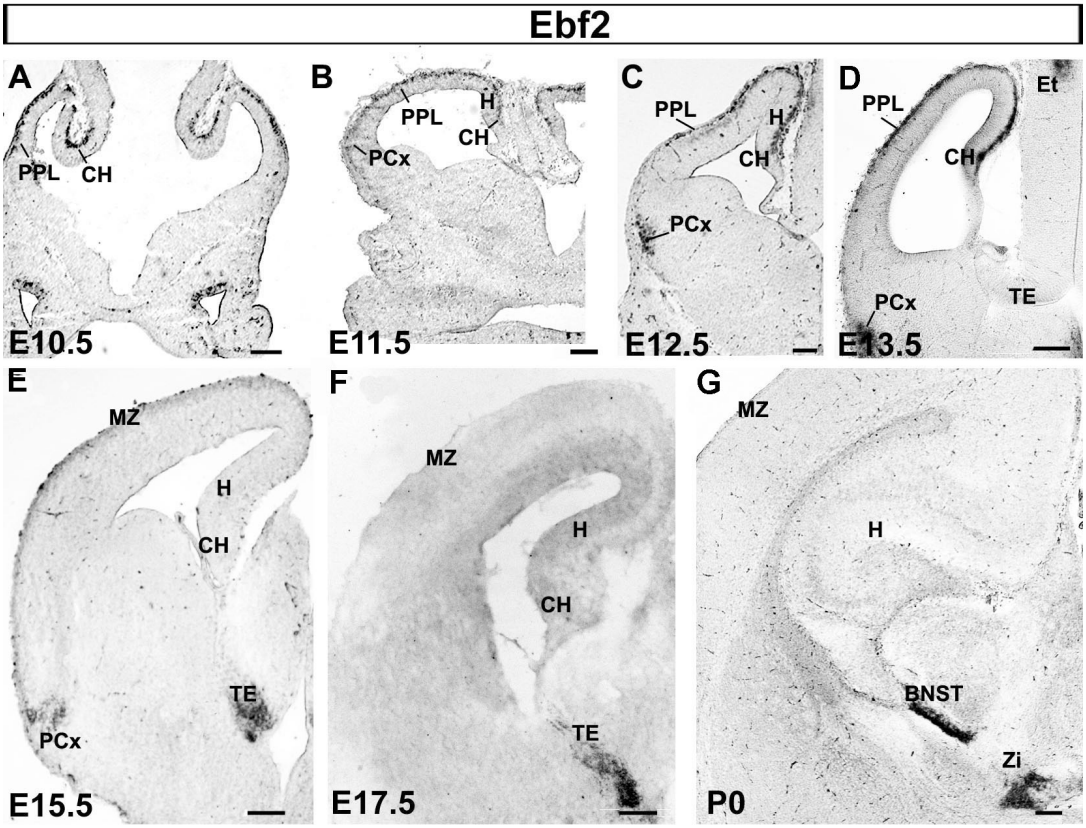
Ebf2
A
PPL
CH
E10.5
B
PPL
H
CH
PCx
E11.5
C
PPL
H
CH
PCx
E12.5
D
PPL
Et
CH
PCx
TE
E13.5
E
MZ
H
CH
TE
PCx
E15.5
F
MZ
H
CH
TE
E17.5
G
MZ
H
BNST
Zi
P0

Figure 3.2 Rostro-caudal expression of *Ebf2* in the developing cortex at E13.5

In situ hybridisation; coronal sections, 40 μm.

A-C: Rostral, medial and caudal sections illustrate the equally distributed expression of *Ebf2 mRNA* along the telencephalic rostro-caudal axis. In B' high magnification of the developing NCx shows the specific signal in the PPL (arrow).

CH: cortical hem, DTB: diencephalic-telencephalic boundary, Et: Epithalamus, H: hippocampus, Hy: hypothalamus, OE: olfactory epithelium, PCx: pyriform cortex, PPL: preplate, Sp: septum, TE: thalamic eminences.

Scale bar: 200 μm (A, B and C), 50 μm (B')

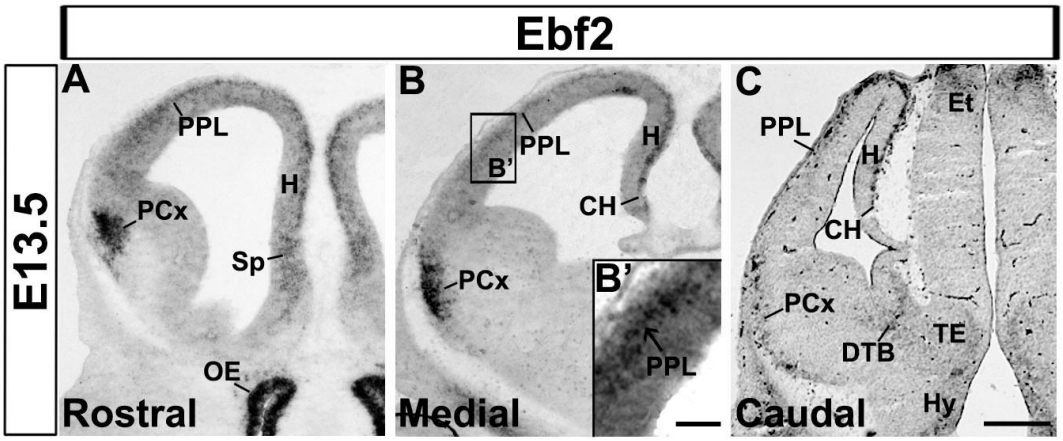
Ebf2
E13.5
A
PPL
H
PCx
Sp
OE
Rostral
B
PPL
B'
H
CH
PCx
B'
PPL
Medial
C
Et
PPL
H
CH
PCx
DTB
TE
Hy
Caudal

Figure 3.3 Higher magnification images of *Ebf2* expression in the PPL and MZ of the developing cortex

In situ hybridisation; coronal sections, 40 μm.

A, B: At E12.5 and E13.5, *Ebf2* is expressed in the PPL/MZ and CH. In **B**, PPL is split in the most ventral part of the pallium into MZ and SP layers by the forming CP. *Ebf2* expression is visible in the SP layer (arrow).
C: *Ebf2* expression is dowregulated in the MZ by E15.5.

CH: cortical hem, CP: cortical plate, IZ: intermediate zone, MZ: marginal zone, PPL: preplate, SP: subplate layer, SVZ: subventricular zone, VZ: ventricular zone.

Scale bar: 100 μm

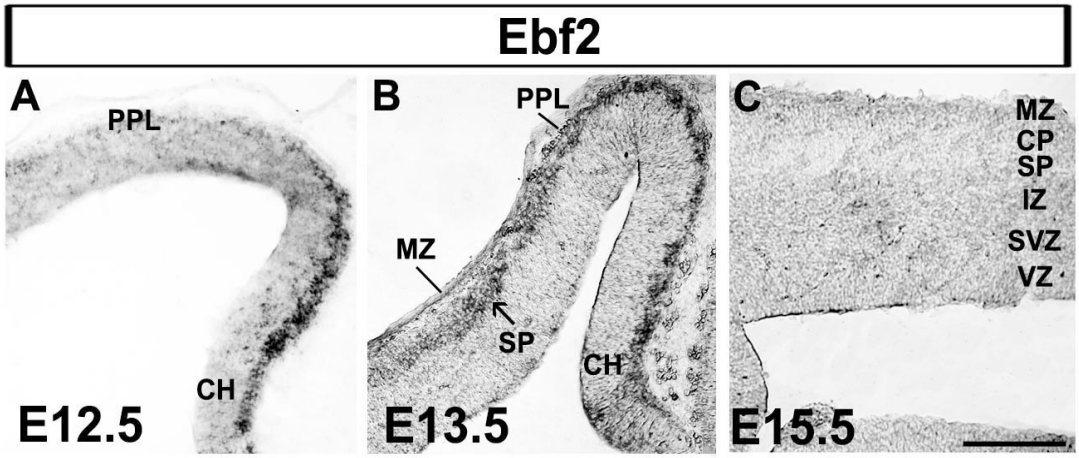
Ebf2
A
PPL
CH
E12.5
B
PPL
MZ
SP
CH
E13.5
C
MZ
CP
SP
IZ
SVZ
VZ
E15.5

Figure 3.4 Expression pattern of *Reelin mRNA* and *Ebf*2 at E13.5

In situ hybridisation; coronal sections, 40 µm.

A, B: *Reelin mRNA* and *Ebf2* expression match in the PPL and CH.
C: Merge of *Reelin mRNA* and *Ebf2* expression. *Reelin mRNA* (brown) and *Ebf2* (purple) signals overlap.
D, E: *Reelin mRNA* and *Ebf2* are both expressed in the septum. The area of the septum is identified by the black dots and subdivided in dorsal (d) and ventral (v) domains. *Reelin* is expressed in d and in v, whereas *Ebf2* expression is confined mainly in d.
F: Merge of *Reelin mRNA* and *Ebf2* expression in the PCx shows no colocalisation in this area.

CH: cortical hem, GE: ganglionic eminences, PCx: pyriform cortex, PPL: preplate, Sp: septum, St: striatum.

Scale bars: (A-C) 100 µm, (D-F) 200 µm

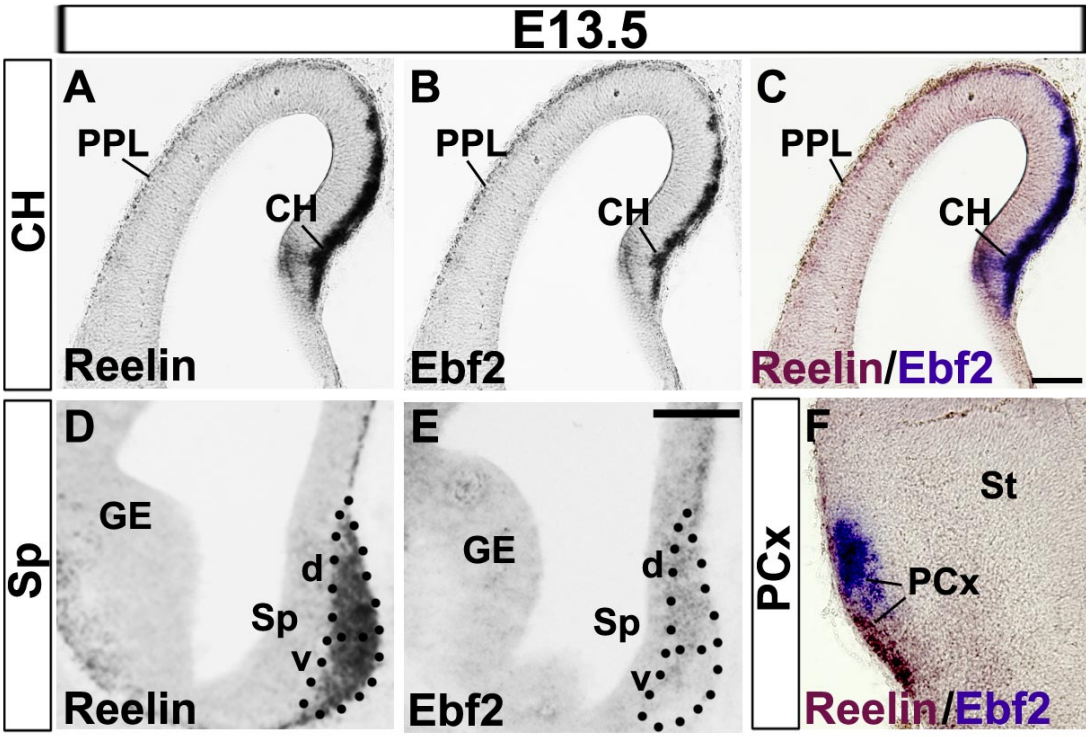
E13.5
CH
A
PPL
CH
Reelin
B
PPL
CH
Ebf2
C
PPL
CH
Reelin/Ebf2
Sp
D
GE
d
Sp
v
Reelin
E
GE
d
Sp
v
Ebf2
PCx
F
St
PCx
Reelin/Ebf2

Figure 3.5 Validation of the *Ebf2*^{GFPiCre} transgenic mouse

In situ hybridisation; coronal sections, 40 µm.

A: The BAC-RP24 contains part the *Ebf2* locus: the hypothetical promoter and the first two exons. The transgene *GFPiCre* was inserted through bacterial recombination in the second exon as shown in the figure.
B, C: E13.5, *Ebf2* and *GFPiCre* are expressed in the same territories.
D, E: E15.5, *GFPiCre* expression is downregulated in the pallial region, as is *Ebf2;* which is still expressed in the PCx.

CH: cortical hem, H: hippocampus, HOM: homology arms for recombination, MZ: marginal zone, PA: polyadenilation signal, PCx: pyriform cortex, PPL: preplate, SP: subplate.

Scale bar: (B-E) 250 µm

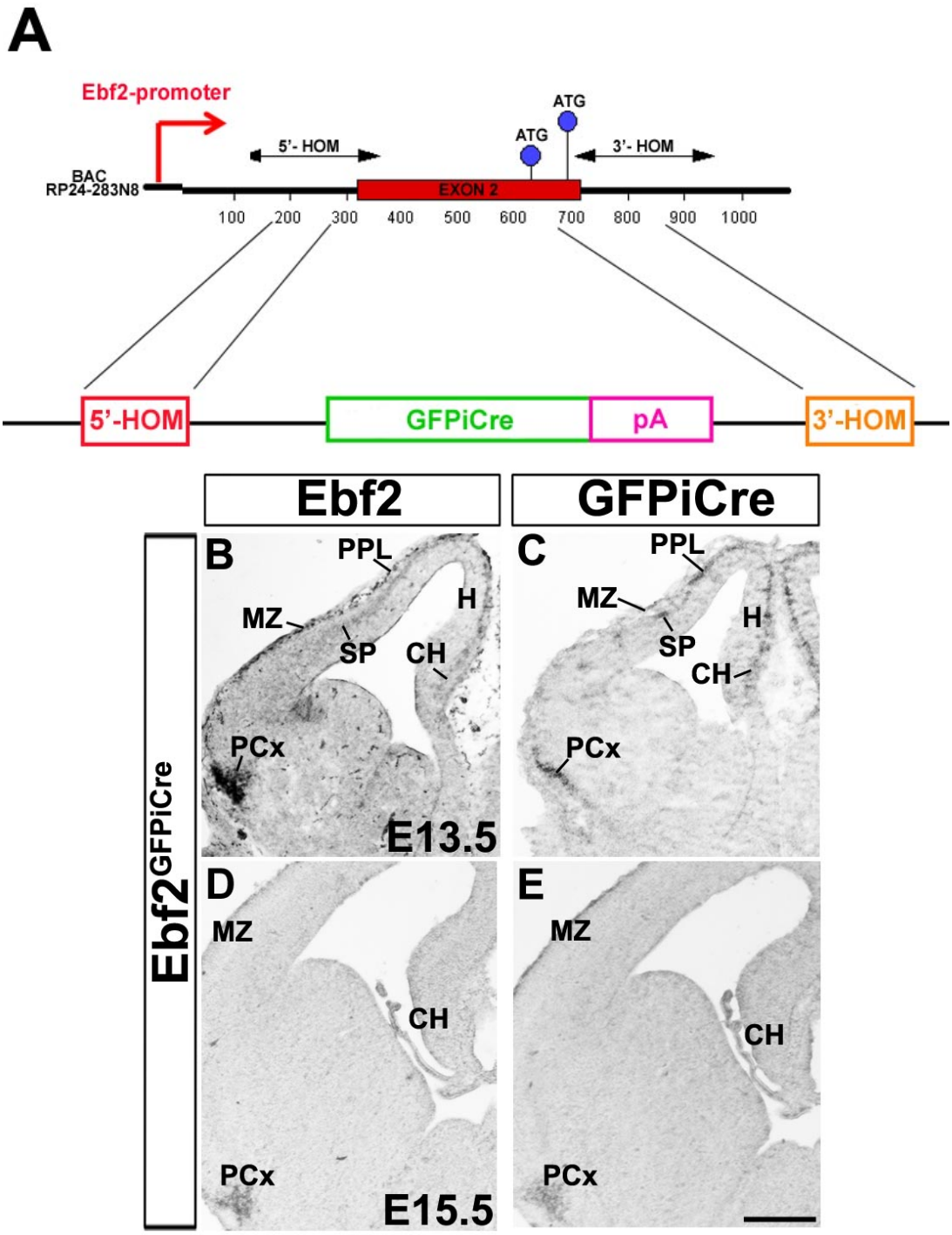
A
Ebf2-promoter
ATG
ATG
5'- HOM
3'- HOM
BAC
RP24-283N8
EXON 2
100
200
300
400
500
600
700
800
900
1000
5'-HOM
GFPiCre
pA
3'-HOM
Ebf2
GFPiCre
Ebf2GFPiCre
B
PPL
H
MZ
SP
CH
PCx
E13.5
C
PPL
MZ
H
SP
CH
PCx
D
MZ
CH
PCx
E15.5
E
MZ
CH
PCx

Figure 3.6 Validation of the Cre-recombinase activity in *Ebf2*^{GFPiCre}

A: The schema shows the loxP recombination driven by the Cre recombinase at the *Rosa26* locus. In the *Ebf2*$^{GFPiCre/R26R\text{-}YFP}$, the activation of the Cre recombinase leads to the excision of the stop signal and the permanent expression of the YFP protein in *Ebf2* expressing cells.
B, C: Whole-mount YFP expression in *Ebf2*$^{GFPiCre/R26R\text{-}YFP}$ at E13.5 and E17.5 shows the activity of Cre recombinase in *Ebf2*$^{+}$ cells.

Cb: cerebellum, F: forebrain, HB: hindbrain, MB: midbrain, OB: olfactory bulb, oe: olfactory epithelium, YFP: yellow fluorescent protein.

Scale bar: (B, C) 50 mm

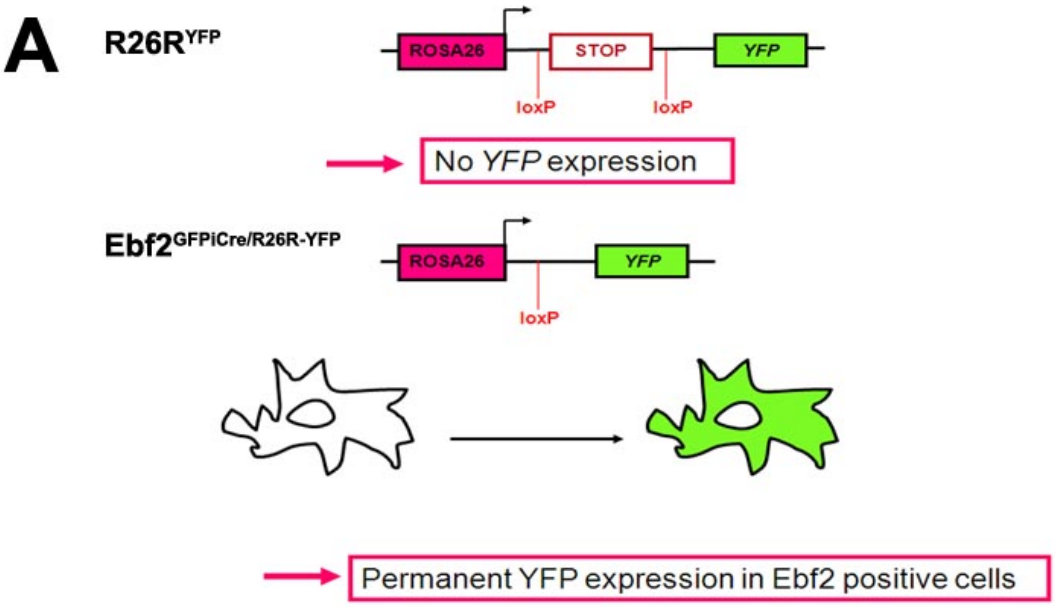
A
R26R^YFP
ROSA26
STOP
YFP
loxP
loxP
No YFP expression
Ebf2^GFPiCre/R26R-YFP
ROSA26
YFP
loxP
Permanent YFP expression in Ebf2 positive cells

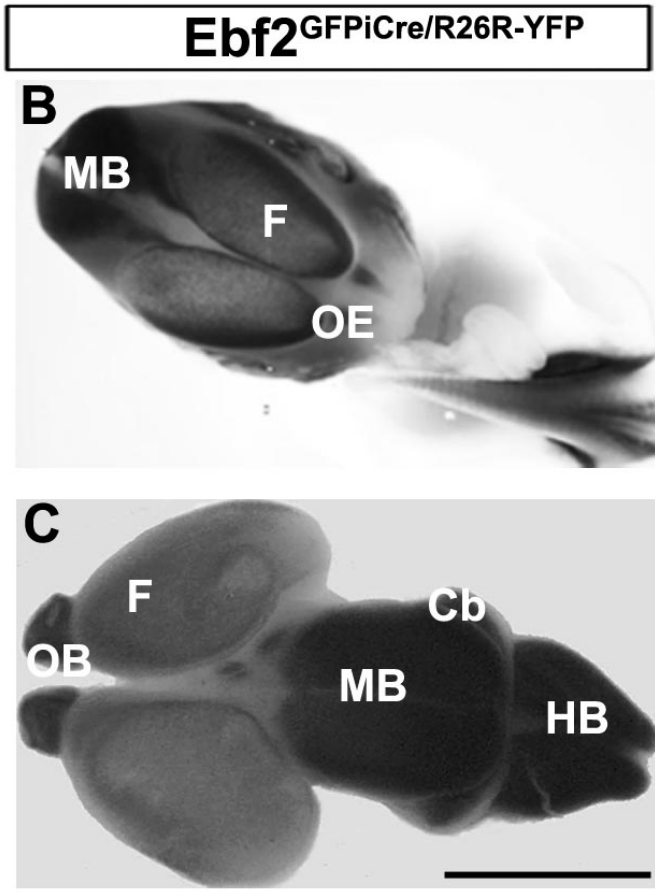
Ebf2^GFPiCre/R26R-YFP
B
MB
F
OE
C
F
Cb
OB
MB
HB

Figure 3.7 Fate mapping of *Ebf2*$^{+}$ cells in *Ebf2*$^{GFPiCre/R26R\text{-}YFP}$

Immunohistochemistry; coronal sections, 20 µm for the embryonic tissue and 40 µm for the adult tissue.

A, B: Expression of YFP at E13.5 and E16.5. The transgene is expressed in the MZ, SP, CH, H, PCx, Sp, Am, H, Et and DTB.
C, D: High magnification images of the pallium at E13.5 and E16.5 reveal that *Ebf2* is not only expressed in CR cells, but also in SP cells and neurons in the CP.
E: YFP cells are found in layer I, as well as in layer V and at the bottom of layer VI (SP cells).

Am: amygdala, CH: cortical hem, CP: cortical plate, DTB: diencephalic-telencephalic boundary, Et: epithalamus, GE: ganglionic eminences, H: hippocampus, Hy: hypothalamus, IZ: intermidiate zone, MZ: marginal zone, SP: subplate, Sp: septum, PCx: pyriform cortex, Th: thalamus.

Scale bars: (A, B, E) 100 µm, (C) 25 µm, (D) 50 µm

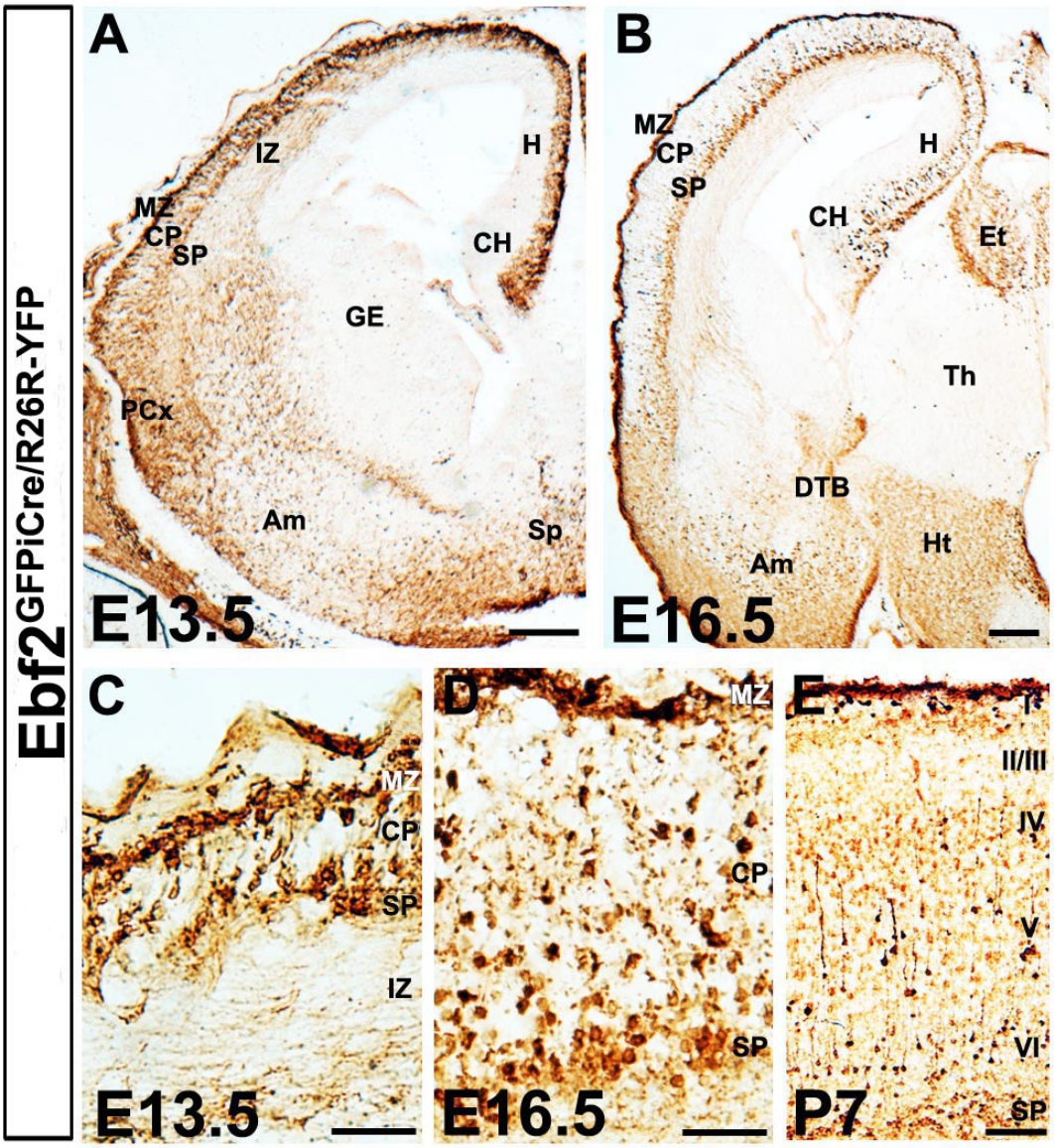
Ebf2GFPiCre/R26R-YFP
A
IZ
H
MZ
CP
SP
CH
GE
PCx
Am
Sp
E13.5
B
MZ
CP
SP
H
CH
Et
Th
DTB
Am
Ht
E16.5
C
MZ
CP
SP
IZ
E13.5
D
MZ
CP
SP
E16.5
E
I
II/III
IV
V
VI
SP
P7

Figure 3.8 Fate mapping of *Ebf2* positive cells in *Ebf2*$^{GFPiCre/R26R\text{-}YFP}$ at E11.5

Immunofluorescence; coronal sections, 20 μm.

A-D': Expression of YFP perfectly matches the expression of p73, a marker of CR cells deriving from the CH and septum (D').
E-H': YFP expression matches the expression of Reelin (H'); however, a proportion of cells expressing YFP did not Reelin (H', arrowhead) and *vice versa* (H', arrow). Cells circled are YFP^{+}/Reelin^{+} (H').
I-L: Square show double positive cells (L'), arrowhead points to YFP^{+}/Calr^{-} cells and arrow points to YFP^{-}/Calr^{+}. Cells circled are YFP^{+}/Calr^{+} (L').

Calr: calretinin, DAPI: 4',6-diamidino-2-phenylindole, PPL: preplate layer, VZ: ventricular zone, YFP: yellow fluorescent protein.

Scale bar: 25 μm

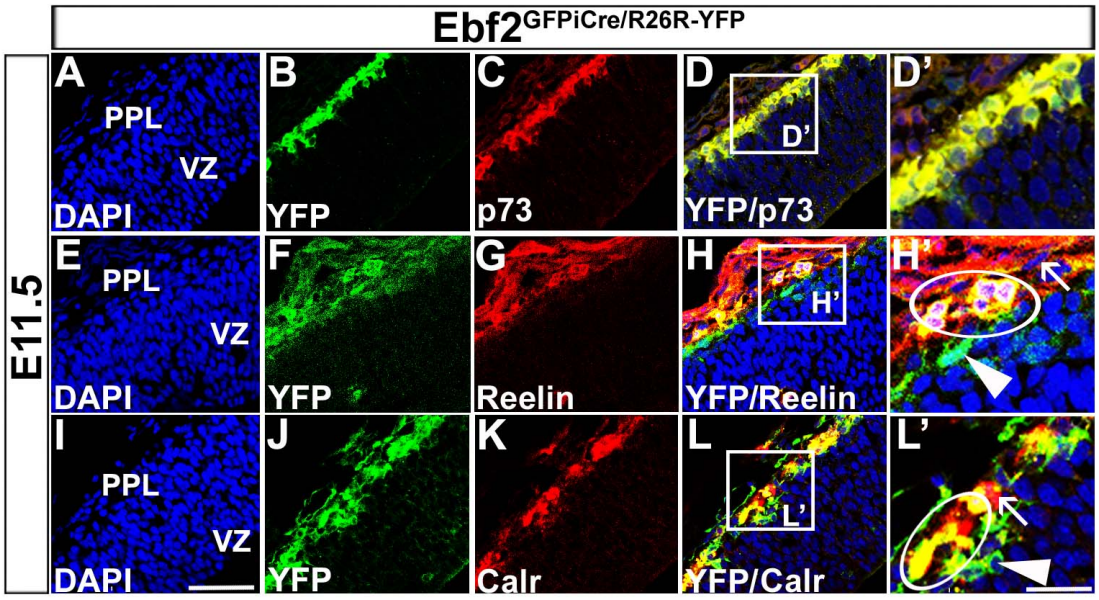
Ebf2GFPiCre/R26R-YFP
E11.5
A
PPL
VZ
DAPI
B
YFP
C
p73
D
D'
YFP/p73
D'
E
PPL
VZ
DAPI
F
YFP
G
Reelin
H
H'
YFP/Reelin
H'
I
PPL
VZ
DAPI
J
YFP
K
Calr
L
L'
YFP/Calr
L'

Figure 3.9 Fate mapping of *Ebf2* positive cells in *Ebf2*$^{GFPiCre/R26R\text{-}YFP}$ at E13.5

Immunofluorescence; coronal sections, 20 µm.

A-D: After the splitting of the PPL, CR cells are positioned in the MZ, whereas SP cells are found in the SP layer (C, circle). $YFP^+/Calr^+$ are present in the MZ (D, square) and in the SP layer (D, circle).
E-H: Expression of Calb (MZ, arrow), a marker for interneurons, does not match the expression of YFP (H, rectangle).

Calb: calbindin, Calr: calretinin, CP: cortical plate, DAPI: 4',6-diamidino-2-phenylindole, IZ: intermediate zone, MZ: marginal zone, SP: subplate layer, SVZ: subventricular zone, VZ: ventricular zone, YFP: yellow fluorescent protein.

Scale bar: 50 µm

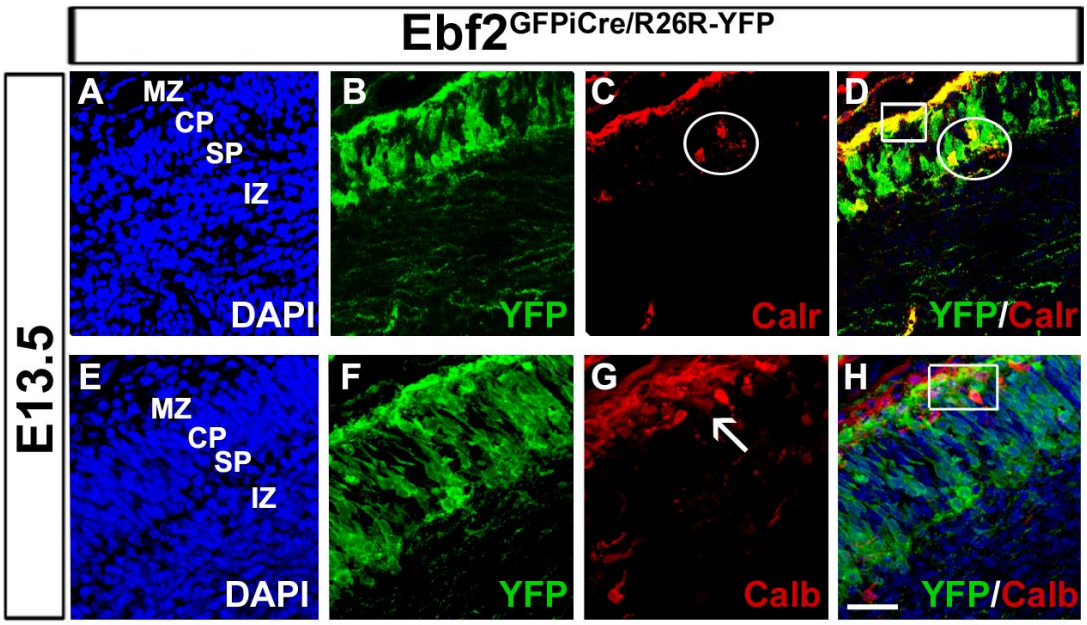
Ebf2GFPiCre/R26R-YFP
E13.5
A
MZ
CP
SP
IZ
DAPI
B
YFP
C
Calr
D
YFP/Calr
E
MZ
CP
SP
IZ
DAPI
F
YFP
G
Calb
H
YFP/Calb

Figure 3.10 Fate mapping of *Ebf2* positive cells in *Ebf2*$^{GFPiCre/R26R\text{-}YFP}$ at P7

Immunofluorescence; coronal sections, 40 µm.

A- C'': Postnatally Calr is expressed in interneurons but, some CR cells still retain this marker at P7. In **C'** cells in the MZ co-express Calr and *Ebf2*. **C''**, high magnification of Calr^{+} interneurons in layer IV which do not show expression of *Ebf2*.
D- F': Expression of Nurr1, a postnatal marker for SP cells, matches the expression of YFP.
G- I': CTIP2, a marker of layers V and VI neurons, co-localises with YFP in layer V (I').

Calr: calretinin, Ctip2: COUP-TF interacting protein 2, Nurr1: nuclear receptor related 1, YFP: yellow fluorescent protein.

Scale bars: (A-I) 250 µm, (C', C'', F', I') 10 µm

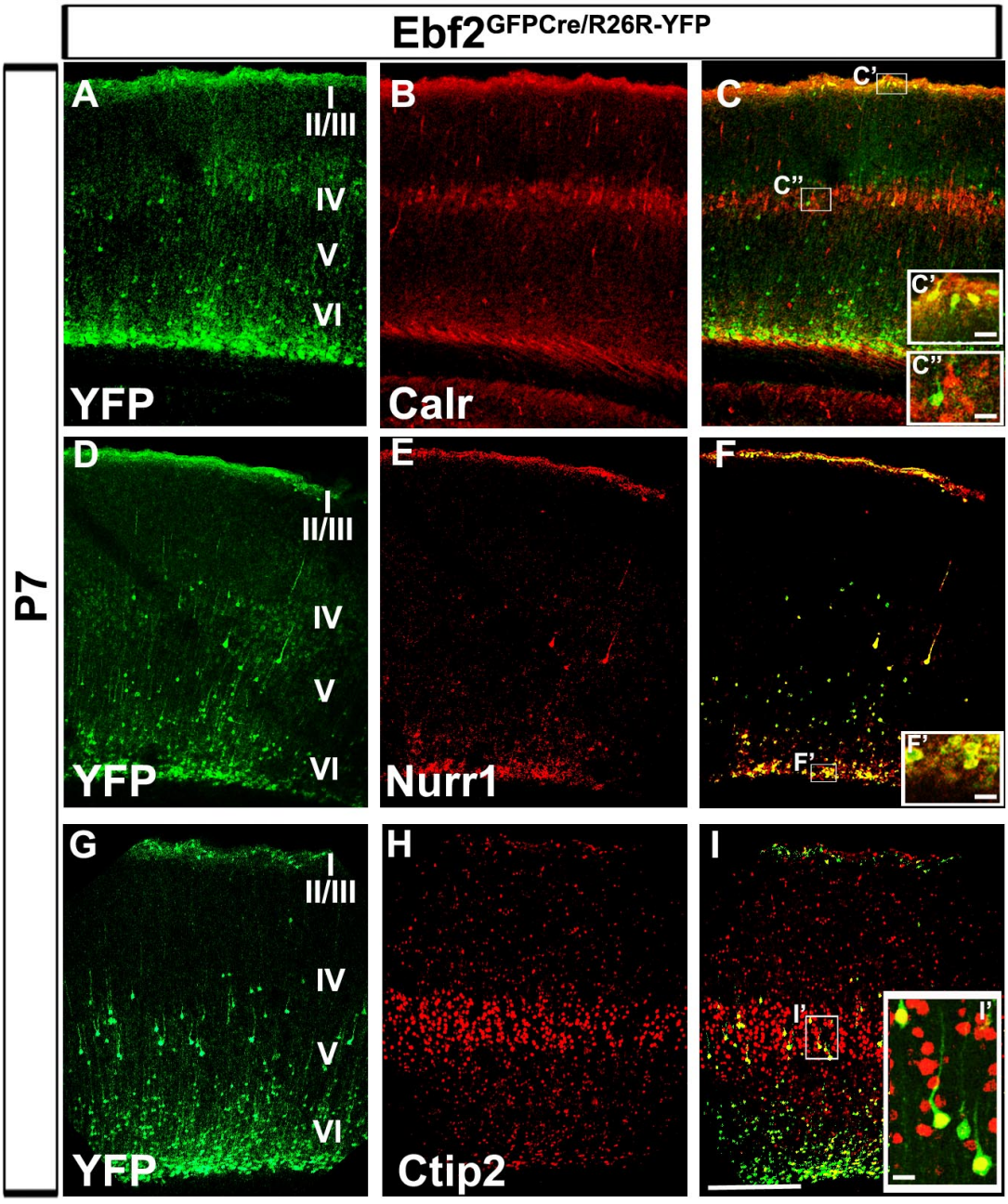
Ebf2GFPCre/R26R-YFP
P7
A
I
II/III
IV
V
VI
YFP
B
Calr
C
C'
C''
C'
C''
D
I
II/III
IV
V
VI
YFP
E
Nurr1
F
F'
F'
G
I
II/III
IV
V
VI
YFP
H
Ctip2
I
I'
I'

3.3 ANALYSIS OF THE CORTICAL STRUCTURE AND CELLULAR ORGANISATION IN *Ebf2*$^{-/-}$ MICE

3.3.1 Development of the CR cell population in *Ebf2*$^{-/-}$ mice

In situ hybridisation and fate mapping studies have shown that *Ebf2* is expressed in CR cells between E10.5 and E13.5 and, as a consequence, it might play a role in their function. In order to study its role in the development of this cell population, I have analysed in *Ebf2*$^{-/-}$ mice the integrity of CR cell specification and migration in the neocortex.

Cajal Retzius cell commitment was analysed through *in situ* hybridizations for transcription factors that are known to be involved in cell specification in the septum, PSPB and CH during early developmental stages (Figure 3.11). *Dbx1*, a homeodomain transcription factor, specifies two CR cell subpopulations originating from the septum and the PSPB. Its expression was found in the expected territories in *Ebf2*$^{-/-}$ mice. However, *Dbx1* signal in the septum of *Ebf2*$^{-/-}$ was reduced, whereas, it was augmented in the PSPB compared to wt controls (Figure 3.11, A compared to B, septum; C compared D, PSPB). *Wnt3a* is, instead, specifically expressed in the CH. Its expression was found in the expected territories of *Ebf2*$^{-/-}$ mice and it looked expanded compared to wt controls (Figure 3.11, E compared F). *Foxg1* is involved in the specification of the telencephalon, and promotes self-renewal of neuronal precursors antagonising their neuronal differentiation (Martynoga *et al*., 2005; Hanashima *et al*., 2004). In fact, loss of function studies show that lack of *Foxg1* leads to abnormal differentiation of early-born cortical progenitors that adopt CR cell fate (Hanashima *et al.* 2004). This consequently causes an increased production of Reelin that alters the expression of *Ebf2*.However, its expression was found to be normal in *Ebf2*$^{-/-}$ mice (Figure 3.11, K compared to L).

I have also analaysed the expression of *Reelin mRNA,* as it is a secreted factor, which plays a pivotal role in the specification of all the CR cell subpopulations. Its expression was found diminished in the septum of *Ebf2*$^{-/-}$ mice compared to wt controls (Figure 3.11, G compared to H). Interestingly, a stronger signal of *Reelin mRNA* was detected in the CH of *Ebf2*$^{-/-}$ mice compared to wt controls (Figure 3.11, I compared to J). Moreover, it was expressed less in the dorsal PPL and more in the

lateral PPL of *Ebf2*$^{-/-}$ mice (Figure 3.11, J; arrow and arrowhead, respectively) compared to wt controls (Figure 3.11, I; arrow and arrowhead, respectively).

Migration was analysed by tracking the position of CR cells using a combination of different CR subpopulation markers such as Calr, Reelin and p73. Firstly, at E13.5, Calr^{+} cells were found in the MZ (Figure 3.12, B' and C') and CH (Figure 3.12, B and C). Cell counts revealed a significant reduction in the number of Calr^{+} cells in the MZ of *Ebf2*$^{-/-}$ mice compared to wt controls (Figure 3.12, A, B', C' and J; *Ebf2*$^{+/+}$ 42±2, *Ebf2*$^{-/-}$ 31±2; n=6; p< 0.001). At the same time, more Calr^{+} cells were found in the CH of mutant animals, suggesting a possible problem in the migration of CR cells from the CH into the cortex (Figure 3.12, A, B, C and J; *Ebf2*$^{+/+}$ 44±3, *Ebf2*$^{-/-}$ 73±3; n=6; p< 0.001). However, Calr alone is not a good marker of CR cells, as it recognises other cell types in the MZ such as SP cells. Reelin^{+} and p73^{+} cells were also examined. Reelin cell number was found to be significantly reduced in the MZ and, on the contrary, increased in the CH and septum of *Ebf2*$^{-/-}$ mice (Figure 3.12, D-F'' and K; MZ, *Ebf2*$^{+/+}$ 88±2, *Ebf2*$^{-/-}$ 79±2; n=6; p<0.01; CH, *Ebf2*$^{+/+}$ 68±1, *Ebf2*$^{-/-}$ 90±1; n=6; p<0.05; Sp, *Ebf2*$^{+/+}$ 64±1, *Ebf2*$^{-/-}$ 86±4; n=6; p<0.05). Six mutants embryos were considered and showed significant differences in Calr and Reelin counts when compared to the respective wt littermates.

Interestingly, p73 cell number was unchanged in the MZ and in the CH, but it was slightly increased in the septum of *Ebf2*$^{-/-}$ mice compared to wt controls (Figure 3.12, G-I'' and L; MZ, *Ebf2*$^{+/+}$ 49±2, *Ebf2*$^{-/-}$ 50±2; n=3; CH, *Ebf2*$^{+/+}$ 126±1, *Ebf2*$^{-/-}$ 120±1; n=3; Sp, *Ebf2*$^{+/+}$ 97±4, *Ebf2*$^{-/-}$ 118±2; n=3; p<0.05). However, this may be explained by the use of unreliable antibody.

CR cell migration in pallial regions is terminated by E16.5, and these cells are positioned in the MZ. Calretinin, Reelin and p73 immunohistochemistry, labelling almost exclusively CR cells in the MZ, did not show any reduction in CR cell numbers in *Ebf2*$^{-/-}$ animals (Figure 3.13 A-C; Calr, *Ebf2*$^{+/+}$ 21±3, *Ebf2*$^{-/-}$ 23±2; n=3; Reelin, *Ebf2*$^{+/+}$ 70±3, *Ebf2*$^{-/-}$ 65±4; n=3; p73, *Ebf2*$^{+/+}$ 44±2, *Ebf2*$^{-/-}$ 46±2; n=3).

In conclusion, it appears that *Ebf2* is not involved in CR cell commitment, but in their early migration. However, the rescue of the migration defect at later stages of development, suggests that this gene alone is not necessary in regulating CR cell migration and function.

Figure 3.11 CR cell fate determination

In situ hybridisation; E12.5 forebrain, coronal section, 40 μm.

A-D: *Dbx1* expression in the septum and PSPB (*Ebf2* is not expressed in this region).
E, F: *Wnt3a* expression in the CH.
G-J: *Reelin mRNA* expression in the CH/PPL and septum, respectively. Arrow indicates dorsal PPL and arrowhead points to lateral PPL.
K, L: *Foxg1* expression in cortical progenitors of the NCx.

CH: cortical hem, *Dbx: developing brain homeobox 1*, *Foxg1: forkhead box G1*, NCx: neocortex, Sp: septum, PPL: preplate, PSPB: pallial subpallial boundary, *Wnt3a: wingless type 3a*.

Scale bar: 100 μm

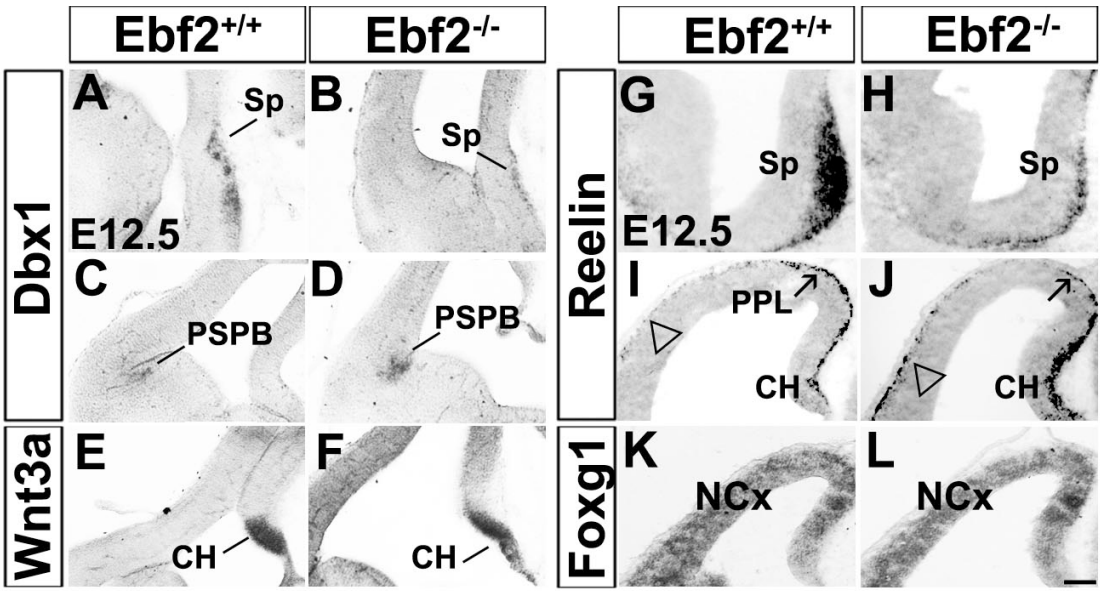
Ebf2+/+
Ebf2-/-
Ebf2+/+
Ebf2-/-
Dbx1
Reelin
Wnt3a
Foxg1
A
Sp
E12.5
B
Sp
G
Sp
E12.5
H
Sp
C
PSPB
D
PSPB
I
PPL
CH
J
CH
E
CH
F
CH
K
NCx
L
NCx

Figure 3.12 CR cell migration

Immunohistochemistry; E13.5, coronal sections, 20 µm.

A, D and G: Schemas indicating the rostro-medial expression areas of Calr, Reelin and p73, respectively.
B-C'; E-F" and H-I": Expression of Calr, Reelin and p73, respectively, in the Sp (E and F, Reelin; H and I, p73), CH (B and C, Calr; E' and F', Reelin; H' and I', p73) MZ (B' and C', Calr; E'' and F'', Reelin; H'' and I'', p73) of *Ebf2*$^{+/+}$ and *Ebf2*$^{-/-}$. Arrows point in each of Calr and Reelin samples to some visible cells that were counted.
J, K and L: Counts of Calr, Reelin and p73, labelled cells in the MZ, CH and Sp.

Calr: calretinin, CH: cortical hem, MZ: marginal zone, Sp: septum.
Scale bars: (B', C', E'', F'', H'', I'') 50 µm, (B, C, E, E', F, F', H, H', I, I') 25 µm

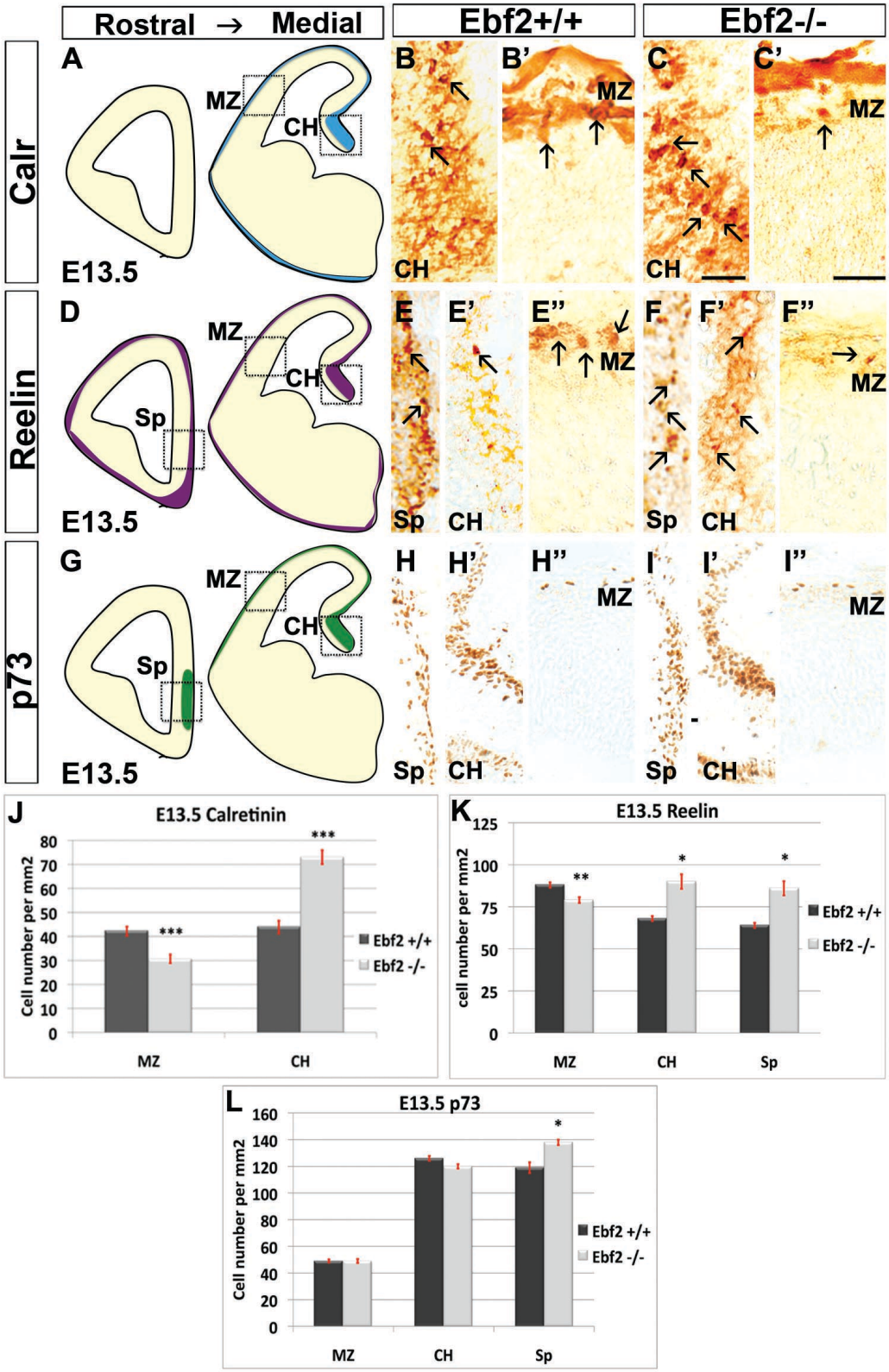
Rostral → Medial
Ebf2+/+
Ebf2-/-
Calr
Reelin
p73
A
B
B'
C
C'
D
E
E'
E''
F
F'
F''
G
H
H'
H''
I
I'
I''
MZ
CH
Sp
E13.5
J
E13.5 Calretinin
Cell number per mm2
Ebf2 +/+
Ebf2 -/-
K
E13.5 Reelin
cell number per mm2
L
E13.5 p73

Figure 3.13 E16.5 CR cell migration

A-C: Calr, Reelin and p73 cell counts in the MZ.

MZ: marginal zone.

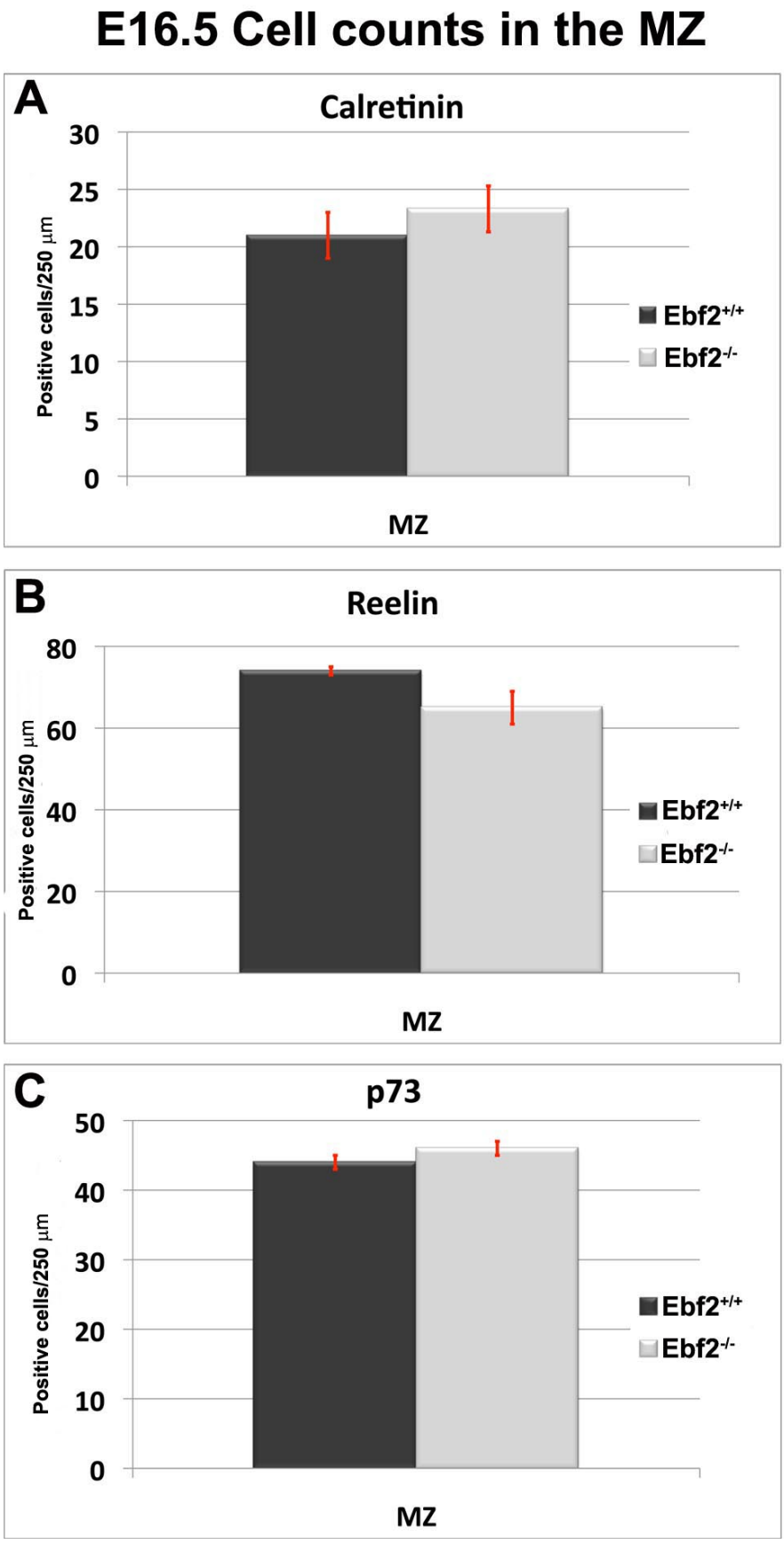
E16.5 Cell counts in the MZ
A
Calretinin
Positive cells/250 µm
30
25
20
15
10
5
0
MZ
Ebf2+/+
Ebf2-/-
B
Reelin
Positive cells/250 µm
80
60
40
20
0
MZ
Ebf2+/+
Ebf2-/-
C
p73
Positive cells/250 µm
50
40
30
20
10
0
MZ
Ebf2+/+
Ebf2-/-

3.3.2 Analysis of the cytoarchitecture of the cerebral cortex of *Ebf2*$^{-/-}$ mice

As previously described, *Ebf2*$^{-/-}$ adult mice appeared smaller compared to wt littermate controls (Corradi et al., 2003; Croci et al., 2006). The overall size and weight of the mutant brains were reduced by approximately 20% compared to wt brains (Figure 3.14, A-C; *Ebf2*$^{+/+}$ 0.525±0.008, *Ebf2*$^{-/-}$ 0.425±0.02; n=10; $p<0.001$). This may be due to the dramatic reduction of the cerebellum, as previously described by Croci and colleagues (2007). The mutant telencephalon did not show any gross defects in the structure (Figure 3.14, A compared to B).

As *Ebf2*$^{-/-}$ mice showed a delayed migration of CR cells at the early stages of development, I have evaluated the presence of phenotypical defects in *Ebf2*$^{-/-}$ cortex by analysing the cortical layer organization postnatally (Figure 3.15). It is known that loss of *Reln* leads to failure of PPL splitting with the formation of a 'superplate' layer and misplaced CP layers in reeler mutants (Caviness and Sidman, 1973). However, it has been shown that ablation of CH or CR cells loss does not necessary lead to major cortical defects, indicating that even a small amount of Reelin may be sufficient for the formation of the correct cortical lamination (Yoshida et al., 2006).

Postnatally, cortical six layer organisation was maintained in *Ebf2*$^{-/-}$ mutants (Figure 3.15, A compared to B). Moreover, immunostaining with specific markers for upper, Cux1, and lower cortical layers, Ctip2, showed that these were not inverted in mutants compared to controls (Figure 3.15, C-F). Although the number of Ctip2 and Cux1 positive cells were unchanged in *Ebf2*$^{-/-}$ mice (Figure 3.15, G and H; Ctip2, *Ebf2*$^{+/+}$ 446±22, *Ebf2*$^{-/-}$ 412±34; n=3; Cux1, *Ebf2*$^{+/+}$ 1474±72, *Ebf2*$^{-/-}$ 1346±65; n=3), an overall reduction of 10% of the cortical thickness along the entire rostro-caudal length of the telencephalon was observed in *Ebf2*$^{-/-}$ (Figure 3.14, D-F; *Ebf2*$^{+/+}$ 970±11, *Ebf2*$^{-/-}$ 935±12; n=10; $p<0.01$). White matter thickness was unchanged in *Ebf2*$^{-/-}$ mutants (Figure 3.14, D-F; *Ebf2*$^{+/+}$ 180±4, *Ebf2*$^{-/-}$ 176±3; n=10). Interestingly, the total thalamo-hypothalamic area was found significantly reduced in *Ebf2*$^{-/-}$ mice compared to wt controls (Figure 3.14, G- I; *Ebf2*$^{+/+}$ 6.17±0.1, *Ebf2*$^{-/-}$ 5.22±0.1; n=10; $p<0.001$).

Figure 3.14 *Ebf2*$^{-/-}$ cortices are reduced in size compared to littermate controls

Nissl staining, coronal sections, 40 μm.

A-C: The brain weight of *Ebf2*$^{-/-}$ mice was significantly reduced (C, $p<0.001$).
D-F: Only the cortical, but not the white matter thickness, was found to be reduced in *Ebf2*$^{-/-}$ mice ($p<0.01$).
G-I: Black dots in **G** and **H** outline the thalamic and hypothalamic areas which are reduced in *Ebf2*$^{-/-}$ mice (I).

Cb: cerebellum, cc: corpus callosum, H: hippocampus, Hb: habenula, Hy: hypothalamus, LV: lateral ventricle, NCx: neocortex, OB: olfactory bulb, SC: spinal cord, St: striatum, TC: telencephalon, Th: thalamus, wm: white matter.

Scale bars: (A, B) 50 mm, (D, E, G, H) 500 μm

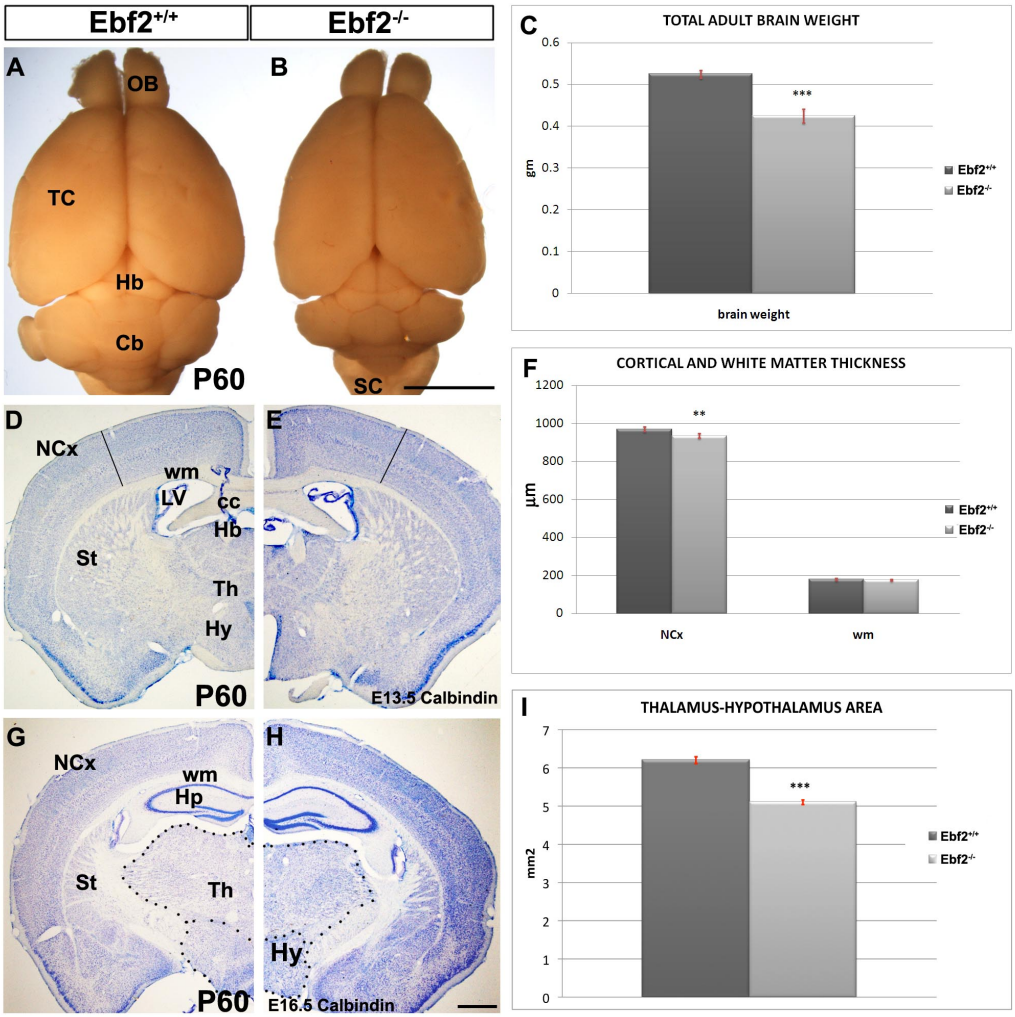
Ebf2+/+
Ebf2-/-
A
OB
TC
Hb
Cb
P60
B
SC
C
TOTAL ADULT BRAIN WEIGHT
0.6
0.5
0.4
0.3
0.2
0.1
0
gm
***
brain weight
Ebf2+/+
Ebf2-/-
D
NCx
wm
LV
cc
Hb
St
Th
Hy
P60
E
E13.5 Calbindin
F
CORTICAL AND WHITE MATTER THICKNESS
1200
1000
800
600
400
200
0
µm
**
NCx
wm
Ebf2+/+
Ebf2-/-
G
NCx
wm
Hp
St
Th
P60
H
Hy
E16.5 Calbindin
I
THALAMUS-HYPOTHALAMUS AREA
7
6
5
4
3
2
1
0
mm2
***
Ebf2+/+
Ebf2-/-

Figure 3.15 Postnatal (adult) cortical layer organisation in *Ebf2* $^{-/-}$ mutants

Immunohistochemistry and Nissl staining, coronal sections, 40 μm.

A, B: The adult *Ebf2* $^{-/-}$ mouse cortex is a six-layer structure, similar to control brains.
C-F: Layers in *Ebf2* $^{-/-}$ mutants are correctly positioned, as confirmed by Ctip2 and Cux1 staining. Despite the reduction in cortical thickness in *Ebf2* $^{-/-}$ mice, cell number in upper and lower cortical layers is not reduced (G and H, respectively).

Ctip2: COUP-TF interacting protein 1, Cux1: Cut-like homeobox 1.

Scale bar: 100 μm.

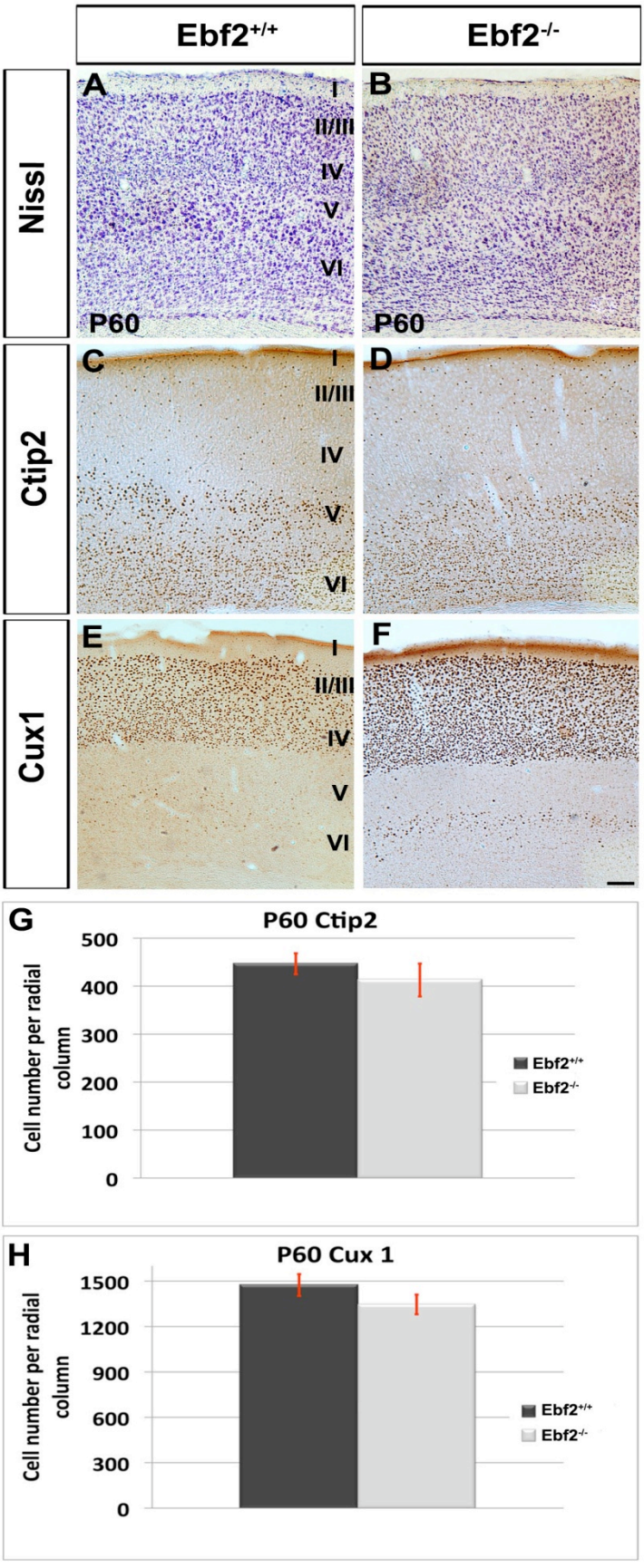
Ebf2+/+
Ebf2-/-
Nissl
Ctip2
Cux1
A
B
C
D
E
F
I
II/III
IV
V
VI
P60
G
P60 Ctip2
Cell number per radial column
500
400
300
200
100
0
Ebf2+/+
Ebf2-/-
H
P60 Cux 1
Cell number per radial column
1500
1200
900
600
300
0
Ebf2+/+
Ebf2-/-

3.3.3 Interneuron migration and organisation is not affected in *Ebf2* $^{-/-}$ mice

Ebf2 is expressed during embryonic development in the PPL and MZ. These layers are used as a route for migration/settlement of three different cell populations, namely CR cells, SP cells and interneurons. In Paragraph 3.2.2 (Figure 3.9), I have shown that *Ebf2* is expressed in CR cells and SP cells, but not in interneurons. However, interneuron development and migration was analysed in *Ebf2*$^{-/-}$ mutants in order to exclude non-cell autonomous effects of *Ebf2* loss of function on this cell population.

Calbindin, a calcium binding protein is expressed in cortical interneurons during embryonic development and adult life. It has been used as a specific interneuron marker, particularly in embryonic stages (Anderson *et al.* 1997; Andrews *et al.* 2006). At E13.5 and E16.5, immmunohistochemistry experiments did not reveal a reduction of Calb expression or impaired migration of Calb^{+} cells in *Ebf2*$^{-/-}$ animals in the cortex (Figure 3.16, E16.5, C, D and F; *Ebf2*$^{+/+}$ 155±6, *Ebf2*$^{-/-}$ 152±7; n=3). Specifically at E13.5, Calb^{+} cells were found in the MZ and IZ, and they were counted in two adjacent (a and b) regions in order to exclude a possible delay in the migration of interneurons from the GE (Figure 3.16, A, B and E; a: MZ, *Ebf2*$^{+/+}$ 101±3, *Ebf2*$^{-/-}$ 109±3; IZ, *Ebf2*$^{+/+}$ 78±3, *Ebf2*$^{-/-}$ 76±3; b: MZ, *Ebf2*$^{+/+}$ 44±2, *Ebf2*$^{-/-}$ 38±3; IZ, *Ebf2*$^{+/+}$ 27±3, *Ebf2*$^{-/-}$ 25±1; n=6)

Postnatally, interneurons, labelled with antibodies to Calb, Calr and Pv, which together stain the vast majority of the adult GABAergic interneurons, did not show any abnormalities in laminar position and number in *Ebf2*$^{-/-}$ mice compare to wt controls (Figure 3.17; Calb, *Ebf2*$^{+/+}$ 77±2, *Ebf2*$^{-/-}$ 82±3; Calr, *Ebf2*$^{+/+}$ 95±3, *Ebf2*$^{-/-}$ 89±3; b: Pv, *Ebf2*$^{+/+}$ 231±9, *Ebf2*$^{-/-}$ 238±10; n=3).

Figure 3.16 Interneuron migration is not affected in *Ebf2* $^{-/-}$ mutants

Immunohistochemistry and Nissl staining, coronal sections, 20 µm.

A-F: During embryonic life, Calb^{+} cells are found migrating in the MZ and IZ. There are no significant changes in their number in *Ebf2* $^{-/-}$ mice compared to wt controls. Arrows point to visible cells.
At E13.5, cells were counted in two different areas, a) at the PSPB, and b) in the NCx.

Calb: calbindin, CP: cortical plate, IZ: intermediate zone, MZ: marginal zone, SP: subplate layer.

Scale bars: 100 µm

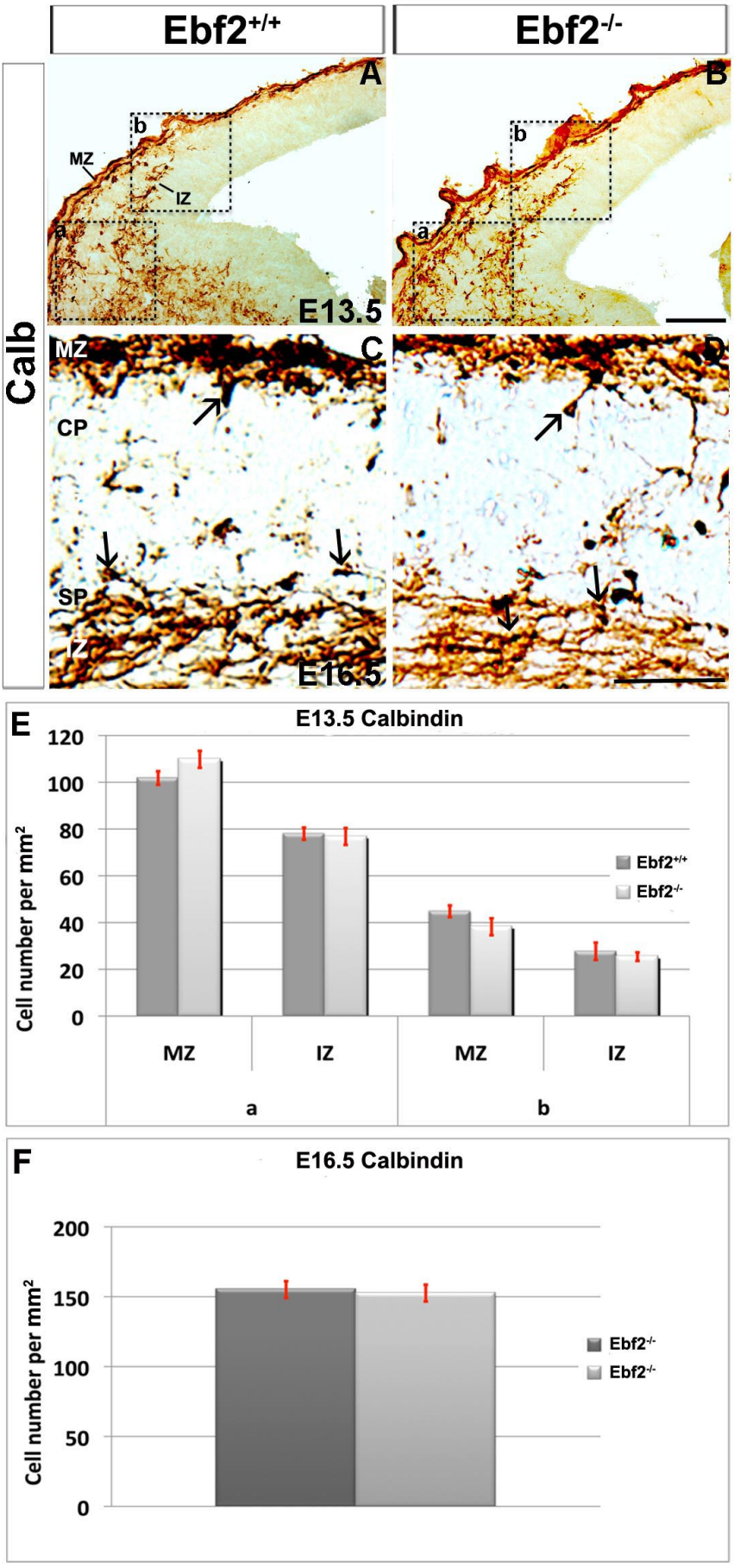
Ebf2+/+
Ebf2-/-
Calb
A
B
C
D
MZ
IZ
a
b
CP
SP
E13.5
E16.5
E
E13.5 Calbindin
Cell number per mm2
120
100
80
60
40
20
0
MZ
IZ
MZ
IZ
a
b
Ebf2+/+
Ebf2-/-
F
E16.5 Calbindin
Cell number per mm2
200
150
100
50
0
Ebf2-/-
Ebf2-/-

Figure 3.17 Postnatal settlement and numbers of interneurons are not affected in *Ebf2* $^{-/-}$ mutants

Immunohistochemistry and Nissl staining; coronal sections, 40 μm.

A-I: Three different markers, Calb, Calr and Pv, were used in order to stain the vast majority of adult cortical interneurons. Cell counts of the three different populations did not reveal significant changes between *Ebf2* $^{-/-}$ mice and wt littermates.

Calb: calbindin, Calr: calretinin, Pv: paravalbumin.

Scale bar: 100 μm

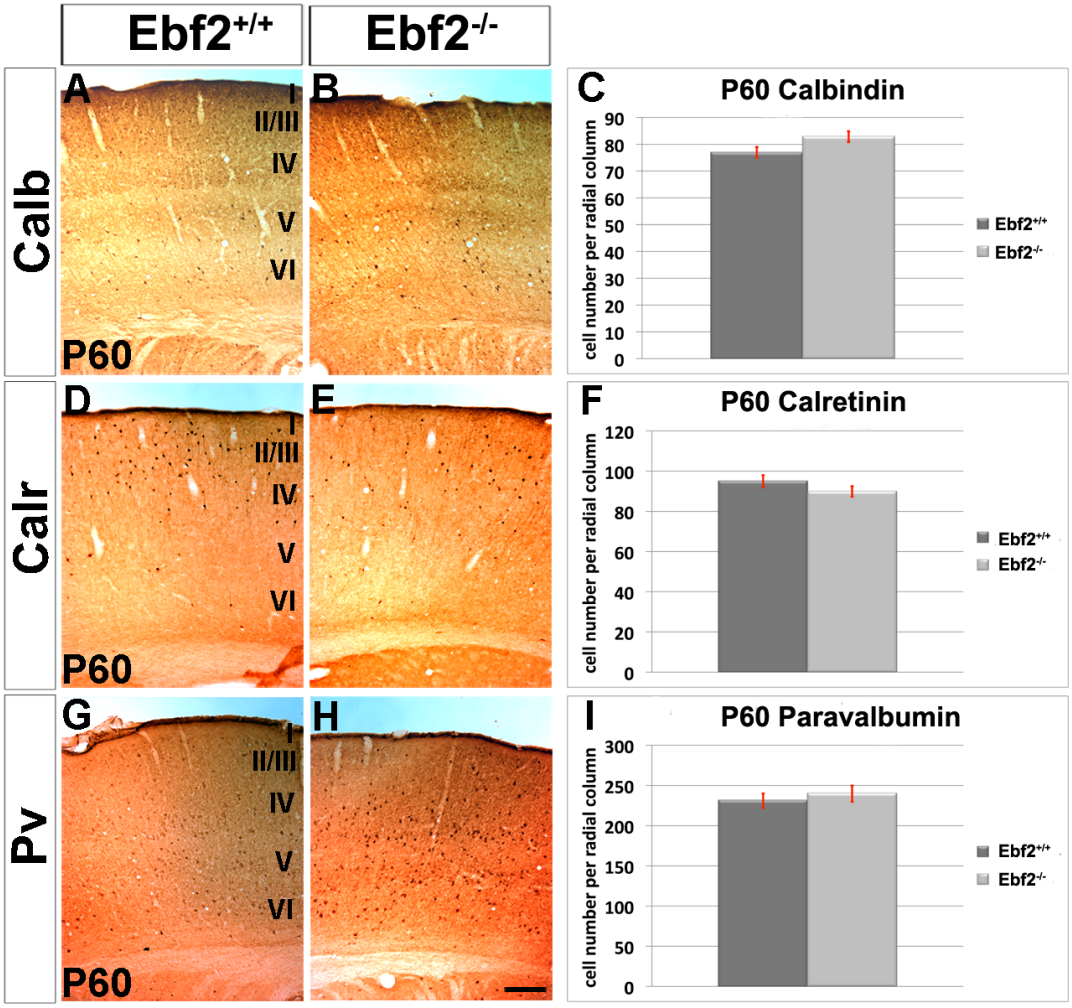
Ebf2+/+
Ebf2-/-
Calb
Calr
Pv
A
B
C
D
E
F
G
H
I
I
II/III
IV
V
VI
P60
P60 Calbindin
P60 Calretinin
P60 Paravalbumin
cell number per radial column
Ebf2+/+
Ebf2-/-

3.3.4 Analysis of SP cells and thalamocortical connections in *Ebf2*$^{-/-}$ mice

Subplate cells, as described in Chapter 1, play a pivotal role during development in guiding the formation of thalamic connections to the correct areas of the cerebral cortex. I have shown and confirmed in the *Ebf2*^{GFPiCRE} line co-expression of Calr or Nurr1 with *Ebf2* in the SP layer during embryonic and postnatal development. At E16.5, SP layer was fully developed, and cells were clearly visible and labelled with Calr. There were no significant changes detected in the cell number in *Ebf2*$^{-/-}$ mice compared to wt littermate controls (Figure 3.18; *Ebf2*$^{+/+}$ 45±3, *Ebf2*$^{-/-}$ 41±2; n=3). Postnatally, the number of Nurr1 positive cells was counted in mutants and compared to wt animals. Changes in position or cell number were not detected in *Ebf2*$^{-/-}$ mice (Figure 3.19; *Ebf2*$^{+/+}$ 104±12, *Ebf2*$^{-/-}$ 103±11; n=3).

In order to exclude thalamic defects, suggested also by the thalamic area reduction seen in mutants, the correct formation of the barrel cortex was analysed. The barrel cortex refers to dark-stained regions found in layer IV of the somatosensory cortex that receive inputs from the thalamus. Barrels are found in rodents and other species that specifically rely on whiskers for proprioception. Inputs from the thalamus carrying information from a given whisker terminate of layer IV forming anatomically distinguishable areas (barrels), which are separated from each other by septa. Neurons within the layer IV barrel cortex directly code for whisker displacement. Postnatally, barrels were visualized by DAPI and cytochrome oxidase (CO) staining in mutants and control animals (Figure 3.20). In mutants, barrels are clearly visible in the DAPI and CO staining (Figure 3.20, A compared to B is a DAPI staining; C compared to D detectes the CO activity; squares and arrows delineate the barrels in C and D), and they are organised with the expected structure (the septa are clearly visible between barrels).

Figure 3.18 Embryonic SP cells counts

Immunohistochemistry; coronal sections, 20 μm.

A, B: $Calr^{+}$ cells are clearly visible in the SP layer.
C: Cell counts do not reveal significant changes in *Ebf2*$^{-/-}$ compared to wt controls.

Calr: calretinin, SP: subplate.

Scale bar: 100 μm

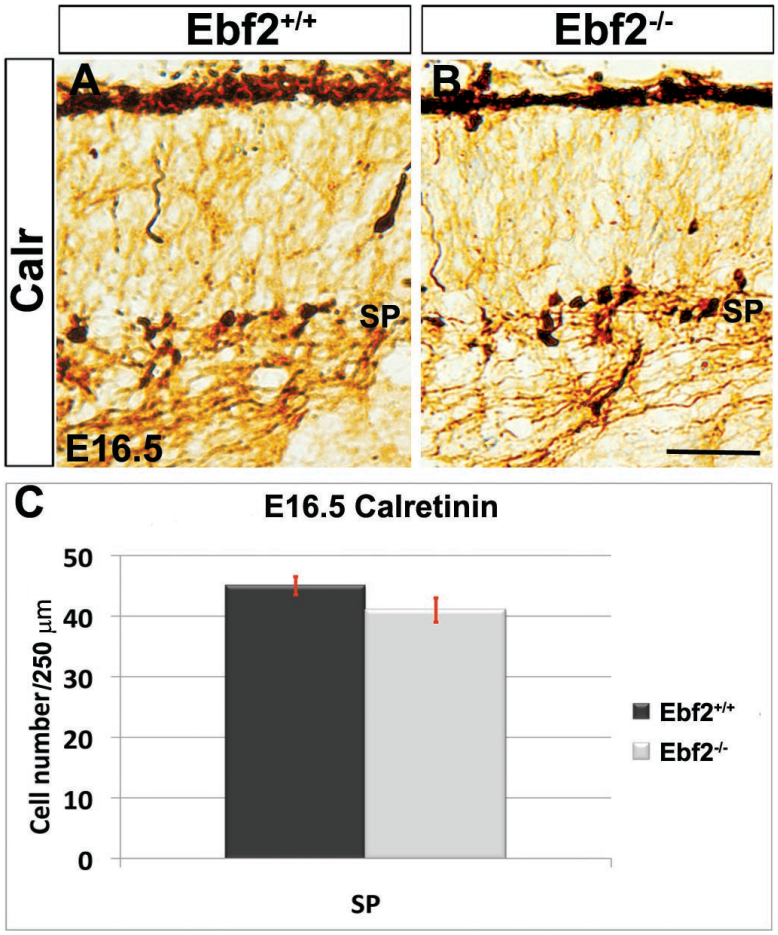
Ebf2+/+
Ebf2-/-
Calr
A
B
SP
SP
E16.5
C
E16.5 Calretinin
Cell number/250 µm
50
40
30
20
10
0
SP
Ebf2+/+
Ebf2-/-

Figure 3.19 Postnatal SP cells counts

Immunohistochemistry; coronal sections, 40 µm.

A, B: Nurr1 is a specific marker of postnatal SP cells.
C: Cell counts do not reveal significant changes in *Ebf2*$^{-/-}$ mice compared to wt controls.

Nurr1: nuclear related receptor 1, SP: subplate.

Scale bar: 150 µm

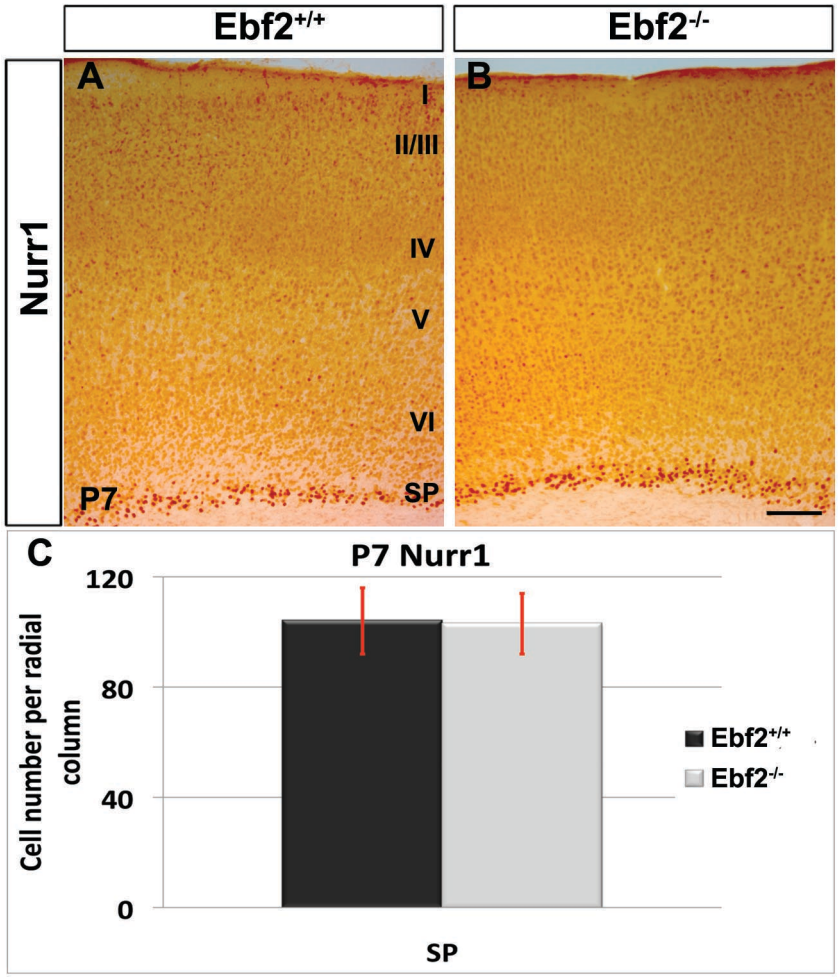
Ebf2+/+
Ebf2-/-
A
B
Nurr1
I
II/III
IV
V
VI
SP
P7
C
P7 Nurr1
120
80
40
0
Cell number per radial column
Ebf2+/+
Ebf2-/-
SP

Figure 3.20 Barrel cortex in *Ebf2*$^{-/-}$ mice

DAPI and CO staining; coronal sections, 40 µm.

A, B: DAPI staining show barrel columns, delimited by the square, in wt and mutant slice.
C, D: Pattern of CO activity in layer IV of wt controls and *Ebf2* mutants. High enzymatic activity characterise the darker areas, called barrels, delimited by black square. The barrels are separated by low metabolic activity regions called septa.

CO: cytochrome oxydase, DAPI: 4',6-diamidino-2-phenylindole.

Scale bars: 100 µm

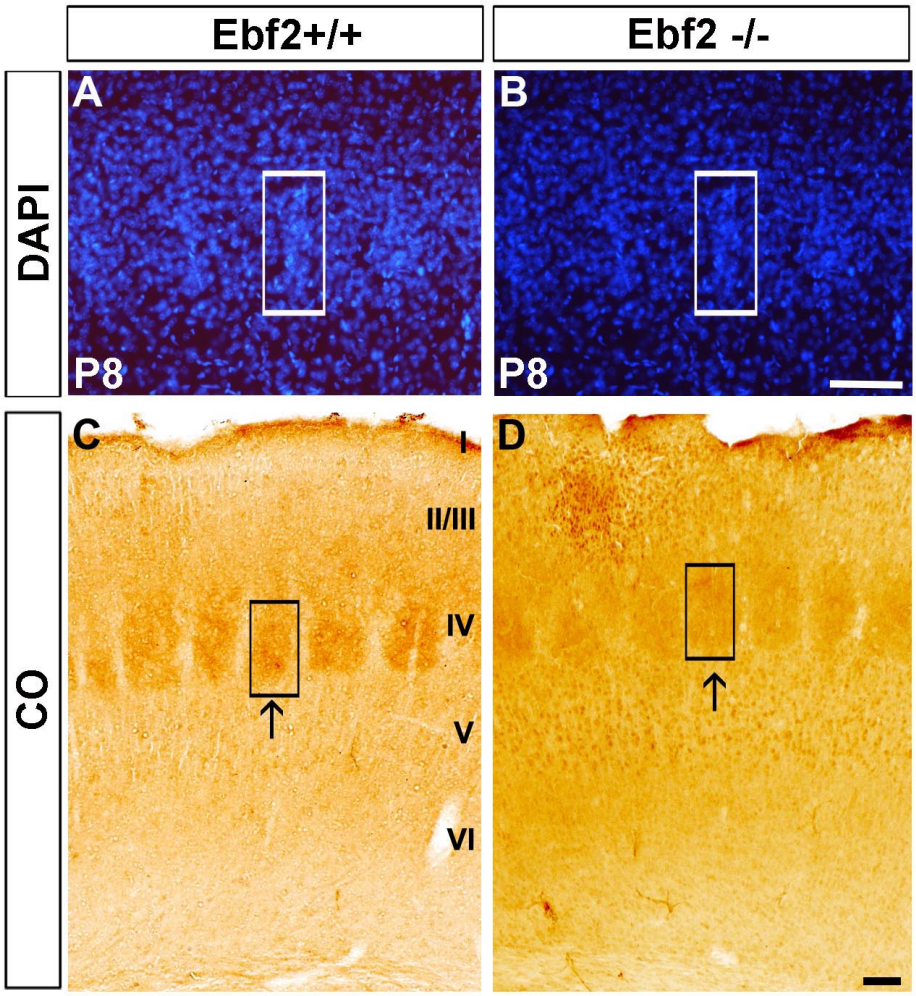
Ebf2+/+
Ebf2 -/-
DAPI
CO
A
B
C
D
P8
P8
I
II/III
IV
V
VI

3.4 DISCUSSION

3.4.1 *Ebf2* is expressed in CR cells and other cortical cell populations during forebrain development

In this chapter, I have shown that *Ebf2* is expressed in the developing mouse forebrain between E10.5 and P0. In the telencephalon, it is expressed in post-mitotic regions of the pallium, such as septum (rostrally), CH (caudally), PPL/MZ (along the entire rostro-caudal axis) and PCx until E14.5. In the diencephalon, it is expressed in the epithalamus, hypothalamus and TE. The expression of *Ebf2* matches the expression of Reelin in CH, PPL/MZ, dorsal part of the septum but, interestingly, not in PSPB/PCx. Reelin, commonly used to label CR cells, is an important secreted factor that plays a pivotal role in cortical layer organisation. Thus, this data have shown a strong correlation between *Ebf2* expression and position of CR cells. However, due to the early cortical downregulation of the gene and the absence of an efficient antibody able to discriminate EBF proteins, the tracking of the *Ebf2* protein expression was so far difficult. Using as genetic approach the mouse transgenic line $Ebf2^{GFPiCre/R26R\text{-}YFP}$ (Chiara F, Badaloni A and Consalez G, unpublished data), I was able for the first time to effectively and permanently labelled *Ebf2* expressing cells in the forebrain. In fact, I have shown that *Ebf2* is expressed in CR cells that have most likely originated from the septum and CH. Three main sites of origin of CR cells have been proposed, namely septum, CH and PSPB; and *Ebf2* is expressed in all but one (PSPB). Three different markers, widely used for labelling CR cells, such as Reelin, Calr and p73, have been used in this chapter to follow the expression of *Ebf2* in CR cells. The expression of these markers was compared with the expression of YFP of caudo-medial coronal sections only, containing mostly CH-derived CR cells (Bielle et *al.*, 2005; Yoshida et *al*., 2006; Griveau et *al*., 2010). Calretinin and Reelin have shown a partial match with *Ebf2* expression, and this is explained as follows. Calretinin labels CR cells derived from CH and PSPB, but not from septum. Thus, $Calr^{+}/Ebf2^{+}$ cells come from the septum and $Calr^{+}/Ebf2^{-}$ cells from the PSPB. Reelin is a broad marker of CR cells originating from septum, CH and PSPB. Thus,

Reelin^{+}/*Ebf2*$^{-}$ cells come from the PSPB. p73 is a specific marker of CR cells derived from the septum and CH; and p73 completely co-localised with *Ebf2* in CH-derived cells and partially in septum-derived cells as *Ebf2* is detected only dorsally in this area.

A recent paper by the Portera-Cailliau group (Chowdhury *et al.* 2010), using a similar transgenic line expressing only the GFP protein under the control of the *Ebf2* promoter, has shown similar results. In contrast with my data, they showed a persistent postnatal expression of *Ebf2* in PPL/MZ cells based only on the study of the mere transgenic expression of the protein GFP. However, it is know that GFP is a stable protein, which is expressed much longer after its mRNA production has ceased (Jusuf *et al.* 2009). In fact, my data have indicated a downregulation of the *Ebf2* promoter activity confirmed in both wt animals and the transgenic line *Ebf2*^{GFPiCre} by the lack of *mRNA* expression after E14.5 in pallial structures. The permanent labelling of *Ebf2*-expressing cells was achieved only by crossing the transgenic line with the reporter line *R26R*^{YFP} allowing a permanent modification of the *Rosa26* locus in *Ebf2*$^{+}$ cells by the Cre recombinase. Even though the these two transgenic lines share similarities, analysis of the cell fate of *Ebf2*$^{+}$ cells is only possible by using the *Ebf2*^{GFPiCre} mice described in this thesis.

Ebf2 is also expressed in SP cells, as confirmed by the embryonic marker Calr and the postnatal marker Nurr1 (Hoerder-Suabedissen *et al.* 2009), and by a subpopulation of layer V pyramidal neurons. *Ebf2* expression in subpallial structures (identified in the adult as BNST and ZI) as well as in diencephalic areas was not analysed in detail, as this study focused primarily on cerebral cortex development.

3.4.2 Early CR cell migration defect is rescued at later stages of development in *Ebf2*$^{-/-}$ mice

Cajal-Retzius cell migration was affected during early development in *Ebf2*$^{-/-}$ mice. At E13.5 the number of Calr^{+} and Reelin^{+} cells was significantly reduced in the PPL/MZ of *Ebf2*$^{-/-}$ animals compared to wt controls, whereas the number of Calr^{+} and Reelin^{+} cells was increased in the septum and CH of mutant animals. At E16.5, the number of Calr^{+} and Reelin^{+} cells in the MZ of *Ebf2*$^{-/-}$ was unchanged compared

to control littermates. Borrell and Marin (2006) show that the meningeal membranes are a necessary and sufficient substrate for the tangential migration of hem-derived CR cells in a CXCR4-dependent manner. My data suggest a delayed migration of CR cells that seem to be retained for longer in the septum and the CH. Thus, *Ebf2* may control CR cell migration targeting directly the expression of CXCR4. Future experiments should analyse in *Ebf2*$^{-/-}$ the integrity of the expression of CXCR4 receptor and the ability of CR cells to respond to its ligand SDF-1. However, the migratory defect is rescued at later stages of development due most likely to a compensatory expression of other genes involved in similar functions. Reelin^{+} cell number defects are in accordance with the changes in the expression of its *mRNA* in the PPL/MZ and CH. In fact, *Reelin mRNA* was expressed more in the CH and less in the dorsal PPL of *Ebf2*$^{-/-}$ mice compared to wt controls suggesting a delay in the migration of CR cells. Interestingly, more signal was, instead, detected in the lateral PPL indicating a possible increase in the migration of CR cells from other sources, such as the PSPB (Griveau *et al*, 2010). This could explain as well the changes detected in the expression of *Dbx1* and *Wnt3a* in the septum/PSPB and CH, respectively, at early developmental stages. However, as only caudo-medial coronal sections were considered, the migration defect was probably CH specific, whereas the changes detected in the other areas were due to rescue mechanisms by a pallial redistribution of other CR cell subpopulations (Yoshida *et al*., 2006; Griveau *et al*, 2010). This hypothesis will be explained in detail in Chapter 4 (see Discussion 4.4.2). Cortical layer organisation was not affected in *Ebf2*$^{-/-}$ by the migratory delay of CR cells. Interestingly, the number of p73^{+} cells in the MZ and CH in *Ebf2*$^{-/-}$ mice remain unaltered, whereas a significant increase in p73 cells was detected only in the septum. However, this may be explained by the use of unreliable antibody.

3.4.3 Subplate cells develop normally in *Ebf2*$^{-/-}$

Subplate neurons are the first cortical neurons to send corticofugal projections, thus pioneering the thalamocortical connections (McConnell *et al.* 1994). Furthermore, a large number of cortical afferents reside in the SP layer and form transient synaptic interactions with SP cells. For thalamic fibers, this is crucial for the

entry of axons to the overlying cortex and their later segregation into layer IV. There is general agreement that most SP cells disappear during postnatal stages by cell death, a few remaining in the adult white matter as interstitial neurons. I have shown that *Ebf2* is expressed in SP cells during development. However, Calr in embryos and Nurr1 in postnatal animals did not reveal significant changes in cell counts or localisation of SP cells in *Ebf2*$^{-/-}$.

Thalamo-cortical axon development in the cortex was not affected in *Ebf2*$^{-/-}$ as revealed by the analysis of the barrel cortex organisation in *Ebf2*$^{-/-}$. Together, these data suggest that *Ebf2* alone may not be required for the correct development of the SP cell population.

3.4.4 Telencephalic organisation is not affected in adult *Ebf2*$^{-/-}$

The overall brain size and the cortical thickness was reduced by approximately 20% in *Ebf2*$^{-/-}$ mice, but counts of pyramidal cells and interneurons as well as Nissl staining analysis did not reveal significant changes in the cell number or distribution. However, the absence of misplaced cortical cells as a result of migratory defects may not be completely excluded. In fact, the techniques used in this thesis were not sensitive enough to detect small changes in the position for example of layer IV or V pyramidal cells that express *Ebf2*. Bromodeoxiurydine (BrdU) injections at different developmental time points and analysis of the position of the BrdU labelled cells in the adult cortex will help to clarify this hypothesis.

The overall reduction of the brain and cortical thickness size could be explained by the fact that *Ebf2*$^{-/-}$ mice are smaller compared to wt littermates, so that the organs adapt to the size of the mutant animal. A bone mass reduction and an increased number of osteoclasts were also detected. Thus, bone development defects could influence the final size of *Ebf2*$^{-/-}$ mice (Kieslinger *et al.* 2005). Moreover, *Ebf2*$^{-/-}$ mice show hypogonadotropic hypogonadism as a consequence of GnRH neuron death during development. This results in decrease or lack of gonadal stimulating pituitary hormones: follicle stimulating hormone (FSH) and luteinizing hormone (LH).

Failure of the hypothalamus-gonads negative feedback regulation could lead to reduce body mass.

3.4.5 Conclusions

The mild defects observed in *Ebf2*$^{-/-}$ mice prompted me to analyse the expression and function in cerebral cortex development of other members of the COE family, *Ebf1* and *Ebf3*. In fact, previous studies suggest that *Ebf1* and *Ebf3* are expressed in overlapping territories of the developing forebrain and may play a redundant role. This hypothesis was analysed in Chapter 4.

CHAPTER 4

A REDUNDANT FUNCTION OF EBF FACTORS IN THE COMMITMENT AND MIGRATION OF CR CELLS

4.1 INTRODUCTION

As presented in Chapter 3, I found that *Ebf2* was transiently expressed in different areas of the developing forebrain. Interestingly, in addition to its expression in the PPL/MZ of the telencephalon, it was found in the septum and CH, known sites for the origin of CR cells. Fate mapping studies on *Ebf2* expressing cells, using the transgenic mouse line $Ebf2^{GFPiCre/R26R\text{-}YFP}$, have revealed that the gene is specifically expressed in the CH and septum-derived CR cell subpopulations, SP cells and a subpopulation of layer V pyramidal neurons. However, the analysis of the development and functions of these cell groups in $Ebf2^{-/-}$ mice did not show any abnormalities, with the exception of a transitory delay in the migration of CR cells from the CH and septum into the PPL/MZ. The mild defects observed in the telencephalon of $Ebf2^{-/-}$ mice suggest that other factors expressed in the telencephalon may compensate its loss of function. Previous studies have implied that *Ebf1* and *Ebf3* are expressed in overlapping territories of the developing forebrain and may play redundant roles (Garel *et al.* 1997). In fact, it has been shown that the mouse EBF proteins show 75% identity. EBF1 and EBF3 are the most similar, whereas EBF2 differs at the carboxy-terminal domain used to interact with other proteins (Crozatier and Vicent, 1999; Dubois and Vicent, 2001). For instance, the olfactory epithelium of $Ebf1^{-/-}$ mice is reported to develop normally due to the redundant function of *Ebf3* (Garel *et al.* 1997; 1999). In contrast, *Ebf2* plays a specific function in this territory. In fact, the olfactory epithelium of $Ebf2^{-/-}$ mice

gives rise to defective GnRH neurons, which are unable to migrate towards their positions in the hypothalamus. Thus, these factors could very well compensate for each other during telencephalic development.

In order to test this hypothesis, I have analysed in this chapter the expression of *Ebf1* and *Ebf3* in the telencephalon of wt and *Ebf2*$^{-/-}$ mice. According to their patterns of expression, I have tested *in vitro* and *in vivo* whether the overexpression or downregulation of the EBFs may affect CR cell specification and migration.

4.2 COE MEMBERS *Ebf1* AND *Ebf3* ARE EXPRESSED IN THE DEVELOPING TELENCEPHALON IN *Ebf2*$^{+}$ TERRITORIES

4.2.1 Analysis of *Ebf1* and *Ebf3* mRNA expression in the developing mouse telencephalon

Previous studies by Garel and colleagues (Garel *et al.* 1997) have reported that *Ebf1* and *Ebf3* are transiently expressed together with *Ebf2* during forebrain development. As mild defects were observed in the migration of CR cells at early embryonic stages (see Chapter 3), I have focused the analysis of their expression in the cerebral cortex. To identify the pattern of expression of *Ebf1* and *Ebf3* in the pallium, brains of mice at different ages were analysed using *in situ* hybridisation. *Ebf1* and *Ebf3* were detected from E10.5 to E15.5, when they were downregulated in a similar fashion as it was previously reported in Chapter 3 for *Ebf2* (Chapter 3.2.1). At E13.5, *Ebf1* and *Ebf3* expression was similar to that of *Ebf2* in the CH and PPL (Figure 4.1, A and C compared to B). Additionally, *Ebf3* was detected in the PSPB (Figure 4.1, C'), which is one of the site of origin of CR cells. In the septum, *Ebf3* was expressed strongly dorso-ventrally (Figure 4.1, F; rectangle), *Ebf2* was detected just in the most dorsal area (Figure 4.1, E; rectangle), whereas *Ebf1* was weakly expressed dorso-ventrally (Figure 4.1, D; rectangle). At E15.5, *Ebf1* expression was downregulated in the pallium (Figure 4.2, A) similar to *Ebf2* (Figure 4.2, B), whereas *Ebf3* was still detected in the CH and MZ (Figure 4.2, C; arrow and arrowhead,

respectively). *Ebf3* expression persisted in these areas also after birth (data not shown).

4.2.2 *Ebf1* and *Ebf3* expression in *Ebf2*$^{-/-}$ mice

Ebf1 and *Ebf3* expression was also analysed in *Ebf2*$^{-/-}$ mice in order to assess whether its loss of function could lead to differences in the *mRNA* expression of these two factors. At E13.3, *in situ* hybridisation experiments showed that *Ebf1* and *Ebf3* were expressed in the CH and PPL (Figure 4.3, A and E compared to B and F, respectively). However, their expression was found diminished in the septum of *Ebf2*$^{-/-}$ mice compared to wt controls (Figure 4.3, C and G compared to D and H, respectively). Furthermore, *Ebf3* expression in the PSPB was increased in *Ebf2*$^{-/-}$ mice compared to wt controls (Figure 4.3, G compared to H).

Figure 4.1 *Ebfs* expression in the cortex at E13.5

In situ hybridisation; coronal sections, 40 μm.

A-C: *Ebf1, Ebf2* and *Ebf3* expression in PPL and CH. *Ebf3* is also detected in PSPB (C')
D-F: *Ebf1, Ebf2* and *Ebf3* expression in the septum. Rectangle divides the area in dorsal (d) and ventral (v)

CH: cortical hem, PCx: pyriform cortex, PPL: preplate, PSPB: pallial subpallial boundary, Sp: septum, St: striatum.

Scale bars: 100 μm

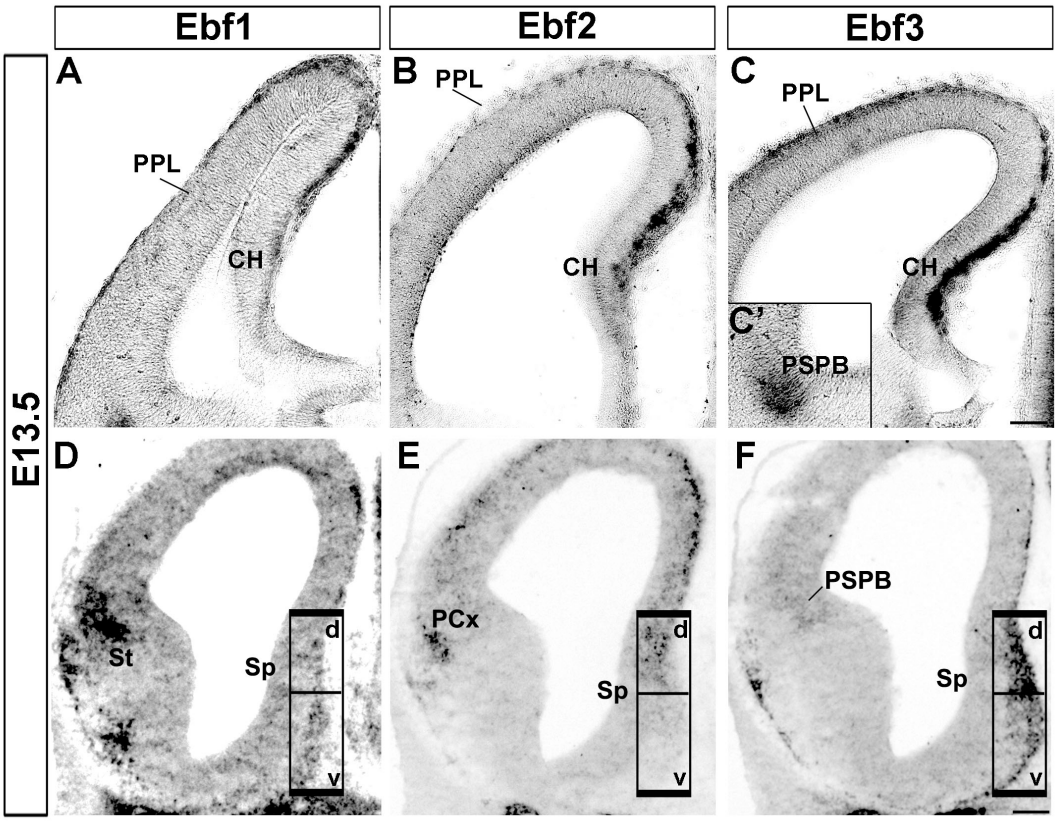
Ebf1
Ebf2
Ebf3
E13.5
A
B
C
C'
D
E
F
PPL
CH
PSPB
St
Sp
PCx
d
v

Figure 4.2 *Ebfs* expression in the cortex at E15.5

In situ hybridisation; coronal sections, 40 µm.

A, B: *Ebf1* and *Ebf2* are downregulated in the MZ and CH
C: *Ebf3* is detected in the CH (arrow) and in MZ (arrowhead)

CH: cortical hem, MZ: marginal zone, St: striatum.

Scale bars: 200 µm

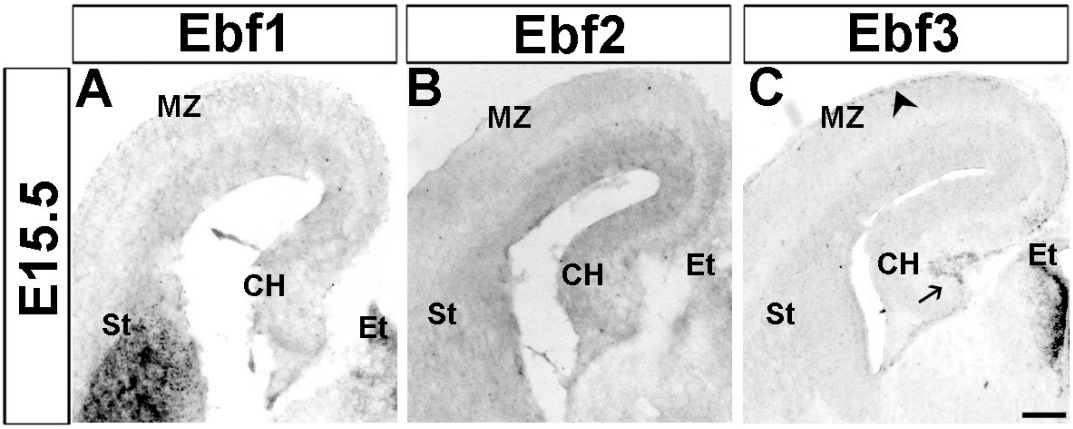
Ebf1
Ebf2
Ebf3
E15.5
A
B
C
MZ
MZ
MZ
CH
CH
CH
St
St
St
Et
Et
Et

Figure 4.3 *Ebf1* and *Ebf3* expression in the cortex of *Ebf2*$^{-/-}$ mice at E13.5

In situ hybridisation; coronal sections, 40 µm.

A-F: *Ebf1* and *Ebf3* are detected in the PPL and CH in wt and in *Ebf2*$^{-/-}$ mice
C-H: *Ebf1* and *Ebf3* are expressed in the septum of wt and in *Ebf2*$^{-/-}$ mice. However, expression in *Ebf2*$^{-/-}$ mice is diminished compared to wt controls, whereas Ebf3 expression is augmented in the PSPB of *Ebf2*$^{-/-}$ mice.

CH: cortical hem, Sp: septum, PPL: preplate.

Scale bar: 100 µm

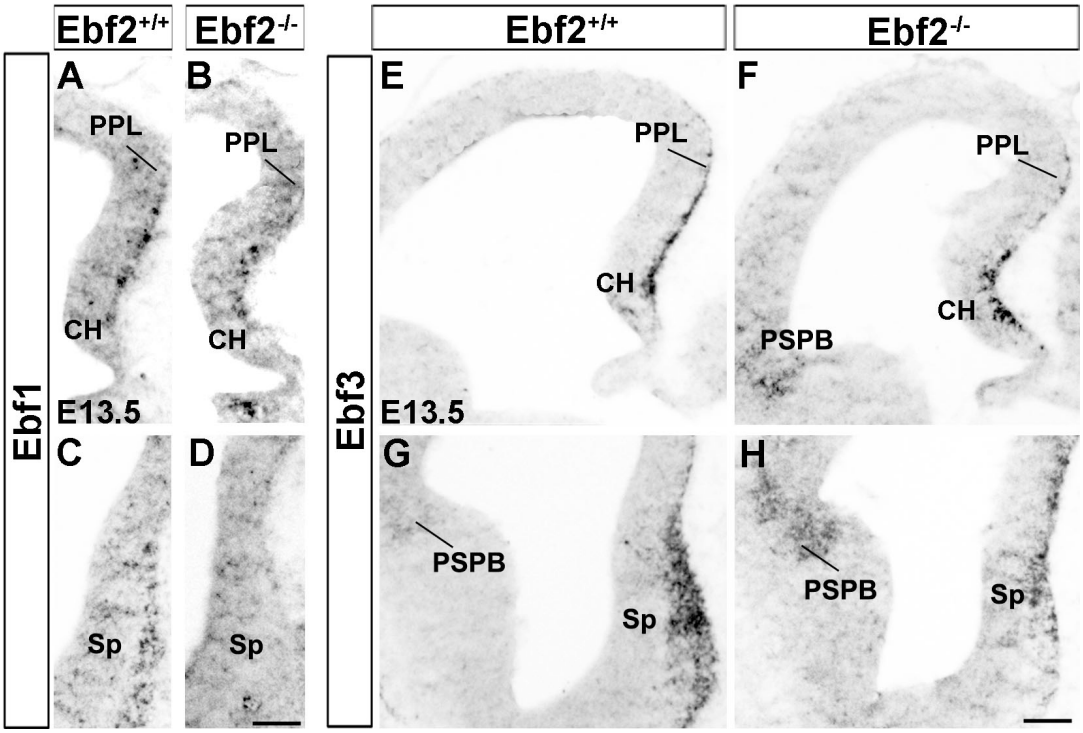
Ebf2+/+
Ebf2-/-
Ebf2+/+
Ebf2-/-
Ebf1
Ebf3
A
B
C
D
E
F
G
H
PPL
CH
Sp
PSPB
E13.5
E13.5

4.3 OVEREXPRESSION AND DOWNREGULATION OF *EBFs* AFFECT CELL MIGRATION

In situ hybridisation analyses revealed that *Ebfs* were transiently expressed in the same pallial structure, specifically in the CH and septum, and PPL/MZ, the site of origin and migration of CR cells, respectively. Thus, they could act together in regulating CR cell development. To test this hypothesis, I have used two different approaches, overexpression and downregulation of single or multiple *Ebf* genes *in vitro* and *in vivo*. The plasmids used in the following experiments were kindly provided by Dr Giacomo G. Consalez.

4.3.1 *In vitro* validation of overexpressing and silencing plasmids

The specificity of the *Ebf-flag* and *short hairpin (sh) Ebf* plasmids were tested *in vitro* in COS cells, which do not express any of the COE genes (data not shown). Confluent COS cells were transfected with *Ebf1/2/3-flag* separately and cultured for 24 h. Cells were split and subsequently transfected with different combinations of *shEbfs* as follows:

1. Ebf1-flag +	*2. Ebf2-flag +*	*3. Ebf3-flag +*
a) shEbf1	*a) shEbf1*	*a) shEbf1*
b) shEbf2	*b) shEbf2*	*b) shEbf2*
c) shEbf3	*c) shEbf3*	*c) shEbf3*
d) shEbf1-2-3	*d) shEbf1-2-3*	*d) shEbf1-2-3*
e) shMock	*e) shMock*	*e) shMock*

Non-transfencted COS cells were used as negative controls and indicated as Blank.

After 72 h past the second transfection with the *shEbfs*, cells were collected and proteins extracted to be used for Western blot analysis. Proteins were quantified and the same amount was used for each sample (Figure 4.4, 1, 2 and 3; α-tubulin shows

protein concentration). The intensity of the *shMock* (containing scattered RNA, used as positive control) band on the blot was used as reference.

A significant reduction in the expression of the EBF proteins compared to *shMock* transfected cells was observed in the following samples (Figure 4.4, 1, 2 and 3; red arrows):

- *Ebf1-flag* transfected COS cells and treated with *shEbf1* and *shEbf1-2-3*
- *Ebf2-flag* transfected COS cells and treated with *shEbf2* and *shEbf1-2-3*
- *Ebf3-flag* transfected COS cells and treated with *shEbf3* and *shEbf1-2-3*

Moreover, immunolabelling for flag and GFP, expressed by the overexpressing and *shEbf* plasmids, respectively, confirmed a downregulation of the EBF proteins in cells co-expressing the specific *shEbfs* (Figure 4.4, 4; A-J, circles). A number of cells espressing the *Ebf-flag* plasmids, not co-tranfected with *shEbfs,* showed anyway a decreased flag signal, raising questions about the specificity and efficiency of the RNAi plasmids. This discrepancy could be due by a different efficiency rate of tranfection as the two plasmids were transfected at different time point. However, the western blot results undoubtely confirmed that the *Ebf-flag* plasmids lead to a specific expression of the EBF proteins in COS cells. Furthermore, EBF proteins can be effectively and specifically silenced by *shEbf* plasmids.

Figure 4.4 Analysis of the function and specificity of overexpressing and silencing *Ebf* plasmids

1-3: Western blot analysis of EBF protein expression in transfected COS cells with different combination of *Ebfs-flag* and *shEbfs* plasmids (See Chapter 4.3.1 for details).

4: Imunnohistochemistry for flag (*Ebf-flag* plasmids) and GFP (*shEbf* plasmids) shows downregulation in the expression of EBF in COS cells co-transfected with *Ebf1-flag* (A-D), *Ebf2-flag* (E-G), *Ebf3-flag* (H-L) and the specific *shEbf* (cells in the circles double tranfected with *shEbf* and *Ebf-flag* show a reduction of the intensity of the flag signal).

α-tub: alpha-tubulin, DAPI: 4'-6-Diamidino-2-phenylindole, GFP: green fluorescent protein, kDa: kilo-Dalton

Scale bar: (A-L) 10 μm

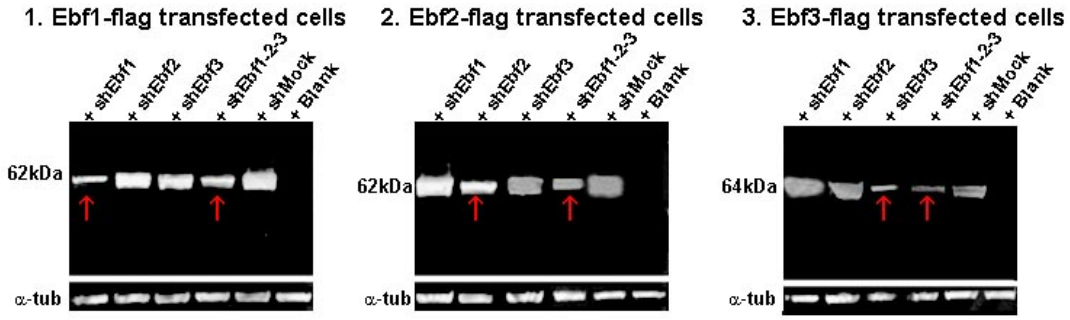
1. Ebf1-flag transfected cells
2. Ebf2-flag transfected cells
3. Ebf3-flag transfected cells
+ shEbf1
+ shEbf2
+ shEbf3
+ shEbf1-2-3
+ shMock
+ Blank
62kDa
62kDa
64kDa
α-tub
α-tub
α-tub

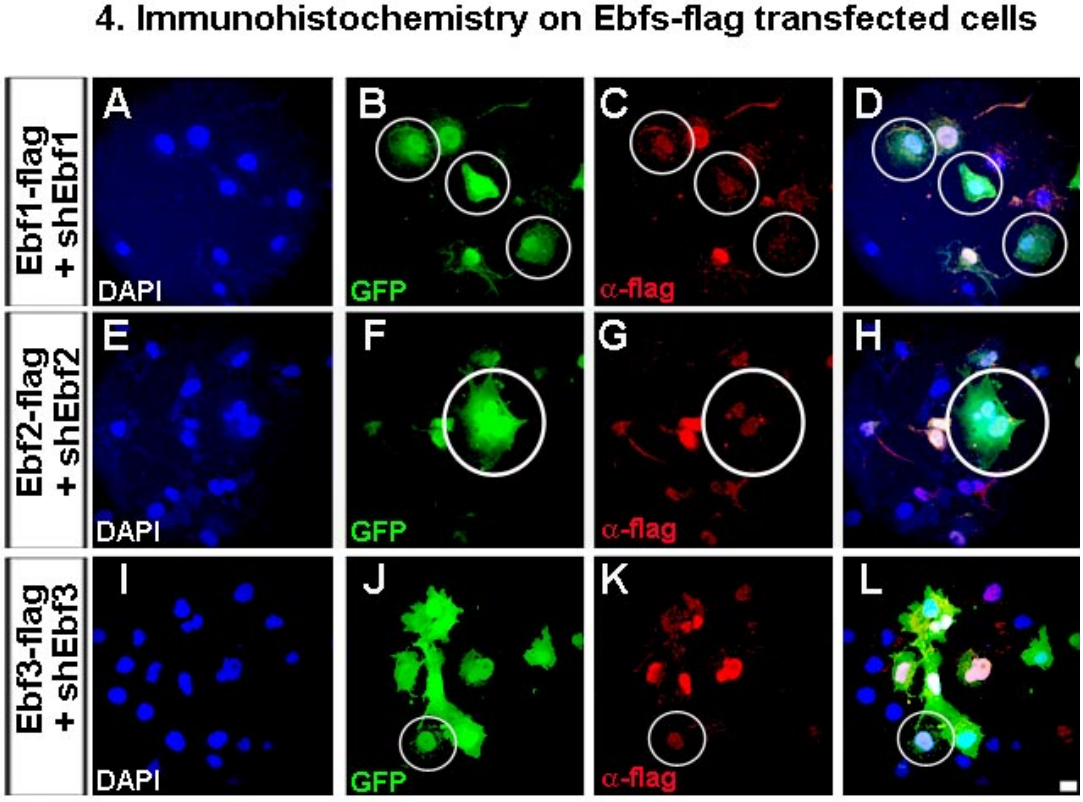
4. Immunohistochemistry on Ebfs-flag transfected cells
Ebf1-flag + shEbf1
Ebf2-flag + shEbf2
Ebf3-flag + shEbf3
A
B
C
D
E
F
G
H
I
J
K
L
DAPI
GFP
α-flag

4.3.2 Overexpression and downregulation of EBF proteins affect the migration of GN11 cells *in vitro*

GN11 cells, a cell line of immortalised immature neurons with high migratory behavior (Radovick et al., 1991), were found to express *Ebf1* and *Ebf3* but not *Ebf2* (Figure 4.5, B). For this reason, they were used as a model to study the role of *Ebf* genes in migration. These cells, maintained in culture, were transfected with the *Ebf-flag* and *shEbf* plasmids, and analysed in a chemotactic assay using the Boyden chamber (Figure 4.5, A).

Firstly, GN11 cells were treated with *Ebf1*, *Ebf2* and *Ebf3-flag* to study the effect of the overexpression of these genes on cell chemotaxis. Cells were transfected with *Ebf-flag* plasmids and cultured 48 h prior the Boyden chamber. GN11 cells transfected with *Ebf1*, *Ebf2* and *Ebf3-flag* migrated more towards the chemoattractant (1% FBS) compared to the control cells (*Mock*) (Figure 4.5, C: a compared to b; c, *Mock* 609±36, *Ebf1-flag* 1522±30, *Ebf2-flag* 1585±24, *Ebf3-flag* 1747±48; n=3; $p<0.001$).

As EBFs overexpression caused an increase in the migration of GN11 cells, I have subsequently analysed the effects of their downregulation on cell chemotaxis. Cells were transfected with *shEbf* plasmids and cultured for 72 h before the chemotactic assay. GN11 cells treated with *shEbf1*, *shEbf3* and *shEbf1-2-3* showed a decreased migration compared to the *Mock* and *shEbf2* treated GN11 (Figure 4.5, D: a compared to b; c, *Mock* 1273±58, *shEbf2* 1200±60, *shEbf1* 544±59, *shEbf3* 603±80, *shEbf1-2-3* 500±36; n=3; $p<0.01$). Interestingly, the migration of *shEbf1-2-3* transfected cells was more affected compared to GN11 cells treated with a single *shEbf*.

Moreover, I have tested whether the defective migration of *shEbf* treated GN11 cells could be rescued by the transfection with plasmids overexpressing the *Ebf* genes *(Ebf-flag)*. Cells were transfected with *shEbf1, shEbf3* and *shEbf1-3*, cultured for 72 h and transfected with *Ebf1/3-flag* plasmids. Boyden chamber was performed after 48 h the second transfection. However, the *flag* constructs used in the following experiment were not *shRNA* resistant. In order to overcome a possible downregulation of the *flag* by the RNAi, a greater quantity of *flag* plasmids was

transfected (according to manufacture's instruction) in order to saturate the *shEbf* plasmids.

The defective migration of GN11 cells caused by the *Ebfs* downregulation was successfully rescued by their later overexpression (Figure 4.6, a compared to b; c, *Mock* 1273±58, *shEbf1* 544±59 and *shEbf1+Ebf1-flag* 1740±66, *shEbf3* 603±80 and *shEbf3+Ebf3-flag* 1740±66, *shEbf1-3* 500±36 and *shEbf1-3+Ebf1-flag* 1679±76, or *+Ebf3-flag* 1594±88, or *+Ebf1/3-flag* 1902±43; n=3; $p<0.001$). Surprisingly, *Ebf3-flag* rescued the migration of *shEbf1* treated cells (Figure 4.6, D; c: *shEbf1* 544±59, *shEbf1+Ebf3-flag* 1501±74, n=3; $p<0.001$) and *Ebf1-flag* of *shEbf3* treated cells (Figure 4.6, D; c: *shEbf3* 603±80, *shEbf3+Ebf1-flag* 1496±63, n=3; $p<0.001$).

In conclusion, these results suggest that *Ebf* factors are strongly involved in neuron migration and compensate for each other's the function *in vitro*.

Figure 4.5 *Ebfs-flag* and *shEbfs* affect the migration of GN11 cells *in vitro*

A: Schema of the Boyden chamber.

B: Agarose gel shows the expression of *Ebf1* and *Ebf3* in GN11 cells.

C: a and b show GN11 cells bound to the porous membrane after the chemotactic assay. Fewer cells are visible in the *Mock* sample (a) compared to the *Ebf-flag* (b). (c) Chart shows the effect on the migration of GN11 cells towards the chemoattractant FBS when treated with *Ebfs* overexpression plasmids. GN11 cells do not migrate towards pure DMEM (left side of the chart).

D: a and b show GN11 cells bound to the porous membrane after the chemotactic assay. More cells are visible in the *Mock* sample (a) compared to the *shEbf* (b). (c) Chart shows the effect on the migration of GN11 cells when treated with *Ebfs* silencing plasmids. GN11 cells do not migrate towards pure DMEM (left side of the chart).

DMEM: Dulbecco modified eagle's medium, FBS: fetal bovine serum.

Scale bar (C: a, b; D: a, b) 25 μm

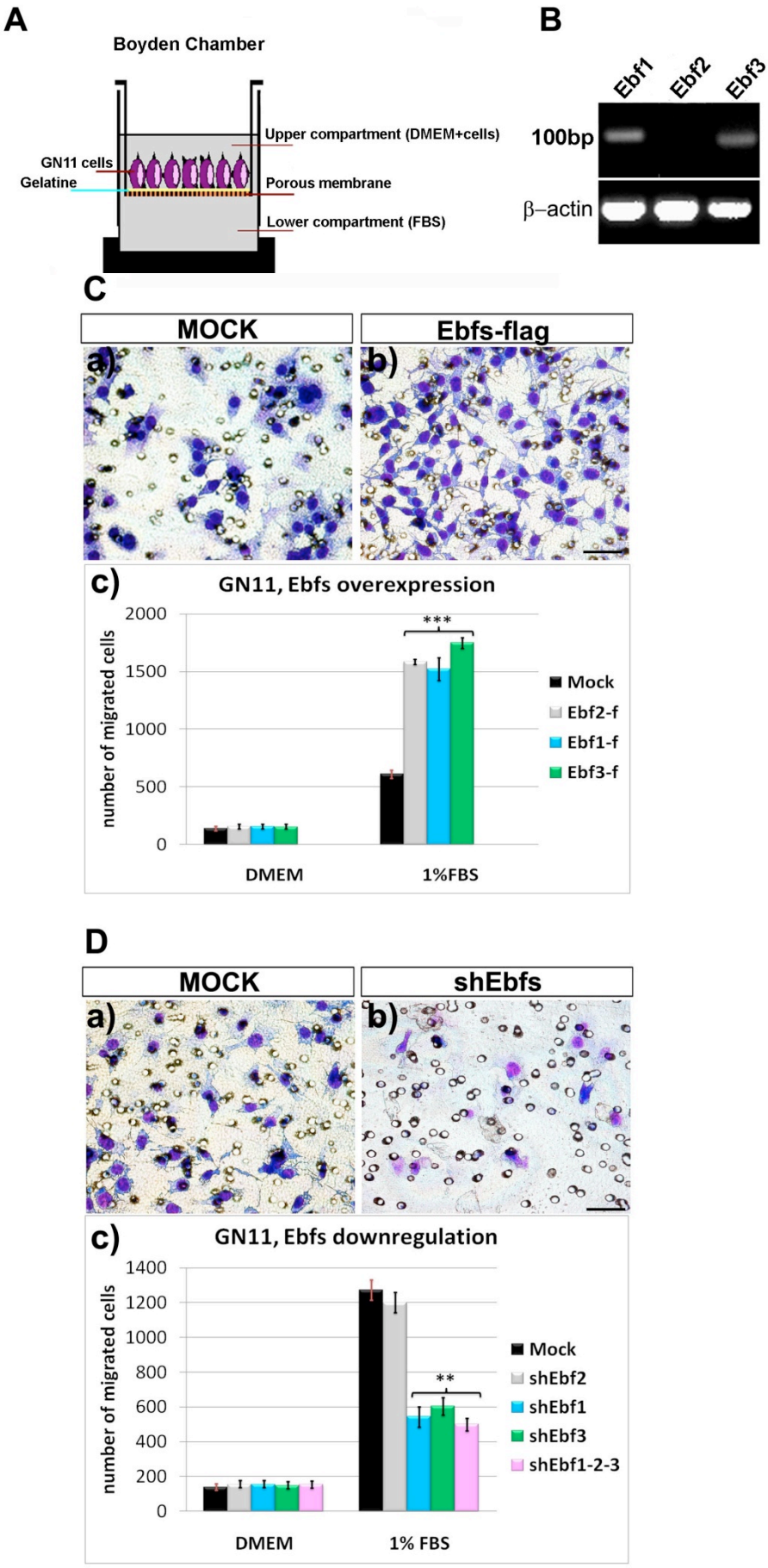
A
Boyden Chamber
Upper compartment (DMEM+cells)
GN11 cells
Gelatine
Porous membrane
Lower compartment (FBS)
B
Ebf1
Ebf2
Ebf3
100bp
β–actin
C
MOCK
Ebfs-flag
a)
b)
c)
GN11, Ebfs overexpression
number of migrated cells
2000
1500
1000
500
0
***
Mock
Ebf2-f
Ebf1-f
Ebf3-f
DMEM
1%FBS
D
MOCK
shEbfs
a)
b)
c)
GN11, Ebfs downregulation
number of migrated cells
1400
1200
1000
800
600
400
200
0
**
Mock
shEbf2
shEbf1
shEbf3
shEbf1-2-3
DMEM
1% FBS

Figure 4.6 The migration of GN11 cells treated with *shEbf1-3* is rescued when transfected with *Ebf1/3-flag* plasmids

A-C: GN11 cells bound to the porous membrane after the chemotactic assay. More cells are visible in the *Mock* sample (a) compared to the *Ebf-flag* (b). However, the migration is rescued after transfection with *Ebf-flag* plasmids.

D: Chart shows the effect on the migration of GN11 cells towards the chemoattractant FBS when treated with *shEbfs* and *Ebf-flag* plasmids. GN11 cells do not migrate towards pure DMEM (left side of the chart).

DMEM: Dulbecco modified eagle's medium, FBS: fetal bovine serum.

Scale bar (A-C) 25 μm

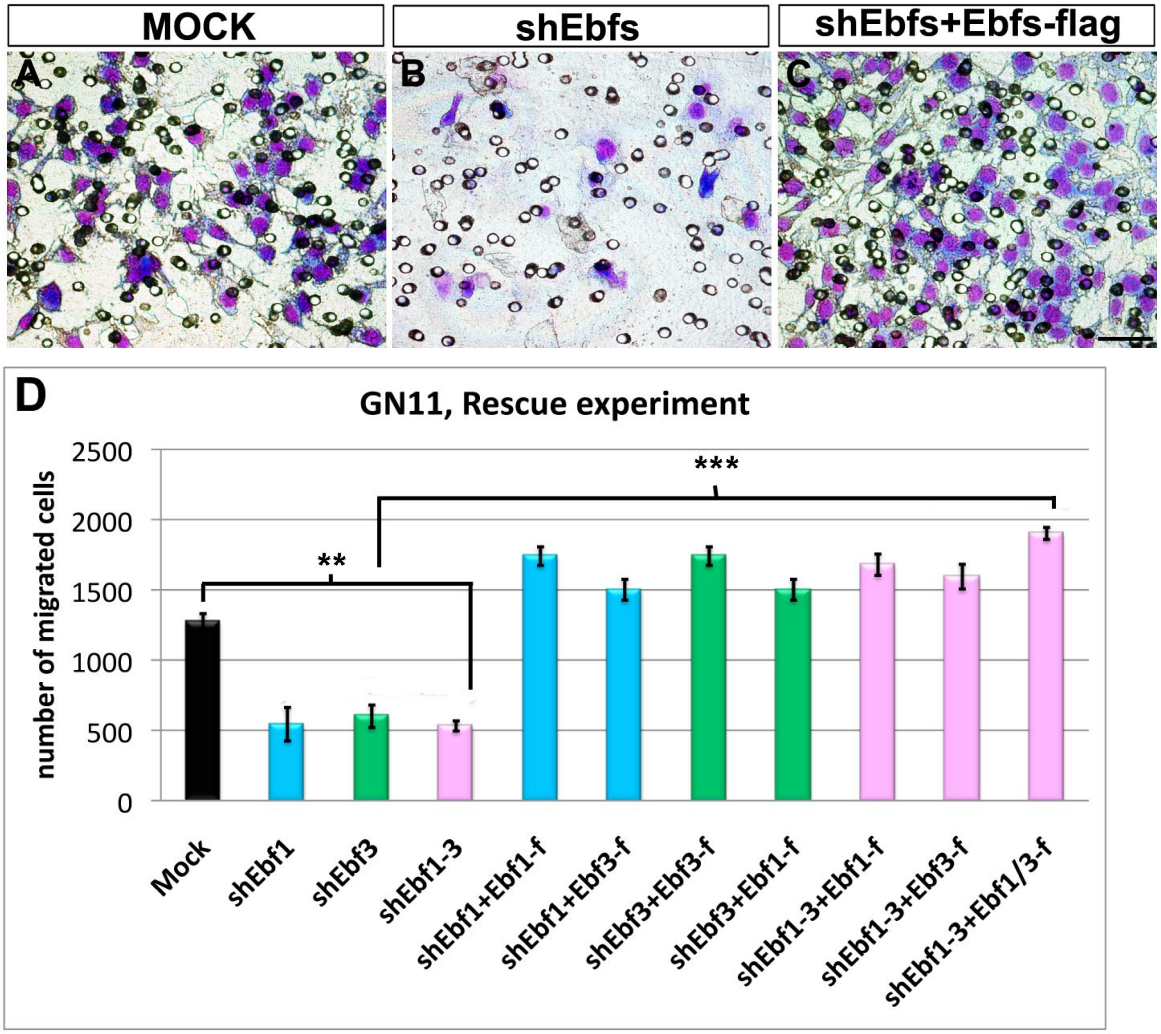
MOCK
shEbfs
shEbfs+Ebfs-flag
A
B
C
D
GN11, Rescue experiment
number of migrated cells
2500
2000
1500
1000
500
0
**
***
Mock
shEbf1
shEbf3
shEbf1-3
shEbf1+Ebf1-f
shEbf1+Ebf3-f
shEbf3+Ebf3-f
shEbf3+Ebf1-f
shEbf1-3+Ebf1-f
shEbf1-3+Ebf3-f
shEbf1-3+Ebf1/3-f

4.3.3 Cortical hem and septum targeted *in utero* electroporation of *shEbf*

Preliminary *in vitro* experiments on GN11 cells *in vitro* have shown that EBFs can strongly affect cell migration and compensate each other loss of function. As they are expressed in overlapping pallial territories (Chapter 4.2), I analysed the effect of a selective downregulation of these factors specifically in CR cells. Embryos at E10.5 were electroporated *in utero* in the CH of left telencephalic hemispheres with different combinations of *shEbf* as follows: *shEbf1-2*, *shEbf2-3* and *shEbf1-2-3*. Electroporated embryos were subsequently collected at E13.5, and CR cell commitment was analysed by *in situ* hybridisation. Expression of *Reelin mRNA*, *Wnt3a* and *Foxg1* in the electroporated telencephalic side (Ep-side) was compared with the non-electroporated side (wt-side). A GFP *in situ* probe visualised the site of the electroporation. *shEbf1-2* were electroporated in the CH (Figure 4.7, A; GFP), but changes were not detected in *Reelin mRNA* (Figure 4.7, A; Ep-side compared to wt-side, arrow), *Wnt3a* and *Foxg1* expression (Figure 4.7, D; Ep-side compared to wt-side, arrow). *shEbf2-3* were electroporated in the CH and neocortex (Figure 4.7, B; GFP), but no significant changes were found in *Reelin mRNA* (Figure 4.7, B; Ep-side compared to wt-side, arrow), *Wnt3a* and *Foxg1* expression (Figure 4.7, E; Ep-side compared to wt-side, arrow). To test whether a downregulation of all the three *Ebfs* was required to give a defective phenotype, *shEbf1-2-3* were electroporated in the CH (Figure 4.7, C; GFP). *shEbf1-2-3* brains did not show changes in *Reelin mRNA* (Figure 4.7, C; Ep-side compared to wt-side, arrow), *Wnt3a* and *Foxg1* expression (Figure 4.7, F; Ep-side compared to wt-side, arrow). Moreover, CR cell migration was followed in *shEbf3* electroporated brains. Embryos were electroporated at E10.5 with *shEbf3* in the CH and collected at E13.5, when CR cell migration was almost completed. Calretinin antibody was used to label CR cells and GFP to discriminate electroporated cells. *shEbf3* was electroporated in the CH and GFP^+ migrating cells were visible in the PPL. Electroporated cells were also positive for Calr, a marker for CR cells (Figure 4.8, C; $GFP^+/Calr^+$, arrow), and localised in the CH and PPL (Figure 4.8, A-C) as in N-Ep (non-electroporated) brains (Figure 4.8, D-F; arrow points to $Calr^+$). In conclusion, the downregulation of *Ebfs* in the CH did not affect the commitment and migration of CR cells. Most likely the lack of

phenotype was due to an insufficient downregulation of the endogenous gene expression by the shRNA *in vivo* as well as the increased complexity of the biological system when compared with cells cultured *in vitro*.

Figure 4.7 CR cell fate *in utero* electroporated brains

In situ hybridisation; E13.5 forebrain, coronal sections, 40 µm.
In utero electroporation was performed at E10.5
Dotted lines separate Ep-side from wt-side.

A, D: Double-colour *in situ* hibridisation on *GFP/Reelin mRNA* (A) and *Wnt3a/Foxg1* (D) *shEbf1-2* electroporated embryos.
B, E: Double-colour *in situ* hibridisation on *GFP/Reelin mRNA* (B) and *Wnt3a/Foxg1* (E)*shEbf2-3* electroporated embryos.
C, F: Double-colour *in situ* hibridisation on *GFP/Reelin mRNA* (C) and *Wnt3a/Foxg1* (F) *shEbf1-2* electroporated embryos.

CH: cortical hem, Ep-side: electroporated side, *Foxg1: forkhead box G1*, MZ: marginal zone NCx: neocortex, PPL: preplate, *Wnt3a: wingless type 3a*, wt-side: wild type side.

Scale bar: 100 µm

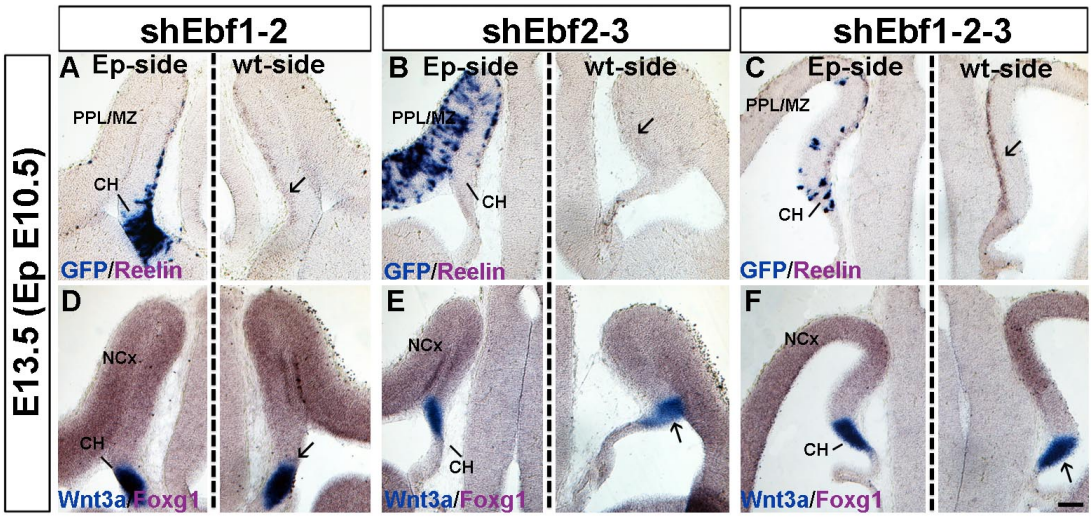
shEbf1-2
shEbf2-3
shEbf1-2-3
E13.5 (Ep E10.5)
A Ep-side
wt-side
B Ep-side
wt-side
C Ep-side
wt-side
PPL/MZ
CH
GFP/Reelin
D
E
F
NCx
Wnt3a/Foxg1

Figure 4.8 CR cell migration is not affected in *shEbf3 in utero* electroporated brains

Immunofluorescence; E13.5 forebrain, coronal section, 20 µm.
In utero electroporation was performed at E10.5

A, C: *shEbf3* electroporation was targeted in the CH (A, GFP^+ cells). $Calretinin^+$ (B) and electroporated cells (GFP^+, C) are migrating out the CH to cover the PPL as expected.
D, F: Non electroporated brain samples show wt migration of $Calr^+$.

Calr: calretinin, CH: cortical hem, GFP: green fluorescent protein, N-Ep: non electroporated, PPL: preplate.

Scale bar: 100 µm

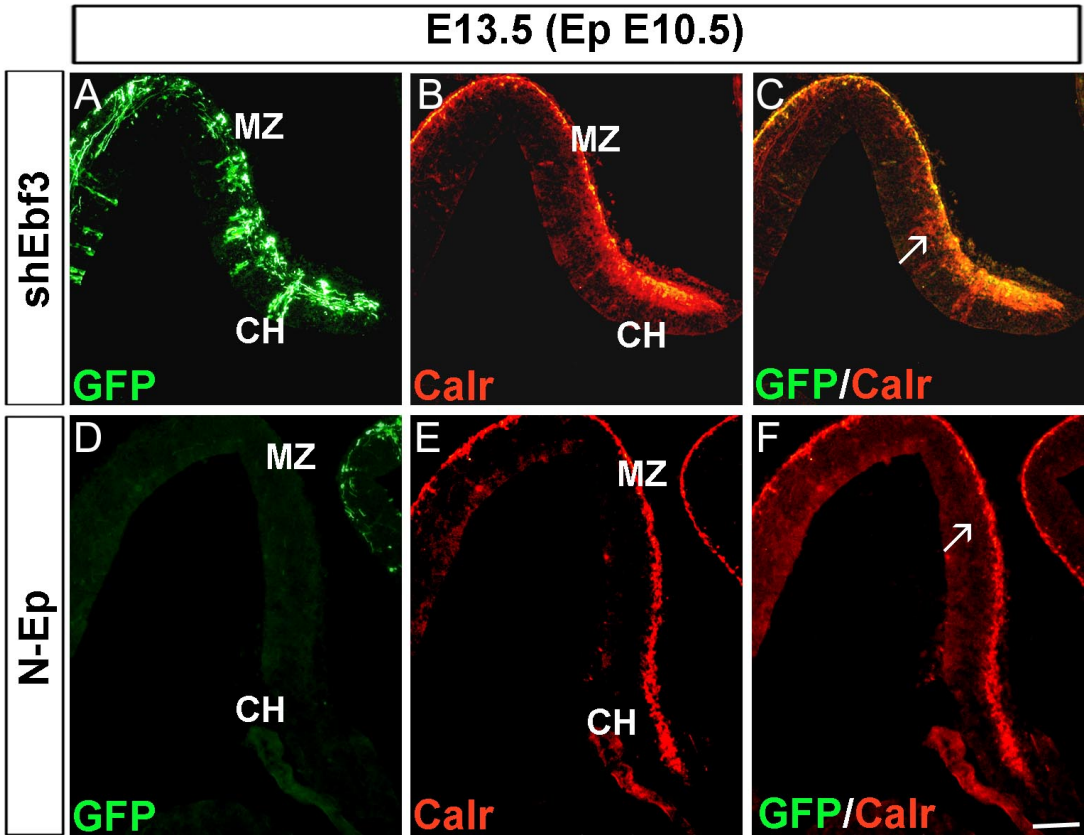
E13.5 (Ep E10.5)
shEbf3
N-Ep
A
MZ
CH
GFP
B
MZ
CH
Calr
C
GFP/Calr
D
MZ
CH
GFP
E
MZ
CH
Calr
F
GFP/Calr

4.4 DISCUSSION

4.4.1 *Ebf1* and *Ebf3* transcription factors are expressed in overlapping pallial territories and compensate the *Ebf2* loss of function

COE genes encode phylogenetically conserved HLH transcription factors and are implicated in various aspects of neural development, such as neuronal differentiation (Dubois *et al.* 1998; Pozzoli *et al*. 2001), migration (Garcia-Dominguez *et al*. 2003; Garel *et al.* 2000) and axon fasciculation and guidance (Garel *et al*. 1999; 2002).

Previous studies have shown that these factors are expressed in overlapping territories in different areas of the developing nervous system, including the olfactory epithelium, forebrain and cerebellum, playing redundant as well as specific functions (Garel *et al.* 1997; Croci *et al*. 2006). For example, *Ebf1* and *Ebf3* play redundant roles in the olfactory epithelium, whereas *Ebf2* is necessary for GnRH neuron migration and its loss of function leads to apoptosis of these cells (Corradi *et al.* 2003). In the cerebellum, all *Ebf* genes are expressed in Purkinje cells. *Ebf1* and *Ebf3* are expressed among the entire cell population, whereas *Ebf2,* which is specifically expressed in a subpopulation, is indispensable for their migration and its loss of function leads to dramatic defects in the topography of the cerebellar cortex (Croci *et al.* 2006). Although *Ebf1*$^{-/-}$ and *Ebf2*$^{-/-}$ mice are available, *Ebf3*$^{-/-}$ mice are not viable (S. Garel and G. Consalez, unpublished), making it difficult to understand its role compared to other members of the COE family. Despite the work of Garel and colleagues (1997), *Ebfs* were never extensively studied during forebrain development. I have, for the first time, specifically characterised *Ebf2* expression and the effects of its loss of function during pallial development. Moreover, in Chapter 4, I have shown that *Ebf1*, *Ebf2* and *Ebf3* are also expressed in the same cortical territories; in particular, within sites of origin and migration of CR cells. These results link the *Ebf* transcription factors to CR cells, and suggest that the lack of gross pallial defects in *Ebf2*$^{-/-}$ mice may be due to a common function of *Ebf* genes in regulating the development of CR cells arising from the CH and septum. Specifically, *Ebfs* are expressed in the CH, PPL/MZ and septum of the pallium at early developmental stages and are subsequently downregulated in these areas at E15.5 (Chapter 4). Interestingly, *Ebf2* and *Ebf3* are strongly expressed in the CH and

PPL/MZ, whereas *Ebf1* is weakly detected in these areas. This suggests two different scenarios responsible for this phenomenon. Firstly, *Ebf2* and *Ebf3* may regulate the level of *Ebf1* expression as they are already co-expressed in the same territory. Secondly, *Ebf1* may be expressed exclusively within a subpopulation of CH derived CR cells, as is the case in the cerebellum. In the septum, a similar trend was observed. *Ebf3* was strongly expressed dorso-ventrally, but *Ebf1* was only expressed weakly and *Ebf2* was confined dorsally. The expression of *Ebf1* and *Ebf3* in *Ebf2*$^{-/-}$ mice was unchanged in the CH and PPL/MZ, whereas it was downregulated in the septum. Previously, in *Xenopus*, Pozzoli and colleagues (2001) have shown that *Ebf2* is activated during Notch signalling and is involved in maintaining high neural potential of precursor cells, but at the same time promotes the commitment into neuronal fate. In this model, *Ebf3* acts downstream of *Ebf2,* stimulating the development of specific cell subtypes.

Moreover, *Ebf3* was the only member of the COE transcription factor family expressed in the PSPB. According to recent findings of Griveau and colleagues, ablation of a CR cell subpopulation cause a redistribution of CR cells from other sources as a compensatory mechanisms. The expansion of the *Ebf3* domain in the PSPB of *Ebf2*$^{-/-}$ mice suggests therefore a non cell-autonomous compensatory mechanism of the migratory defect seen in the mutants.

In conclusion, these data suggest that *Ebf2* may be involved in regulating the expression of *Ebf1* and *Ebf3* in the septum, affecting CR cell migration from this region, while *Ebf1* and *Ebf3* compensate its loss from the CH, and *Ebf3* from the PSPB.

4.4.2 Alternative mechanisms are involved in the compensation of *Ebf2*$^{-/-}$ mouse phenotype

Cajal-Retzius cells are a complex, transient population organized into subpopulations specified by different domains, such as the CH, septum and PSPB (Bielle *et al.* 2005, Griveau *et al.* 2010). The combinations of these different CR cell subtypes populate distinct regions of the pallium rostro-caudally. Recently, Griveau and colleagues (2010) have shown that the genetic ablation of the septum leads to a redistribution of PSPB and CH-derived CR cells along with changes in early

patterning events and cell division and differentiation. However, alterations to cell division and differentiation do not lead to major cortical defects (Griveau *et al.* 2010). These findings could suggest a possible redistribution along the rostro-caudal axis of CR cell subpopulations in *Ebf2*$^{-/-}$ mice, as well as increased production of CR cells from other sources. In fact, *Ebf2*$^{-/-}$ mice have shown a decreased number in Reelin and Calr positive cells in the MZ of caudo-medial sections and an increase of Reelin and Calr cells in the CH, suggesting a delay in the migration of CR cells from this region. Conversely, *Dbx1* expression was diminished in the septum, together with *Ebf1* and *Ebf3,* suggesting that *Ebf2* may be an upstream factor regulating its expression and function in this area as well as the CR cell commitment and migration (Pozzoli *et al.* 2001). Moreover, the number of mitotic cells (PH3 positive, data not shown) was decreased in the pallial VZ at E11.5, whereas it was increased in the CH at E12.5. According to recent findings of Griveau and colleagues, these data suggest compensatory mechanisms, which induce a precocious generation of postmitotic neurons to populate the early preplate (Kowalczyk *et al.* 2009) and a possible redistribution of the other CR subpopulations, as suggested by the expansion of the *Dbx1* and *Ebf3* domains in the PSPB of *Ebf2*$^{-/-}$ mice. Furthermore, these defects correlate with changes in the size and positioning of cortical areas at postnatal stages without affecting signaling centers or cortical lamination (Griveau *et al.* 2010; Yoshida *et al.* 2006), which could also be the case in *Ebf2*$^{-/-}$ mice. In fact, the reduction of cortical thickness in these mutants may mask arealisation defects, which were not examined in this thesis. Thus, *Ebf2* loss of function may be recouped by two different mechanisms, a redundant expression of *Ebf1* and *Ebf3* in the CH as well as CR cell redistribution, possibly from the PSPB.

4.4.3 *Ebf* factors influence the migration of immortalized immature neurons *in vitro*

Ebf factors are strictly connected with cell migration in different species. *Ebf2* is involved in the migration of a subpopulation of Purkinje cells in the cerebellum and GnRH neurons from the olfactory epithelium to the hypothalamus (Corradi *et al.* 2003; Croci *et al.* 2006). In Chapter 3, I have shown that *Ebf2*$^{-/-}$ mice displayed a transitory migration defect in CR cells restored later by compensatory mechanisms.

Therefore, I have tested whether the overexpression and silencing of one or a combination of more *Ebfs* could affect the migration of neurons, with a specific focus on the activity of migration. As a model, I have used GN11 cells, which are neurons derived from immature, immortalised GnRH cells. RT-PCR and micro-array analysis have confirmed that these cells express *Ebf1* and *Ebf3*, but not *Ebf2*. (A. Cariboni, unpublished). Overexpression of *Ebf1* and *Ebf3* genes in GN11 cells lead to increased migration in comparison with control mock-transfected cells (Chapter 4). Interestingly, *Ebf2* overexpression caused an increase in cell migration, suggesting that this gene, even when not expressed, can trigger migratory mechanisms most likely acting through the same signal pathway as for *Ebf1* and *Ebf3*.

On the other hand, downregulation of *Ebf1* and *Ebf3* caused a significant decrease in cell migration compared to the non-treated control cells. Downregulation of both genes caused a stronger phenotype, suggesting that the function of *Ebf* genes may be dose-dependent. As expected, downregulation of *Ebf2* did not lead to significant changes in GN11 cell behavior. Moreover, transfection of *Ebf1* and *Ebf3* in shRNA-treated GN11 cells were able to rescue the defective migration of these cells. Interestingly, *Ebf1* was able to rescue the phenotype caused by *shEbf3* and *vice versa*. Thus, this suggests that *Ebfs* can play a redundant function and complement each other.

Taken together this data confirm that *Ebf* factors are involved in neuron migration. They may play redundant functions and, most likely, affect the migration of other neuron types expressing *Ebfs*, in particular, CR cells.

4.4.4 Target *in vivo* downregulation of Ebfs expression in CR cells by in utero electroporation

Single mutants are available for *Ebf1* and *Ebf2*. However, *Ebf3* single mutants are not yet available. Alternatively, *in utero* electroporation, performed in collaboration with Dr T. Shimogori (Riken BSI, Tokyo), was used to specifically downregulate the expression of *Ebf* genes in the CH where they are expressed at high levels. The electroporation was performed at E10.5 and the electroporated embryos analysed at E13.5. Cell commitment and migration was studied in successfully electroporated

cells. Changes were not detected in any of the electroporated brains for any of the different combinations of *shRNA* used. Technical limitations render these experiments extremely challenging. Firstly, to target the CH and septum in early embryos was extremely difficult because of the size and positions of the anatomical areas. Moreover, the viability of the electroporated embryos was very low, especially when two or more *shEbfs* were combined together, suggesting possible toxic effects of the plasmids. On the other hand, the lack of phenotype was most likely due to an insufficient downregulation of the endogenous gene expression by the shRNA *in vivo* as well as the increased complexity of the biological system when compared with cells cultured *in vitro*.

4.4.5 Conclusions and Future experiments

The present thesis provides several pieces of evidence that *Ebf* factors may play an important role in the development of CR cells. However, different hypothesis should be still tested to further complete my work.

First, I have shown that *Ebf* factors strongly affect the migration and compensate each other's functions in GN11 neurons *in vitro*. However, due to technical limitations the experiments were not yet reproducible specifically in CR cells. For this reason, I am currently pursuing a different approach to target the expression of EBF proteins in CR cells in collaboration with Dr Eikcholt (King's College London). This approach consists of dissociating cells from murine CH at E11.5 and, after transfection by electroporation (Lonza) with overexpression or silencing *Ebf* plasmids, tests their ability of migration *in vitro* by stripe assays. Stripe assays test the ability of cells to migrate on a coverslip coated with various protein combinations such as laminin or CR cell chemoattractants, for example, SDF-1.

Second, $Ebf2^{-/-}$ mice displayed changes in the expression of different genes in the CH, PSPB, neocortex (PPL/MZ) and septum. However, these results were confirmed only by *in situ* hybridization experiments. A specific microarray analysis on $Ebf2^{+}$ cells may clarify the targets of *Ebf2* transcription factor, which are still mostly unknown. In particular, I would cross breed the $Ebf2^{-/-}$ mice with $Ebf2^{GFPiCre/R26R\text{-}YFP}$ line, specifically isolate the YFP expressing cells and compare them with YFP^{+} cells from the pure $Ebf2^{GFPiCre/R26R\text{-}YFP}$ line. This strategy will permit to follow the

commitment and migration of *Ebf2* expressing cells in the mutant and wt background, even after the downregulation of the endogenous gene.

Moreover, several evidences in the *Ebf2*$^{-/-}$ mice showed a possible redistribution of CR cells populations in the cortex, possibly from the PSPB. To confirm this hypothesis, it would be useful to cross *Ebf2*$^{-/-}$ mice with the transgenic *Dbx1*$^{\beta\text{-}gal}$ line (Bielle *et al*. 2005) and follow the fate of *Dbx1*$^{+}$ cells compared to *Dbx1*$^{+}$ cells in the wt background. Calretinin antibody would be used to distinguish PSPB-*Dbx1* and septum-*Dbx1* derived CR cell subpopulations.

Finally, most of the information on the functions of *COE* genes comes from the analysis of *Ebf1* and *Ebf2* mutants. It is known that *COE* members control neuronal commitment and cell migration during CNS development, playing redundant as well as specific functions, but little is still known about *Ebf3* transcription factor. I have shown that *Ebf* factors are expressed in sites of origin of CR cells. However, the analysis of *Ebf1* (Garel *et al.* 1999) and *Ebf2* mutants did not reveal a specific role in the development of CR cells. The creation and phenotypic analysis of conditional *Ebf3*$^{-/-}$ mice, as *Ebf3*$^{-/-}$ mice are reported to be embryonically lethal, may elucidate an unique role of this factor in the development of CR cells.

CONCLUDING REMARKS

GENETIC NETWORKS AND REDUNDANCY DEFINE THE COMPLEXITY OF BIOLOGICAL SYSTEMS

Genetic redundancy is an amazing property of genomes and has only recently become evident as a result of negative knockout experiments. In fact, knockout strategies have demonstrated that the function of many genes cannot be studied by simply disrupting them in model organisms because the inactivation of these genes does not lead to any phenotypic effects. For living systems, the phenomenon of genetic redundancy seems common (Borger, 2008). Genetic redundancy involves two or more genes that can perform overlapping functions (Tautz, 1992; Nowak *et al.* 1997), but recent findings suggest that this is not always the case. In the following paragraph I will present two theories explaining the genetic redundancy and its effects.

Most common ideas still follow the Darwin theories on gene evolution. Susumo Ohno writes in his book "*Evolution by Gene Duplication"*, that duplications of genes provide redundancies, which then accumulate mutations and adopt novel biological functions. Duplicates transforming into improved, novel genes are then favored by natural selection as they have an advantage over other genes. Meanwhile, the genetic redundancy will protect old functions, reducing the lethality of mutations. He also provides an explanation for the knockouts without phenotype: if genes duplicate fairly often, then it is expected to find redundancy in most genomes, because, according to natural selection, duplicates provide an organism with "back-up" genes (Ohno, 1970). However, in 2000, Wagner demonstrated that genes considered not essential are not more likely to have duplicates than other "essential" genes that cause a phenotype when they are knocked out. Wagner concluded that the no-

phenotype effect cannot be caused exclusively by gene duplication and redundancy, but concomitant with interactions between unrelated genes (Wagner, 2000). The molecular biologist Peter Borger suggests that no-phenotype knockouts are explained if we take into account the non-linearity of biochemical systems. He argues that biological systems do not work like linear causality, where A causes B causes C causes D causes E. Biological systems are, instead, designed as a complex networks. He proposes instead a "simple non-linear biological system with nodes" where A may cause B, but A also causes D independent of B and C. Thus, if A fails to make the link with D, there are still B and C to make the connection. This theory gives the idea that not only gene duplication is important to maintain the stability of a living organism, but also the cross-talk between different genes, which could potentially give rise to an organization of genetic networks. Thus, genetic networks stabilize the complex regulatory mechanisms of living systems. They control homeostasis, regulate the maintenance of genomes and provide regulatory feedback on gene expression (Borger, 2008).

In conclusion, if we consider complex biological systems such as mammals, it is most likely then these two mechanisms may coexist and cooperate together. Mario Cappecchi, a pioneer in the development of knockout technology, once said: "I don't believe that there is a single mouse (knockout) that does not have a phenotype. We just aren't asking the right questions." (Quoted from H. Pearson, 2002), suggesting that in biology there is far more behind the expression and function of one simple gene.

REFERENCES

Abellan, A., A. Menuet, C. Dehay, L. Medina and S. Retaux (2010). "Differential expression of LIM-homeodomain factors in Cajal-Retzius cells of primates, rodents, and birds." Cereb Cortex 20(8): 1788-98.

Aguilo, A., T. H. Schwartz, V. S. Kumar, Z. A. Peterlin, A. Tsiola, E. Soriano and R. Yuste (1999). "Involvement of cajal-retzius neurons in spontaneous correlated activity of embryonic and postnatal layer 1 from wild-type and reeler mice." J Neurosci 19(24): 10856-68.

Anderson, S. A., D. D. Eisenstat, L. Shi and J. L. Rubenstein (1997). "Interneuron migration from basal forebrain to neocortex: dependence on Dlx genes." Science 278(5337): 474-6.

Andrews, W., A. Liapi, C. Plachez, L. Camurri, J. Zhang, S. Mori, F. Murakami, J. G. Parnavelas, V. Sundaresan and L. J. Richards (2006). "Robo1 regulates the development of major axon tracts and interneuron migration in the forebrain." Development 133(11): 2243-52.

Anton, E. S., J. A. Kreidberg and P. Rakic (1999). "Distinct functions of alpha3 and alpha(v) integrin receptors in neuronal migration and laminar organization of the cerebral cortex." Neuron 22(2): 277-89.

Aravind, L. and E. V. Koonin (1999). "Gleaning non-trivial structural, functional and evolutionary information about proteins by iterative database searches." J Mol Biol 287(5): 1023-40.

Arias, M. S., J. Baratta, J. Yu and R. T. Robertson (2002). "Absence of selectivity in the loss of neurons from the developing cortical subplate of the rat." Brain Res Dev Brain Res 139(2): 331-5.

Assimacopoulos, S., E. A. Grove and C. W. Ragsdale (2003). "Identification of a Pax6-dependent epidermal growth factor family signaling source at the lateral edge of the embryonic cerebral cortex." J Neurosci 23(16): 6399-403.

Ayala, R., T. Shu and L. H. Tsai (2007). "Trekking across the brain: the journey of neuronal migration." Cell 128(1): 29-43.

Bielle, F., A. Griveau, N. Narboux-Neme, S. Vigneau, M. Sigrist, S. Arber, M. Wassef and A. Pierani (2005). "Multiple origins of Cajal-Retzius cells at the borders of the developing pallium." Nat Neurosci 8(8): 1002-12.

Borger, P. (2008). “Evidence for the design of life.” J Creation 22(2): 79-84.

Borrell, V. and O. Marin (2006). "Meninges control tangential migration of hem-derived Cajal-Retzius cells via CXCL12/CXCR4 signaling." Nature Neuroscience 9(10): 1284-93.

Bulchand, S., E. A. Grove, F. D. Porter and S. Tole (2001). "LIM-homeodomain gene Lhx2 regulates the formation of the cortical hem." Mech Dev 100(2): 165-75.

Butt, S. J., M. Fuccillo, S. Nery, S. Noctor, A. Kriegstein, J. G. Corbin and G. Fishell (2005). "The temporal and spatial origins of cortical interneurons predict their physiological subtype." Neuron 48(4): 591-604.

Caviness, V. S., Jr. (1982). "Neocortical histogenesis in normal and reeler mice: a developmental study based upon [3H]thymidine autoradiography." Brain Res 256(3): 293-302.

Caviness, V. S., Jr. and R. L. Sidman (1973). "Retrohippocampal, hippocampal and related structures of the forebrain in the reeler mutant mouse." J Comp Neurol 147(2): 235-54.

Chowdhury, T. G., J. C. Jimenez, J. M. Bomar, A. Cruz-Martin, J. P. Cantle and C. Portera-Cailliau (2010). "Fate of cajal-retzius neurons in the postnatal mouse neocortex." Front Neuroanat 4: 10.

Clancy, B., M. Silva-Filho and M. J. Friedlander (2001). "Structure and projections of white matter neurons in the postnatal rat visual cortex." J Comp Neurol 434(2): 233-52.

Cobos, I., U. Borello and J. L. Rubenstein (2007). "Dlx transcription factors promote migration through repression of axon and dendrite growth." Neuron 54(6): 873-88.

Cobos, I., M. E. Calcagnotto, A. J. Vilaythong, M. T. Thwin, J. L. Noebels, S. C. Baraban and J. L. Rubenstein (2005). "Mice lacking Dlx1 show subtype-specific loss of interneurons, reduced inhibition and epilepsy." Nature Neuroscience 8(8): 1059-68.

Cobos, I., J. E. Long, M. T. Thwin and J. L. Rubenstein (2006). "Cellular patterns of transcription factor expression in developing cortical interneurons." Cerebral Cortex 16 Suppl 1: i82-8.

Copeland, N. G., N. A. Jenkins and D. L. Court (2001). "Recombineering: a powerful new tool for mouse functional genomics." Nat Rev Genet 2(10): 769-79.

Corbin, J. G., N. Gaiano, R. P. Machold, A. Langston and G. Fishell (2000). "The Gsh2 homeodomain gene controls multiple aspects of telencephalic development." Development 127(23): 5007-20.

Corradi, A., L. Croci, V. Broccoli, S. Zecchini, S. Previtali, W. Wurst, S. Amadio, R. Maggi, A. Quattrini and G. G. Consalez (2003). "Hypogonadotropic hypogonadism and peripheral neuropathy in Ebf2-null mice." Development 130(2): 401-10.

Croci, L., V. Barili, D. Chia, L. Massimino, R. van Vugt, G. Masserdotti, R. Longhi, P. Rotwein and G. G. Consalez (2011). "Local insulin-like growth factor I expression is essential for Purkinje neuron survival at birth." Cell Death Differ 18(1): 48-59.

Croci, L., S. H. Chung, G. Masserdotti, S. Gianola, A. Bizzoca, G. Gennarini, A. Corradi, F. Rossi, R. Hawkes and G. G. Consalez (2006). "A key role for the HLH transcription factor EBF2COE2,O/E-3 in Purkinje neuron migration and cerebellar cortical topography." Development 133(14): 2719-29.

Crozatier, M., D. Valle, L. Dubois, S. Ibnsouda and A. Vincent (1996). "Collier, a novel regulator of Drosophila head development, is expressed in a single mitotic domain." Curr Biol 6(6): 707-18.

Crozatier, M. and A. Vincent (1999). "Requirement for the Drosophila COE transcription factor Collier in formation of an embryonic muscle: transcriptional response to notch signalling." Development 126(7): 1495-504.

D'Arcangelo, G., R. Homayouni, L. Keshvara, D. S. Rice, M. Sheldon and T. Curran (1999). "Reelin is a ligand for lipoprotein receptors." Neuron 24(2): 471-9.

D'Arcangelo, G., G. G. Miao, S. C. Chen, H. D. Soares, J. I. Morgan and T. Curran (1995). "A protein related to extracellular matrix proteins deleted in the mouse mutant reeler." Nature 374(6524): 719-23.

de Carlos, J. A., L. Lopez-Mascaraque and F. Valverde (1996). "Dynamics of cell migration from the lateral ganglionic eminence in the rat." J Neurosci 16(19): 6146-56.

Dubois, L. and A. Vincent (2001). "The COE--Collier/Olf1/EBF--transcription factors: structural conservation and diversity of developmental functions." Mech Dev 108(1-2): 3-12.

Dubois, L., L. Bally-Cuif, M. Crozatier, J. Moreau, L. Paquereau and A. Vincent (1998). "XCoe2, a transcription factor of the Col/Olf-1/EBF family involved in the specification of primary neurons in Xenopus." Curr Biol 8(4): 199-209.

Fishell, G. (2007). "Perspectives on the developmental origins of cortical interneuron diversity." Novartis Found Symp 288: 21-35; discussion 35-44, 96-8.

Flames, N., R. Pla, D. M. Gelman, J. L. Rubenstein, L. Puelles and O. Marin (2007). "Delineation of multiple subpallial progenitor domains by the combinatorial expression of transcriptional codes." J Neurosci 27(36): 9682-95.

Fode, C., Q. Ma, S. Casarosa, S. L. Ang, D. J. Anderson and F. Guillemot (2000). "A role for neural determination genes in specifying the dorsoventral identity of telencephalic neurons." Genes Dev 14(1): 67-80.

Fuccillo, M., M. Rallu, A. P. McMahon and G. Fishell (2004). "Temporal requirement for hedgehog signaling in ventral telencephalic patterning." Development 131(20): 5031-40.

Fukuchi-Shimogori, T. and E. A. Grove (2001). "Neocortex patterning by the secreted signaling molecule FGF8." Science 294(5544): 1071-4.

Garcia-Dominguez, M., C. Poquet, S. Garel and P. Charnay (2003). "Ebf gene function is required for coupling neuronal differentiation and cell cycle exit." Development 130(24): 6013-25.

Garcia-Moreno, F., L. Lopez-Mascaraque and J. A. De Carlos (2007). "Origins and migratory routes of murine Cajal-Retzius cells." J Comp Neurol 500(3): 419-32.

Garel, S., K. Yun, R. Grosschedl and J. L. Rubenstein (2002). "The early topography of thalamocortical projections is shifted in Ebf1 and Dlx1/2 mutant mice." Development 129(24): 5621-34.

Garel, S., M. Garcia-Dominguez and P. Charnay (2000). "Control of the migratory pathway of facial branchiomotor neurones." Development 127(24): 5297-307.

Garel, S., F. Marin, R. Grosschedl and P. Charnay (1999). "Ebf1 controls early cell differentiation in the embryonic striatum." Development 126(23): 5285-94.

Garel, S., F. Marin, M. G. Mattei, C. Vesque, A. Vincent and P. Charnay (1997). "Family of Ebf/Olf-1-related genes potentially involved in neuronal differentiation and regional specification in the central nervous system." Dev Dyn 210(3): 191-205.

Gelman, D. M., F. J. Martini, S. Nobrega-Pereira, A. Pierani, N. Kessaris and O. Marin (2009). "The embryonic preoptic area is a novel source of cortical GABAergic interneurons." J Neurosci 29(29): 9380-9.

Gong, S., C. Zheng, M. L. Doughty, K. Losos, N. Didkovsky, U. B. Schambra, N. J. Nowak, A. Joyner, G. Leblanc, M. E. Hatten and N. Heintz (2003). "A gene expression atlas of the central nervous system based on bacterial artificial chromosomes." Nature 425(6961): 917-25.

Gotz, Magdalena. "Cerebral Cortex Development." Encyclopedia of Life Sciences. 2001.

Griveau, A., U. Borello, F. Causeret, F. Tissir, N. Boggetto, S. Karaz and A. Pierani (2010). "A novel role for Dbx1-derived Cajal-Retzius cells in early regionalization of the cerebral cortical neuroepithelium." PLoS Biol 8(7): e1000440.

Grove, E. A. and S. Tole (1999). "Patterning events and specification signals in the developing hippocampus." Cereb Cortex 9(6): 551-61.

Guillemot, F., Z. Molnar, V. Tarabykin and A. Stoykova (2006). "Molecular mechanisms of cortical differentiation." Eur J Neurosci 23(4): 857-68.

Gulacsi, A. and S. A. Anderson (2006). "Shh maintains Nkx2.1 in the MGE by a Gli3-independent mechanism." Cerebral Cortex 16 Suppl 1: i89-95.

Hack, I., S. Hellwig, D. Junghans, B. Brunne, H. H. Bock, S. Zhao and M. Frotscher (2007). "Divergent roles of ApoER2 and Vldlr in the migration of cortical neurons." Development 134(21): 3883-91.

Hagman, J., M. J. Gutch, H. Lin and R. Grosschedl (1995). "EBF contains a novel zinc coordination motif and multiple dimerization and transcriptional activation domains." EMBO J 14(12): 2907-16.

Hanashima, C., M. Fernandes, J. M. Hebert and G. Fishell (2007). "The role of Foxg1 and dorsal midline signaling in the generation of Cajal-Retzius subtypes." Journal of Neuroscience 27(41): 11103-11.

Hanashima, C., S. C. Li, L. Shen, E. Lai and G. Fishell (2004). "Foxg1 suppresses early cortical cell fate." Science 303(5654): 56-9.

Hashimoto-Torii, K., M. Torii, M. R. Sarkisian, C. M. Bartley, J. Shen, F. Radtke, T. Gridley, N. Sestan and P. Rakic (2008). "Interaction between Reelin and Notch signaling regulates neuronal migration in the cerebral cortex." Neuron 60(2): 273-84.

Hata, A., J. Seoane, G. Lagna, E. Montalvo, A. Hemmati-Brivanlou and J. Massague (2000). "OAZ uses distinct DNA- and protein-binding zinc fingers in separate BMP-Smad and Olf signaling pathways." Cell 100(2): 229-40.

Hatten, M. E. (1999). "Central nervous system neuronal migration." Annu Rev Neurosci 22: 511-39.

Heintz, N. (2004). "Gene expression nervous system atlas (GENSAT)." Nat Neurosci 7(5): 483.

Hernandez-Miranda, L. R., J. G. Parnavelas and F. Chiara (2010). "Molecules and mechanisms involved in the generation and migration of cortical interneurons." ASN Neuro 2(2): e00031.

Hevner, R. F., T. Neogi, C. Englund, R. A. Daza and A. Fink (2003). "Cajal-Retzius cells in the mouse: transcription factors, neurotransmitters, and birthdays suggest a pallial origin." Brain Res Dev Brain Res 141(1-2): 39-53.

Hevner, R. F., L. Shi, N. Justice, Y. Hsueh, M. Sheng, S. Smiga, A. Bulfone, A. M. Goffinet, A. T. Campagnoni and J. L. Rubenstein (2001). "Tbr1 regulates differentiation of the preplate and layer 6." Neuron 29(2): 353-66.

Hiesberger, T., M. Trommsdorff, B. W. Howell, A. Goffinet, M. C. Mumby, J. A. Cooper and J. Herz (1999). "Direct binding of Reelin to VLDL receptor and ApoE receptor 2 induces tyrosine phosphorylation of disabled-1 and modulates tau phosphorylation." Neuron 24(2): 481-9.

Hoerder-Suabedissen, A., W. Z. Wang, S. Lee , K. E. Davies , A. M. Goffinet , S. Rakić , J. Parnavelas , K. Reim , M. Nicolić , O. Paulsen , Z. Molnár (2009). "Novel markers reveal subpopulations of subplate neurons in the murine cerebral cortex." Cereb Cortex. 19(8):1738-50.

Howell, B. W., R. Hawkes, P. Soriano and J. A. Cooper (1997). "Neuronal position in the developing brain is regulated by mouse disabled-1." Nature 389(6652): 733-7.

Hsieh-Li, H. M., D. P. Witte, J. C. Szucsik, M. Weinstein, H. Li and S. S. Potter (1995). "Gsh-2, a murine homeobox gene expressed in the developing brain." Mech Dev 50(2-3): 177-86.

Inoue, T., M. Ogawa, K. Mikoshiba and J. Aruga (2008). "Zic deficiency in the cortical marginal zone and meninges results in cortical lamination defects resembling those in type II lissencephaly." J Neurosci 28(18): 4712-25.

Jimenez, M. A., P. Akerblad, M. Sigvardsson and E. D. Rosen (2007). "Critical role for Ebf1 and Ebf2 in the adipogenic transcriptional cascade." Mol Cell Biol 27(2): 743-57.

Jossin, Y. and A. M. Goffinet (2007). "Reelin signals through phosphatidylinositol 3-kinase and Akt to control cortical development and through mTor to regulate dendritic growth." Mol Cell Biol 27(20): 7113-24.

Jusuf, P. R. and W. A. Harris (2009). "Ptf1a is expressed transiently in all types of amacrine cells in the embryonic zebrafish retina." Neural Dev 4: 34.

Kandel, E. R., J.H. and T.M. Jessell (2000). "Principles of Neural Science." Fourth Ed. McGrown -Hill pp250-298.

Kanold, P. O., H. J.Luhmann (2010). "The subplate and early cortical circuits." Ann Rev Neurosci 33, 23-48.

Kanold, P. O., P. Kara, R. C. Reid and C. J. Shatz (2003). "Role of subplate neurons in functional maturation of visual cortical columns." Science 301(5632): 521-5.

Kieslinger, M., S. Folberth, G. Dobreva, T. Dorn, L. Croci, R. Erben, G. G. Consalez and R. Grosschedl (2005). "EBF2 regulates osteoblast-dependent differentiation of osteoclasts." Dev Cell 9(6): 757-67.

Konig, N. and R. Marty (1981). "Early neurogenesis and synaptogenesis in cerebral cortex." Bibl Anat(19): 152-60.

Kroll, T. T. and D. D. O'Leary (2005). "Ventralized dorsal telencephalic progenitors in Pax6 mutant mice generate GABA interneurons of a lateral ganglionic eminence fate." Proc Natl Acad Sci U S A 102(20): 7374-9.

Kowalczyk, T., A. Pontious, C. Englund, R. A. Daza, F. Bedogni, R. Hodge, A. Attardo, C. Bell, W. B. Huttner and R. F. Hevner (2009). "Intermediate

neuronal progenitors (basal progenitors) produce pyramidal-projection neurons for all layers of cerebral cortex." Cereb Cortex 19(10): 2439-50.

Lee, E. C., D. Yu, J. Martinez de Velasco, L. Tessarollo, D. A. Swing, D. L. Court, N. A. Jenkins and N. G. Copeland (2001). "A highly efficient Escherichia coli-based chromosome engineering system adapted for recombinogenic targeting and subcloning of BAC DNA." Genomics 73(1): 56-65.

Liberg, D., M. Sigvardsson and P. Akerblad (2002). "The EBF/Olf/Collier family of transcription factors: regulators of differentiation in cells originating from all three embryonal germ layers." Mol Cell Biol 22(24): 8389-97.

Lopez-Bendito, G., J. A. Sanchez-Alcaniz, R. Pla, V. Borrell, E. Pico, M. Valdeolmillos and O. Marin (2008). "Chemokine signaling controls intracortical migration and final distribution of GABAergic interneurons." J Neurosci 28(7): 1613-24.

Maggi, R., F. Pimpinelli, L. Molteni, M. Milani, L. Martini and F. Piva (2000). "Immortalized luteinizing hormone-releasing hormone neurons show a different migratory activity in vitro." Endocrinology 141(6): 2105-12.

Malgaretti, N., O. Pozzoli, A. Bosetti, A. Corradi, S. Ciarmatori, M. Panigada, M. E. Bianchi, S. Martinez and G. G. Consalez (1997). "Mmot1, a new helix-loop-helix transcription factor gene displaying a sharp expression boundary in the embryonic mouse brain." J Biol Chem 272(28): 17632-9.

Mallamaci, A., R. Iannone, P. Briata, M.L. Pintonello, S. Mercurio, E. Boncinelli, G. Corte (1998). "EMX2 protein in the developing brain and olfactory area." Mech Dev 77:165-172.

Marin, O. and J. L. Rubenstein (2003). "Cell migration in the forebrain." Annu Rev Neurosci 26: 441-83.

Marin-Padilla, M. (1978). "Dual origin of the mammalian neocortex and evolution of the cortical plate." Anat Embryol 152:109-126.

Marin-Padilla M. (1988) "Early ontogenesis of the human cerebral cortex. In: Cerebral cortex, Vol VII, Development and maturation of the cerebral cortex." (Peters A, Jones EG, eds), pp 1-30. New York: Plenum.

Marin-Padilla, M. (1990). "Three-dimensional structural organization of layer I of the human cerebral cortex: a Golgi study." J Comp Neurol 299(1): 89-105.

Martynoga, B., H. Morrison , D. J. Price , J. O. Mason (2005). "Foxg1 is required for specification of ventral telencephalon and region-specific regulation of dorsal telencephalic precursor proliferation and apoptosis." Dev Biol 283(1): 113-27.

Mayr, Ernst. (1984). "The Growth of Biological Thought: Diversity, Evolution and Inheritance." Cambridge: Harvard University Press.

McConnell, S. K., A. Ghosh and C. J. Shatz (1994). "Subplate pioneers and the formation of descending connections from cerebral cortex." J Neurosci 14(4): 1892-907.

Metin, C., J. P. Baudoin, S. Rakic and J. G. Parnavelas (2006). "Cell and molecular mechanisms involved in the migration of cortical interneurons." Eur J Neurosci 23(4): 894-900.

Meyer, G., C. G. Perez-Garcia, H. Abraham and D. Caput (2002). "Expression of p73 and Reelin in the developing human cortex." J Neurosci 22(12): 4973-86.

Mione, M. C., J. F. Cavanagh, B. Harris and J. G. Parnavelas (1997). "Cell fate specification and symmetrical/asymmetrical divisions in the developing cerebral cortex." J Neurosci 17(6): 2018-29.

Molnar, Z., C. Metin, A. Stoykova, V. Tarabykin, D. J. Price, F. Francis, G. Meyer, C. Dehay and H. Kennedy (2006). "Comparative aspects of cerebral cortical development." Eur J Neurosci 23(4): 921-34.

Molyneaux, B. J., P. Arlotta, J. R. Menezes and J. D. Macklis (2007). "Neuronal subtype specification in the cerebral cortex." Nature Reviews Neuroscience 8(6): 427-37.

Monuki, E. S. and C. A. Walsh (2001). "Mechanisms of cerebral cortical patterning in mice and humans." Nature Neuroscience 4 Suppl: 1199-206.

Muzio, L., B. DiBenedetto, A. Stoykova, E. Boncinelli, P. Gruss and A. Mallamaci (2002). "Conversion of cerebral cortex into basal ganglia in Emx2(-/-) Pax6(Sey/Sey) double-mutant mice." Nat Neurosci 5(8): 737-45.

Muzio, L. and A. Mallamaci (2003). "Emx1, emx2 and pax6 in specification, regionalization and arealization of the cerebral cortex." Cereb Cortex 13(6): 641-7.

Nadarajah, B., P. Alifragis, R. O. Wong and J. G. Parnavelas (2002). "Ventricle-directed migration in the developing cerebral cortex." Nat Neurosci 5(3): 218-24.

Nadarajah, B., J. E. Brunstrom, J. Grutzendler, R. O. Wong and A. L. Pearlman (2001). "Two modes of radial migration in early development of the cerebral cortex." Nat Neurosci 4(2): 143-50.

Nieto, M., C. Schuurmans, O. Britz and F. Guillemot (2001). "Neural bHLH genes control the neuronal versus glial fate decision in cortical progenitors." Neuron 29(2): 401-13.

Niu, S., A. Renfro, C. C. Quattrocchi, M. Sheldon and G. D'Arcangelo (2004). "Reelin promotes hippocampal dendrite development through the VLDLR/ApoER2-Dab1 pathway." Neuron 41(1): 71-84.

Niu, S., O. Yabut and G. D'Arcangelo (2008). "The Reelin signaling pathway promotes dendritic spine development in hippocampal neurons." J Neurosci 28(41): 10339-48.

Noctor, S. C., V. Martinez-Cerdeno, L. Ivic and A. R. Kriegstein (2004). "Cortical neurons arise in symmetric and asymmetric division zones and migrate through specific phases." Nat Neurosci 7(2): 136-44.

Nowak, M. A., M. C. Boerlijst, J. Cooke and J. M. Smith (1997). "Evolution of genetic redundancy." Nature 388(6638): 167-71.

O'Leary, D. D. (1989). "Do cortical areas emerge from a protocortex?" Trends Neurosci 12(10): 400-6.

O'Leary, D. D., S. J. Chou and S. Sahara (2007). "Area patterning of the mammalian cortex." Neuron 56(2): 252-69.

O'Leary, D. D., B. L. Schlaggar and R. Tuttle (1994). "Specification of neocortical areas and thalamocortical connections." Annu Rev Neurosci 17: 419-39.

Ogawa, M., T. Miyata, K. Nakajima, K. Yagyu, M. Seike, K. Ikenaka, H. Yamamoto and K. Mikoshiba (1995). "The reeler gene-associated antigen on Cajal-Retzius neurons is a crucial molecule for laminar organization of cortical neurons." Neuron 14(5): 899-912.

Ohno, S. (1970). “Evolution by gene duplication.” New York:Springer-Verlag.

Panganiban, G. and J. L. Rubenstein (2002). "Developmental functions of the Distal-less/Dlx homeobox genes." Development 129(19): 4371-86.

Paredes, M. F., G. Li, O. Berger, S. C. Baraban and S. J. Pleasure (2006). "Stromal-derived factor-1 (CXCL12) regulates laminar position of Cajal-Retzius cells in normal and dysplastic brains." J Neurosci 26(37): 9404-12.

Parnavelas, J. G. and S. M. Edmunds (1983). "Further evidence that Retzius-Cajal cells transform to nonpyramidal neurons in the developing rat visual cortex." J Neurocytol 12(5): 863-71.

Parnavelas, J. G. and B. Nadarajah (2001). "Radial glial cells. are they really glia?" Neuron 31(6): 881-4.

Pearson, H. (2002). "Surviving a knockout blow." Nature 415(6867): 8-9.

Pla, R., V. Borrell, N. Flames and O. Marin (2006). "Layer acquisition by cortical GABAergic interneurons is independent of Reelin signaling." J Neurosci 26(26): 6924-34.

Portera-Cailliau, C., R. M. Weimer, V. De Paola, P. Caroni and K. Svoboda (2005). "Diverse modes of axon elaboration in the developing neocortex." PLoS Biol 3(8): e272.

Pozzoli, O., A. Bosetti, L. Croci, G. G. Consalez and M. L. Vetter (2001). "Xebf3 is a regulator of neuronal differentiation during primary neurogenesis in Xenopus." Dev Biol 233(2): 495-512.

Prasad, B. C., B. Ye, R. Zackhary, K. Schrader, G. Seydoux and R. R. Reed (1998). "unc-3, a gene required for axonal guidance in Caenorhabditis elegans, encodes a member of the O/E family of transcription factors." Development 125(8): 1561-8.

Radnikow, G., D. Feldmeyer and J. Lubke (2002). "Axonal projection, input and output synapses, and synaptic physiology of Cajal-Retzius cells in the developing rat neocortex." J Neurosci 22(16): 6908-19.

Radovick, S., S. Wray , E. Lee , D. K. Nicols , Y. Nakayama , B. D. Weintraub , H. Westphal , G. B. Jr Cutler , F. E. Wondisford (1999). “Migratory arrest of gonadotropin-releasing hormone neurons in transgenic mice.” Proc Natl Acad Sci U S A. 88(8):3402-6.

Rakic, P. (1988). "Specification of cerebral cortical areas." Science 241(4862): 170-6.

Rakic, P., A. E. Ayoub, J. J. Breunig and M. H. Dominguez (2009). "Decision by division: making cortical maps." Trends in Neurosciences 32(5): 291-301.

Rakic, P., K. Hashimoto-Torii and M. R. Sarkisian (2007). "Genetic determinants of neuronal migration in the cerebral cortex." Novartis Found Symp 288: 45-53; discussion 53-8, 96-8.

Ramón y Cajal S. (1911) "Histologie du Systeme Nerveux de l’Homme et des Vertebres." Vol. 2. Paris: Maloine

Retzius, G. (1894) "Weitere Beiträge zur Kenntniss der Cajal'schen Zellen der Grosshirnrinde des Menschen." Biologische Untersuchungen. Neue Folge 6:29–36.

Rice, D. S. and T. Curran (2001). "Role of the reelin signaling pathway in central nervous system development." Annu Rev Neurosci 24: 1005-39.

Sahara, S., Y. Kawakami, J. C. Izpisua Belmonte and D. D. O'Leary (2007). "Sp8 exhibits reciprocal induction with Fgf8 but has an opposing effect on anterior-posterior cortical area patterning." Neural Dev 2: 10.

Sarnat, H. B. and L. Flores-Sarnat (2002). "Cajal-Retzius and subplate neurons: their role in cortical development." Eur J Paediatr Neurol 6(2): 91-7.

Scardigli, R., N. Baumer, P. Gruss, F. Guillemot and I. Le Roux (2003). "Direct and concentration-dependent regulation of the proneural gene Neurogenin2 by Pax6." Development 130(14): 3269-81.

Schmid, Y., G. A. Grassl, O. T. Buhler, M. Skurnik, I. B. Autenrieth and E. Bohn (2004). "Yersinia enterocolitica adhesin A induces production of interleukin-8 in epithelial cells." Infect Immun 72(12): 6780-9.

Schuurmans, C., O. Armant, M. Nieto, J. M. Stenman, O. Britz, N. Klenin, C. Brown, L. M. Langevin, J. Seibt, H. Tang, J. M. Cunningham, R. Dyck, C. Walsh, K. Campbell, F. Polleux and F. Guillemot (2004). "Sequential phases of cortical specification involve Neurogenin-dependent and -independent pathways." EMBO J 23(14): 2892-902.

Schwartz, T. H., D. Rabinowitz, V. Unni, V. S. Kumar, D. K. Smetters, A. Tsiola and R. Yuste (1998). "Networks of coactive neurons in developing layer 1." Neuron 20(3): 541-52.

Sheng, H. Z., S. Bertuzzi, C. Chiang, W. Shawlot, M. Taira, I. Dawid and H. Westphal (1997). "Expression of murine Lhx5 suggests a role in specifying the forebrain." Dev Dyn 208(2): 266-77.

Shimogori, T., V. Banuchi, H. Y. Ng, J. B. Strauss and E. A. Grove (2004). "Embryonic signaling centers expressing BMP, WNT and FGF proteins interact to pattern the cerebral cortex." Development 131(22): 5639-47.

Shimogori, T. and M. Ogawa (2008). "Gene application with in utero electroporation in mouse embryonic brain." Development Growth & Differentiation 50(6): 499-506.

Shimshek, D. R., J. Kim, M. R. Hubner, D. J. Spergel, F. Buchholz, E. Casanova, A. F. Stewart, P. H. Seeburg and R. Sprengel (2002). "Codon-improved Cre recombinase (iCre) expression in the mouse." Genesis 32(1): 19-26.

Siegenthaler, J. A. and M. W. Miller (2008). "Generation of Cajal-Retzius neurons in mouse forebrain is regulated by transforming growth factor beta-Fox signaling pathways." Dev Biol 313(1): 35-46.

Sigvardsson, M., D. R. Clark, D. Fitzsimmons, M. Doyle, P. Akerblad, T. Breslin, S. Bilke, R. Li, C. Yeamans, G. Zhang and J. Hagman (2002). "Early B-cell factor, E2A, and Pax-5 cooperate to activate the early B cell-specific mb-1 promoter." Mol Cell Biol 22(24): 8539-51.

Soda, T., R. Nakashima, D. Watanabe, K. Nakajima, I. Pastan and S. Nakanishi (2003). "Segregation and coactivation of developing neocortical layer 1 neurons." J Neurosci 23(15): 6272-9.

Soriano, E., R. M. Alvarado-Mallart, N. Dumesnil, J. A. Del Rio and C. Sotelo (1997). "Cajal-Retzius cells regulate the radial glia phenotype in the adult and developing cerebellum and alter granule cell migration." Neuron 18(4): 563-77.

Soriano, E. and J. A. Del Rio (2005). "The cells of cajal-retzius: still a mystery one century after." Neuron 46(3): 389-94.

Stoykova, A., O. Hatano, P. Gruss and M. Gotz (2003). "Increase in reelin-positive cells in the marginal zone of Pax6 mutant mouse cortex." Cereb Cortex 13(6): 560-71.

Stoykova, A., D. Treichel, M. Hallonet and P. Gruss (2000). "Pax6 modulates the dorsoventral patterning of the mammalian telencephalon." J Neurosci 20(21): 8042-50.

Stuhmer, T., S. A. Anderson, M. Ekker and J. L. Rubenstein (2002). "Ectopic expression of the Dlx genes induces glutamic acid decarboxylase and Dlx expression." Development 129(1): 245-52.

Sussel, L., O. Marin, S. Kimura and J. L. Rubenstein (1999). "Loss of Nkx2.1 homeobox gene function results in a ventral to dorsal molecular respecification within the basal telencephalon: evidence for a transformation of the pallidum into the striatum." Development 126(15): 3359-70.

Takiguchi-Hayashi, K., M. Sekiguchi, S. Ashigaki, M. Takamatsu, H. Hasegawa, R. Suzuki-Migishima, M. Yokoyama, S. Nakanishi and Y. Tanabe (2004). "Generation of reelin-positive marginal zone cells from the caudomedial wall of telencephalic vesicles." J Neurosci 24(9): 2286-95.

Tamagnone, L. and P. M. Comoglio (2004). "To move or not to move? Semaphorin signalling in cell migration." EMBO Rep 5(4): 356-61.

Tautz, D. (1992). "Redundancies, development and the flow of information." Bioessays 14(4): 263-6.

Testa, G., Y. Zhang, K. Vintersten, V. Benes, W. W. Pijnappel, I. Chambers, A. J. Smith, A. G. Smith and A. F. Stewart (2003). "Engineering the mouse genome with bacterial artificial chromosomes to create multipurpose alleles." Nat Biotechnol 21(4): 443-7.

Tissir, F. and A. M. Goffinet (2003). "Reelin and brain development." Nature Reviews Neuroscience 4(6): 496-505.

Tissir, F., A. Ravni, Y. Achouri, D. Riethmacher, G. Meyer and A. M. Goffinet (2009). "DeltaNp73 regulates neuronal survival in vivo." Proc Natl Acad Sci U S A 106(39): 16871-6.

Toresson, H., S. S. Potter and K. Campbell (2000). "Genetic control of dorsal-ventral identity in the telencephalon: opposing roles for Pax6 and Gsh2." Development 127(20): 4361-71.

Tsai, L. H. and J. G. Gleeson (2005). "Nucleokinesis in neuronal migration." Neuron 46(3): 383-8.

Tsai, R. Y. and R. R. Reed (1997). "Cloning and functional characterization of Roaz, a zinc finger protein that interacts with O/E-1 to regulate gene expression: implications for olfactory neuronal development." J Neurosci 17(11): 4159-69.

Wagner, A. (2000). "Robustness against mutations in genetic networks of yeast." Nat Genet 24(4): 355-61.

Wang, S. S., A. G. Betz and R. R. Reed (2002). "Cloning of a novel Olf-1/EBF-like gene, O/E-4, by degenerate oligo-based direct selection." Mol Cell Neurosci 20(3): 404-14.

Wang, S. S., R. Y. Tsai and R. R. Reed (1997). "The characterization of the Olf-1/EBF-like HLH transcription factor family: implications in olfactory gene regulation and neuronal development." J Neurosci 17(11): 4149-58.

Wang W. Z., A. Hoerder-Suabedissen, F. M. Oeschger, N. Bayatti, B. Kar Ip, S. Lindsay, V. Supramanian, L. Srinivasan, M. Rutherford, K. Mollgard, G. J. Clowry, Z. Molnar (2010). "Subplate in the developing cortex of mouse and human." J. Anat. 217:368-380.

Xu, Q., I. Cobos, E. De La Cruz, J. L. Rubenstein and S. A. Anderson (2004). "Origins of cortical interneuron subtypes." J Neurosci 24(11): 2612-22.

Xu, Q., C. P. Wonders and S. A. Anderson (2005). "Sonic hedgehog maintains the identity of cortical interneuron progenitors in the ventral telencephalon." Development 132(22): 4987-98.

Yamazaki, H., M. Sekiguchi, M. Takamatsu, Y. Tanabe and S. Nakanishi (2004). "Distinct ontogenic and regional expressions of newly identified Cajal-Retzius cell-specific genes during neocorticogenesis." Proceedings of the National Academy of Sciences of the United States of America 101(40): 14509-14.

Yoshida, M., S. Assimacopoulos, K. R. Jones and E. A. Grove (2006). "Massive loss of Cajal-Retzius cells does not disrupt neocortical layer order." Development 133(3): 537-45.

Yu, H. H. and A. L. Kolodkin (1999). "Semaphorin signaling: a little less perplexin." Neuron 22(1): 11-4.

Yun, K., S. Fischman, J. Johnson, M. Hrabe de Angelis, G. Weinmaster and J. L. Rubenstein (2002). "Modulation of the notch signaling by Mash1 and Dlx1/2 regulates sequential specification and differentiation of progenitor cell types in the subcortical telencephalon." Development 129(21): 5029-40.

Yun, K., S. Potter and J. L. Rubenstein (2001). "Gsh2 and Pax6 play complementary roles in dorsoventral patterning of the mammalian telencephalon." Development 128(2): 193-205.

Zhao, S., X. Chai, E. Forster and M. Frotscher (2004). "Reelin is a positional signal for the lamination of dentate granule cells." Development 131(20): 5117-25.

Zhao, Y., H. Z. Sheng, R. Amini, A. Grinberg, E. Lee, S. Huang, M. Taira and H. Westphal (1999). "Control of hippocampal morphogenesis and neuronal differentiation by the LIM homeobox gene Lhx5." Science 284(5417): 1155-8.

Zhou, C., S. Y. Tsai and M. J. Tsai (2001). "COUP-TFI: an intrinsic factor for early regionalization of the neocortex." Genes Dev 15(16): 2054-9.

Zimmer, C., J. Lee, A. Griveau, S. Arber, A. Pierani, S. Garel and F. Guillemot (2010). "Role of Fgf8 signalling in the specification of rostral Cajal-Retzius cells." Development 137(2): 293-302.

Zimmer, C., M. C. Tiveron, R. Bodmer and H. Cremer (2004). "Dynamics of Cux2 expression suggests that an early pool of SVZ precursors is fated to become upper cortical layer neurons." Cerebral Cortex 14(12): 1408-20.